

The role of inorganic polyphosphates in Escherichia coli sepsis

Die Rolle von anorganischen Polyphosphaten in der Escherichia coli Sepsis

Inauguraldissertation

zur Erlangung des Doktorgrades der Medizin

des Fachbereichs Medizin der

Johannes Gutenberg-Universität

Mainz

vorgelegt von

Georgios Stavrides

aus Lefkosia, Republik Zypern

Mainz, 2022

Tag der Promotion: 12. Juli 2022

Für meine Familie und meine Freunde

I. Table of contents

I.	Table of contents.....	I
II.	List of tables.....	V
III.	List of figures.....	VI
IV.	Abbreviations.....	VIII
1.	Introduction – Working hypothesis.....	1
2.	Literature review.....	3
2.1	Initiation of inflammation after bacterial infection.....	3
2.1.1	Mediators of immune response.....	4
2.1.2	Macrophages.....	7
2.1.3	Toll-like receptors and signalling.....	9
2.1.4	Cytokine release and inflammatory response.....	10
2.1.5	Chemokines and inflammatory response.....	11
2.1.6	The role of nitric oxide (NO).....	12
2.2	Sepsis and septic shock.....	12
2.2.1	Definition of sepsis and septic shock.....	12
2.2.2	Incidence and mortality of sepsis.....	13
2.2.3	The pathomechanism of sepsis.....	14
2.2.4	Sepsis interventional management.....	16
2.2.5	Murine sepsis models and evaluation of septic infection.....	16
2.2.6	Human endotoxemia experiments.....	17
2.3	Inorganic polyphosphates.....	17
2.3.1	Introduction – a polymer with many functions.....	17

2.3.2	PolyP in diverse organisms	18
2.3.3	The effect of PolyP on blood coagulation in mammalian species	19
2.3.4	Interaction of PolyP with inflammatory mediators	21
2.3.5	Working Hypothesis.....	24
3.	Materials and methods.....	25
3.1	Material	25
3.1.1	Consumable materials.....	25
3.1.2	Media and buffer.....	26
3.1.3	Reagents	28
3.1.4	Assay kits	30
3.1.5	Biochemicals	31
3.1.6	Cells and E. coli strains	31
3.1.7	Antibodies.....	32
3.1.8	Primers and vectors.....	32
3.1.9	Instruments. Equipment and software analysis	33
3.2	Mouse strains.....	35
3.3	In vivo Experiments.....	36
3.3.1	Establishment of live E. coli sepsis model	36
3.3.2	Live E. coli sepsis and administration of inorganic polyphosphates.	38
3.3.3	Live E. coli sepsis and treatment with recombinant exopolyphosphatase from <i>Saccharomyces cerevisiae</i> (ScPPX).....	38
3.3.4	Extraction of blood plasma and peritoneal lavage after sepsis	39
3.4	In vitro experiments.....	39
3.4.1	Bacterial growth curve	39

3.4.2	Flow cytometric count of the bacterial inoculum for live E. coli sepsis	40
3.4.3	Purification of Saccharomyces cerevisiae exopolyphosphatase (ScPPX) .	40
3.4.4	Bacterial killing assay by macrophages	41
3.4.5	Preparation of bone marrow-derived macrophages.....	42
3.4.6	MH-S macrophage culture.....	43
3.4.7	MLE-12 cell culture	43
3.4.8	Determination of cell numbers for in vitro experiments	44
3.4.9	In vitro stimulation and sample preparation	44
3.5	Biochemical methods	45
3.5.1	DNA extraction from bacteria using Trizol Reagent.....	45
3.5.2	Genotyping of E. coli by polymerase-chain-reaction (PCR).....	46
3.5.3	Enzyme-linked immunosorbent (ELISA) assay.....	46
3.5.4	Sample preparation for quantitative PCR analysis	47
3.5.5	Bioplex assay	49
3.5.6	Flow cytometry of mouse cells.....	50
3.5.7	Bradford assay	51
3.5.8	Grieff assay	51
3.5.9	Enzymatic activity measurement of ScPPX using Biomol Green assay	51
3.5.10	Statistical analysis.....	52
4.	Results	53
4.1	Estimation of bacterial concentration needed for in vivo bacterial sepsis.....	53
4.2	Sepsis from bacterial strains deficient of polyphosphate metabolising enzymes resulted in an altered outcome	55
4.3	L-PolyP dysbalance the inflammatory response and impair the outcome of E. coli sepsis	58

4.4	Short-chain polyphosphates do not influence E. coli sepsis survival.....	65
4.5	Recombinant exopolyphosphatase improved the outcome of E. coli sepsis	66
4.6	Administration of L-PolyP during endotoxemia in mice	68
4.7	L-PolyP triggered CXCL4 release during E. coli sepsis	70
4.8	The presence of L-PolyP decreased bacterial killing by macrophages	72
4.9	The bacterial growth of E. coli is not affected by exogenous L-PolyP and ScPPX.....	74
5.	Discussion.....	76
5.1	Establishment of live E. coli sepsis model.....	76
5.2	L-PolyP are a modulator of sepsis outcome.....	77
5.3	The presence of L-PolyP increases the systemic inflammatory response	79
5.4	L-PolyP induce PF4 (CXCL4) release during inflammatory response.....	82
5.5	ScPPX as a potential drug candidate for sepsis.....	83
5.6	Conclusion	86
6.	Summary (Zusammenfassung).....	87
7.	References.....	89
V.	Curriculum vitae	109

II. List of tables

Table 1: Consumable material	25
Table 2: Media and buffer	26
Table 3: Reagents	28
Table 4: Assay kits	30
Table 5: Biochemicals	31
Table 6: Cell lines.....	31
Table 7: E. coli strains.....	31
Table 8: Flow cytometry antibodies.....	32
Table 9: RT-PCR and qPCR primers and plasmid vectors.....	32
Table 10: Instruments.....	33
Table 11: Software	34
Table 12: Mouse strains	35
Table 13: Clinical severity scoring system.....	37
Table 14: Preparation of cDNA	48
Table 15: qPCR program	48

III. List of figures

Figure 1: Schematic representation of inorganic polyphosphate polymer and its metabolism as regulated by Ppk and Ppx enzymes.....	18
Figure 2: Schematic representation of E. coli strains.	24
Figure 3: Schematic representation of the intraperitoneal injection of the bacterial suspension in sex- and age-matched C57BL/6 mice.	37
Figure 4: Growth curve of E. coli MG1665 based on optical density.....	53
Figure 5: Gating strategy for quantification of injected E. coli bacteria.	54
Figure 6: Survival rate after live E. coli sepsis induction with E. coli MG1655 (wt-bacteria).....	54
Figure 7: Growth curve of used bacterial stains in terms of optical density.	55
Figure 8: Sepsis experiments with E. coli strains deficient of polyphosphate metabolising enzymes.....	56
Figure 9: The administration of L-PolyP increases mortality rates during E. coli bacteremia.....	58
Figure 10: L-PolyP increased clinical severity score (CSS) in septic mice.....	59
Figure 11: L-PolyP increase bacterial burden and aggravate symptoms of sepsis.....	60
Figure 12: Gating strategy for quantification of peritoneal cells.	61
Figure 13: Quantification of peritoneal immune cells during E. coli sepsis.	62
Figure 14: Quantification of chemokines in the peritoneal lavage in the presence or absence of exogenous L-PolyP during E. coli sepsis.....	63
Figure 15: Quantification of pro- and anti-inflammatory cytokines in the peritoneal lavage in the presence or absence of L-PolyP during E. coli sepsis.	63
Figure 16: Quantification of chemokines in the peritoneal lavage in the presence or absence of L-PolyP during E. coli sepsis (Bioplex assay).....	64
Figure 17: The presence of S-PolyP does not affect survival during E. coli sepsis. ...	65

Figure 18: Treatment with recombinant exopolyphosphatase from <i>Saccharomyces cerevisiae</i> improves the survival rate during <i>E. coli</i> sepsis.....	66
Figure 19: Treatment with recombinant exopolyphosphatase from <i>Saccharomyces cerevisiae</i> improves the clinical signs of sepsis.	67
Figure 20: ScPPX treatment caused a decrease in bacterial burden during <i>E. coli</i> sepsis.....	68
Figure 21: Studies on the administration of L-PolyP in LPS-induced endotoxemia. ...	69
Figure 22: L-PolyP reduces iNOS activity in the context of LPS-induced TLR4 signalling.....	70
Figure 23: L-PolyP increases platelet-factor 4 release in blood plasma and peritoneal lavage during <i>E. coli</i> sepsis.....	71
Figure 24: L-PolyP results in platelet-factor 4 release from MH-S macrophages.....	72
Figure 25: L-PolyP reduce the efficiency of phagocytosis in vitro.....	73
Figure 26: L-PolyP and ScPPX do not influence <i>E. coli</i> bacterial growth in vitro	75

IV. Abbreviations

AIM-2	Absent in melanoma 2
ALR	AIM-2 like receptor
APC	Antigen-presenting cell
B-On	Overnight bacterial culture
BSA	Bovine serum albumin
CARS	Compensatory anti-inflammatory response syndrome
CCL	CC chemokine ligand
CD	Cluster of differentiation
CFU	Colony forming units
CLR	C-type lectin receptors
CO ₂	Carbon dioxide
°C	Celcius
DC	Dendritic cells
DMSO	Dimethyl sulphoxide
DNA	Deoxyribonucleic acid
E. coli	Escherichia coli
E.g	Exempli gratia
EDTA	Ethylenediaminetetraacetic acid

ELISA	Enzyme-linked immunosorbent assay
eNOS	Endothelial nitric oxide synthase
Et al.	<i>Et alia</i>
FACS	Fluorescence-activated cell sorting
FCS	Fetal calf serum
FiO ₂	Fraction of inspired oxygen
FI-XII(a)	Factor 1 to 12(a=activated)
GM-CSF	Granulocyte-macrophage colony-stimulating factor
HBSS	Hank's balanced salt solution
HMGB1	High mobility box group 1
i.p	Intra-peritoneal, intra-peritoneally (when used as an adverb)
ICAM-1	Intercellular adhesion molecule 1
IFN	Interferon
IL	Interleukin
iNOS	Inducible nitric oxide synthase
IPTG	Isopropyl-β-D1-thiogalactopyranoside
IRF	Interferon regulatory factors
KC	Keratinocyte chemoattractant
LAM	Lipoarabinomannan

L-PolyP	Long-chain polyphosphates
MAL	MyD88-adaptor-like
MAP	Mean arterial pressure
MAPK	Mitogen-activated protein kinase
MHC	Major histocompatibility complex
MLE-12-Cells	Murine lung epithelial cells
MyD88	Myeloid differentiation primary response 88
M ϕ	Macrophage
NaCl	Sodium chloride
NF- κ B	Nuclear factor kappa-lightchain-enhancer of activated B cells
NLR	Nod-like receptors
nNOS	Neuronal nitric oxide synthase
NO	Nitric oxide
Nod	nucleotide-binding oligomerization domain- receptors
OD ₆₀₀	Optical density of solution, measured at 600nm
P2Y1	Purinergic receptor Y1
PAGE	Polyacrylamide gel electrophoresis
PAMP	Pathogen-associated molecular pattern
PaO ₂	partial pressure of oxygen

PBS	Phosphate buffered saline
PenStrep	Penicillin-Streptomycin
PF4	Platelet-derived factor 4
Pi	Phosphate group
PolyP	Inorganic polyphosphates
Ppk	Polyphosphate kinase
PPR	Pattern recognition receptor
Ppx	Exopolyphosphatase
qSOFA	Quick Sequential (Sepsis-related) Organ Failure Assessment
RAGE	Receptor for advanced glycation endproducts
rec.	Recombinant
RLR	RIG-I-like receptors
RNA	Ribonucleic acid
rpm	Rounds per minute
RPMI	Roswell Park Memorial Institute
RT	Room temperature
ScPPX	Exopolyphosphatase, derived from <i>Saccharomyces cerevisiae</i>
SDS	Sodium dodecyl sulfate
S.E.M	Standard error of the median

SIRS	Systemic inflammatory response syndrome
SOFA	Sequential (Sepsis-related) Organ Failure Assessment
S-PolyP	Short-chain polyphosphates
TEMED	Tetramethylethylenediamine
TGF- β	Transforming growth factor beta
TICAM1	TIR-domain-containing molecule 1
TIRAP	TIR-associated protein
TLR	Toll-like receptor
TNF- α	Tumour necrosis factor α
tPA	Tissue plasminogen activator
TRAM	TRIF-related adaptor molecule
TRIF	TIR-domain-containing adaptor protein-inducing IFN- β
VCAM-1	Vascular cell adhesion molecule 1
wt	Wild type
Δ ppk	Deficiency of the enzyme exopolyphosphatase
Δ ppx	Deficiency of the enzyme polyphosphate kinase

1. Introduction – Working hypothesis

Inorganic polyphosphates (PolyP) are a linear polymer consisting of many orthophosphates linked together by phosphoanhydride bonds. PolyP are present in all living organisms and their size varies from short-chain polyphosphates (S-PolyP), found in platelets, to long-chain polyphosphates (L-PolyP), located in prokaryotic cells, e.g. bacteria. Intracellular polyphosphates modulate energy metabolism as a phosphate storage for ATP synthesis and as an energy reservoir in stress conditions. It was also found that PolyP play an essential role in the blood-clotting pathway. Inorganic polyphosphates work as activators of Factor XII and as amplifiers of the activation of factor XI by enhancing the thrombin feedback and activation of Factor V. The main enzymes participating in microbial PolyP metabolism are polyphosphate kinase (Ppk), which catalyses the synthesis of polymers from anionic phosphate monomers, and exopolyphosphatase (Ppx), which catalyses the subsequent degradation of PolyP into monomers.

Inorganic polyphosphates also act as modulators of the immune system in mammals. Through the activation and initiation of the contact pathway, vasoactive and inflammatory factors such as bradykinin are released. The presence of S-PolyP increases the endothelial leakage and promotes cell migration after the initiation of the NF- κ B pathway¹. Inorganic polyphosphates were proposed to activate through interaction with RAGE and P2Y1 receptors² and the mammalian target of rapamycin complexes 1 and 2 (mTORC1, mTORC2)³, leading to activation of the NF- κ B pathway. Furthermore, inorganic polyphosphates result in a downregulation of the complement system response and a destabilisation of the C5b/C6 complex⁴. Inorganic polyphosphates cause a reduction of the iNOS expression from peritoneal macrophages after LPS-stimulation, thus limiting the immune response⁵.

Based on the various effects of inorganic polyphosphates on the immune response, bacterial virulence, and coagulation, we formulated the major **hypothesis** if L-PolyP alter the endpoints and severity of sepsis by modulating the innate immune response. Therefore, this dissertation aims to investigate the influence of PolyP on sepsis and inflammation during bacterial peritonitis, focusing on the effects of inorganic

polyphosphates on sepsis outcome, immune-modulating cells, cytokines and changes in coagulant and procoagulant factors.

A murine peritoneal sepsis model after intraperitoneal injection of *E. coli* mutants was established, which models either overexpression or deficiency of bacterial polyphosphates. In addition, the administration of L-PolyP, S-PolyP and exogenous recombinant exopolyphosphatase during sepsis were investigated.

The presence of L-PolyP during sepsis resulted in a significant increase in mortality and migration of immune cells such as neutrophils and macrophages, leukocyte-derived cytokines, thrombin-antithrombin complexes and platelet-derived mediators. On the other hand, the treatment of septic mice with ScPPX resulted in a significant increase in the survival rate, confirming the hypothesis that inorganic polyphosphates are an immune modulator.

According to our results, PolyP modulate the inflammatory response in bacterial sepsis. PolyP not only influence the virulence and stress reaction of bacteria, as suggested by previous studies but also interfere with the immune system components of eukaryotes. PolyP could serve as a future target in the fight against sepsis and inflammation for achieving better outcomes in human patients.

2. Literature review

2.1 Initiation of inflammation after bacterial infection

The presence of microbial organisms is often associated with infection and inflammatory responses, although it has been known for years, that most of the vertebral eukaryotic organisms have a symbiotic relationship with prokaryotes^{6,7}. Prokaryotic organisms like bacteria or fungi are present in significant populations in anatomical structures like the oropharyngeal cavity, colon, and epidermis⁸. The interaction between host and microbiota facilitates essential functions such as digestion and affects disease vulnerability. Studies in germ-free mice revealed that the equilibrium of interactions between microbiota and the host innate immunity affect the development of infection, autoimmunity and chronic diseases⁹, metabolic syndrome¹⁰ and cancer¹¹.

However, prokaryotes are often regarded as pathogens because they can cause the initiation of the inflammatory response in host organisms after exceeding the threshold to establish an infection. Injuries, wounds, immune suppression, simultaneous infection and iatrogenic manipulation may provide the perfect environment for opportunistic colonisation causing local infection, which could be generated in the form of sepsis or septic shock under certain circumstances¹².

Bacteria are prokaryotic organisms divided into four major groups according to their outer wall structure and pathogenesis: Gram-positive and Gram-negative, mycobacteria, and spirochetes¹³. The main characteristic and potential virulence factor of Gram-positive bacteria is a thick cell wall containing structures like peptidoglycan, lipoteichoic acid, and lipopeptides. These cell wall components are immunologically active and act as potential agents of inflammation. The main immunologically active component of gram-negative bacteria is LPS, which interacts with recognition pathways of innate immunity and contains lipid A. Mycobacteria interact with the immune system because of the main structural element of their outer membrane, lipoarabinomannan (LAM)¹⁴. Some spirochetes use LPS as a virulence factor, but it is also considered that their outer membrane lipoproteins interact with the immune system.

Invasion of extracorporeal prokaryotic microorganisms (e.g., bacteria, viruses)¹⁵ eukaryotic cells (e.g. fungi) or extracorporeal/synthetic material (e.g. prosthetic material)¹⁶ activates the first-line defence of the host organism, which is the innate immune system. The innate immune system initiates the inflammatory response by activating multiple mechanisms, including complement activation. It also serves as the starting point for adaptive immunity. If the inflammatory response fails to control pathogen invasion, the infection generalizes, leading to sepsis, which can progress to septic shock with a high mortality rate. The interaction between different immune defence agents is facilitated by the release of cytokines and the direct interaction between the cellular agents via receptors.

2.1.1 Mediators of immune response

The immune system's main components are innate immunity, consisting of monocytes, macrophages, neutrophils and the complement system, and adaptive immunity, consisting of lymphocytes and immunoglobulins. After the recognition of microbial invasion by the pathways of innate immunity, adaptive immunity is activated. Both systems interact by direct contact and release and recognition of inflammatory cytokines.

2.1.1.1 Innate Immunity

The innate immune system is responsible for the immediate activation of host defenses against pathogen invasion, infection or tissue injury. Vertebrate species recognise the presence of microorganisms such as bacteria by engagement of pattern recognition receptors (PRRs), which detect pathogen-associated molecular patterns (PAMPs)¹⁷. PAMPs include a variety of structural characteristics of microorganisms, including polysaccharides, lipoproteins, glycolipids, nucleic acids or nucleotides. Toll-like receptors (TLRs), nucleotide-binding oligomerization domain- receptors (Nod), leucine-repeat-containing receptors, also called Nod-like receptors (NLRs), RIG-I-like receptors (RLRs), and C-type lectin receptors (CLRs), AIM-2-like Receptors (ALRs) and intracellular sensors for nucleic acids are essential classes of PRRs, which are widely studied¹⁸. PRRs

are characterised by their cellular compartment localisation, e.g. plasma membrane, endosome, lysosome or cytosol, and tissue-specific expression^{19,20}. Some PRRs are involved in the intracellular (cell-intrinsic) recognition of microbial patterns and others are responsible for the cell-extrinsic pathogen recognition. TLRs are membrane-bound receptors that sense various microbial components and are involved in the activation of both immunity mechanisms²¹. They are divided into subfamilies according to the recognition of related PAMPs and can be found in antigen-presenting cells, including macrophages, dendritic cells (DCs) and B-lymphocytes. They are the most studied PRRs so far²². Cytosolic pattern recognition of PAMPs is mediated by intracellular PRRs. Nod1, Nod2, and NLRs detect bacterial components such as peptidoglycan fragments and flagellin in the cytoplasm^{23,24}. RLRs detect viral DNA and RNA released during viral replication in infected cells²⁵. CLR plays an essential role in recognising bacterial and fungal infection after binding with structures like LAM on the surface of *Mycobacterium tuberculosis* or components of fungal cell walls such as β -(1,3) glucan^{26,27}. Innate immunity not only recognizes structural microbial components but also detects danger signals through a complex structure, termed inflammasome²⁸. The oligomerisation of the proteins of this complex leads to activation of caspase-1, which catalyses the production of active interleukin-1 (IL-1) by proteolytic cleavage from its precursor pro-IL-1. Different families of inflammasomes recognize different danger signals or PAMPs through their respective NLR²⁸⁻³⁰. For example, NLRP3 inflammasome is activated by bacterial exotoxins and viroporins³¹. The binding of PAMPs to PRRs leads to the triggering of orchestrated signalling pathways. The signals are transmitted through a series of adaptor molecules such as myeloid differentiation primary response 88 (MyD88), TIR-associated protein (TIRAP), MyD88-adaptor-like (MAL), TIR-domain-containing adaptor protein-inducing IFN- β (TRIF), TIR-domain-containing molecule 1 (TICAM1) and TRIF-related adaptor molecule (TRAM), that determine the specificity of the response^{18,32}. Signal transmission is performed via phosphorylation, ubiquitination, or protein-protein interactions, resulting in the upregulation of transcription factors that regulate the expression of genes that play an important role in inflammation and immune response. Three very crucial regulatory factors of gene expression are nuclear factor kappa-lightchain-enhancer of activated B cells (NF- κ B), mitogen-activated protein kinases

(MAPKs), and interferon regulatory factors (IRFs)^{22,33,34}. NF- κ B and MAPKs are involved in the impairment of proinflammatory response and IRFs are essential for stimulation of the interferon (IFN) production³⁵. The upregulation of gene transcription results in the production of cytokines and chemokines, which cause a local inflammatory response and accumulation of immune cells. Furthermore, the upregulation of the expression of cell adhesion molecules, such as intercellular adhesion molecule-1 (ICAM-1) and E-selectin, leads to cell migration to the site of infection¹⁸. Antigen-presenting cells (APCs) such as mononuclear phagocytes can then migrate from the infection site to secondary lymphoid areas, where they activate the cells of adaptive immunity by cell-cell contacts (i.e. MHC/TCR) and cytokines³⁶.

2.1.1.2 Adaptive Immunity

The adaptive immune system requires the T-lymphocytes, which are produced and selected in the thymus, and the B-lymphocytes, which are produced in the bone marrow and are responsible for antibody production³⁷. After lymphocytes mature in primary lymphoid organs, they migrate to secondary lymphoid organs (lymph nodes, spleen), where they can be activated by antigens after cell-mediated antigen presentation. The adaptive immune response is mediated by the migration of lymphocytes from the spleen and lymph nodes to infection sites and the following pathogen killing, release of chemokines or antibodies³⁸. Various adhesion molecules and chemokine receptors facilitate lymphocyte migration and activation. Mature T cells, found in the thymus, possess a functional T-cell Receptor, which contains Variable (V-), Diversity (D-) and Joining (J-) Segments, encoded by different genes, ensuring large diversity³⁹. T-cells are then activated after the interaction of their TCRs with MHC-presented antigens if in the context of co-stimulatory signals. Mature T-cells express cluster of differentiation 4 (CD4) or cluster of differentiation 8 (CD8), which are the main interaction partners of the major histocompatibility complex (MHC) of APCs. The largest group of T-cells in the body is the CD4+ TCR population, known to have a helper function (T_H cells)⁴⁰. Activated T_H cells produce a range of cytokines. It was shown that there are two main categories of T_H cells, T_{H1} and T_{H2} cells. T_{H1} cells produce IFN- γ and IL-2 and their differentiation is provoked by

IL-12 and IFN- γ effects on naive T_{H0} precursors. T_{H2} cells release IL-4, IL-5, IL-10, and IL-13⁴⁰. The cytokines released from T_{H1} cells cause activation of mononuclear phagocytes, natural killer (NK) cells, and cytotoxic T-cells to destroy intracellular microbes and cells infected by viruses. Cytokines released from T_{H2} cells promote antibody production, hypersensitivity and immunological response against parasitic invasion⁴¹. Natural killer T (NKT) cells are a subset of T cells, which interact with antigens presented by MHC molecules of the CD1 family. NKT cells are characterised by the T-cell expression, containing CD3 and TCR, and NK cell antigens (CD56). Activated NKT cells produce cytokines, e.g., IL-4, rapidly and are involved in allergic pathogenesis⁴². B-Lymphocytes are responsible for the production of antibodies⁴³. Active B-lymphocytes can differentiate into plasma cells, which secrete low-affinity antibodies, or memory cells in a lymph follicle centre by producing IgG, IgA and IgE instead of IgM or IgD^{44,45}. Memory cell development facilitates a faster immune response after the future invasion of the same pathogenic antigens. The production of high-affinity antibodies like IgG, IgA and IgE instead of IgM or IgD is called class-switching and is based on gene rearrangement mechanisms⁴⁶⁻⁴⁸.

2.1.2 Macrophages

Macrophages are essential cells for innate immunity. Their role is to encounter the microbial invasion in closed cavities or organs such as peritoneum, pleura, lung, liver, or barrier surfaces, namely the skin and gut. To successfully minimize the effects of microbial infection and their replication, macrophages interact with immune cells such as dendritic cells, neutrophils, and NK-Lymphocytes. A major characteristic of macrophages is abundant the presence of PRRs, as mentioned above, to recognize pathogen patterns (PAMPs). The initiation of the immune response, engaging both innate and adaptive immunity, is described above and is facilitated by cytokine expression and direct contact between pathogen patterns and innate and adaptive immune cells.⁴⁹

The primary defence mechanisms of macrophages are based on phagocytosis through bacterial lysosome elimination and the production of bactericidal reactive oxygen species (ROS) and nitrite oxide (NO)⁵⁰. In addition, macrophages serve as antigen-presenting

cells, interacting with T_H cells-TCR via MHC-II antigen presentation⁵¹. Macrophages produce various chemokines and cytokines⁵², facilitating the involvement of other innate or adaptive immune cells in the inflammatory response against microbial infection. Tissue macrophages, such as alveolar macrophages in the lung, are derived from erythro-myeloid progenitors from the yolk sac without connection with hematopoietic stem cells. A vast majority of macrophages are derived from the bone marrow's myeloid colony-forming unit (M-CFU)⁵³.

Macrophages are heterogeneous and can polarize into distinctive phenotypes: M1-Macrophages, which are activated after stimulation with bacterial LPS or IFN- γ , and M2-Macrophages, which are further divided into various subgroups like M2a after stimulation with T lymphocyte-derived IL-4, M2b, after stimulation with LPS + IL-1 β or immune complexes + IL-1ra, and M2c, derived after stimulation with TGF- β and IL-10⁵⁴.

M1 macrophages have a pro-inflammatory role. They destruct microbial invasion by phagocytosis, and their aim is the elimination of pathogen via ROS and NO release⁵⁵. NO is produced under the catalytic action of nitric oxide synthase (iNOS), an enzyme used to quantify the M1 polarization³¹. Living microbes or pathogen released proteins are taken up in endolysosomes via phagocytosis or pinocytosis, where high acidic concentrations and proteolytic enzymes ensure their destruction. The resulting fragments are processed and presented to the MHC II complex on the cell surface, enabling the interaction with adaptive immune cells.

M2 macrophages possess anti-inflammatory functions and promote wound healing. M2 macrophages release IL-10, which has autocrine and paracrine effects. IL-10 inhibits a subset of inflammatory genes of macrophages and enables a decrease in the production of regulating factors such as cytokines released by T_{H1} cells⁵⁶.

Following microbial invasion, neutrophils are chemotactically attracted to the site of infection, followed by M1-polarizing macrophages, whose actions orchestrate the inflammatory response with the goal of pathogen elimination. If successful, the number of pathogens decreases, enabling the development of M2 macrophages to reduce inflammation and promote the elimination of dead neutrophils and macrophages.

2.1.3 Toll-like receptors and signalling

Toll-like-receptors (TLRs) belong to pattern recognition receptors and interact with PAMPs, including cell wall components, genetic information (DNA), peptides, and toxins, released from bacteria, viruses, fungi, and parasites²⁰. TLRs are localised in membranes and composed of a leucine-rich external domain, which interacts with PAMPs and an intracellular Toll-IL-1 receptor (TIR), which initiates signalling after activation.

TLRs can be found on the outer cell membrane, acting as cell receptors for extracellular pathogens or pathogen virulence mediators or in the cytosol, enabling the initiation of immunity against intracellular pathogens. There exist 10 known human TLRs and 13 mouse TLRs.^{20,21,35} Some TLRs can bind more than one pathogen-related pattern. Cell surface-bound TLRs include TLR1, TLR2, TLR4, TLR5, and TLR6. TLR3, TLR7, TLR8, and TLR9, TLR11 are found in the intracellular membranes to facilitate the recognition of nucleic acids derived from viruses or components of intracellularly replicated bacteria or parasites²¹.

The interaction of TLRs with the appropriate PAMPs leads to signalling activation to initiate the immune response. TLRs signalling is promoted mainly by two pathways: MyD88 and TIR-domain-containing adapter-inducing interferon- β (TRIF)²⁰. Most Toll-like receptors (TLR7, TLR8, TLR9, TLR11, TLR12, TLR13, and heterodimers TLR2/1 and TLR2/6) use MyD88 as signal initiator, while TLR3 utilises TRIF²². TLR4, the TLR receptor which interacts with LPS, activates both signalling pathways stated above. TLR5 uses mainly the MyD88 signalling pathway. Most TLRs (except TLR3) and members of the IL-1 receptor family signal via MyD88, which results in NF- κ B and MAP kinase activation³⁴. Alternatively, TLR3 and TLR4 utilize TRIF to activate NF- κ B and IRFs to induce type I IFN and inflammatory cytokine production. Additionally, TLR2 and TLR4 use TIRAP to recruit MyD88^{57,58}.

After interaction with bacterial LPS, under the catalytic action of LPS binding protein (LBP) and CD14,⁵⁹ TLR4 signals via MyD88 dependent and TRIF dependent pathways. The early response via MyD88 pathway activation results in the activation of mainly pro-inflammatory genes such as CXCL1, CXCL2, TNF- α , and IL-1 β via mitogen-activated protein kinase (MAPK) and NF- κ B pathway. This is known as the early LPS induced TLR4 response⁶⁰.

Following the endocytosis of the TLR4-LPS-CD14 complex, TRIF signalling is initiated, which causes the induction of CCL5, CXCL10, IFIT1, IFIT2, OASL1, and MS4A4C, as well as many other genes. TRAM-TRIF– dependent signalling pathway activates IRF3, facilitating the production type I IFNs. Type I IFNs (IFN α/β) promote interferon-stimulated genes (ISG) through Jak-STAT signalling. The activation of IFN β signalling after LPS induction promotes the macrophage inflammatory responses by inducing nitric oxide synthase (iNOS), IL-12 (p40), and the signal adaptor MyD88^{61,62}.

2.1.4 Cytokine release and inflammatory response

Cytokines are proteins produced by immune cells during the initiation of the immune response. They are often divided into pro-inflammatory, anti-inflammatory cytokines and chemokines⁶³. To the pro-inflammatory mediators belong, for example, Interleukin 1 (IL-1), Interleukin 6 (IL-6), Interleukin 8 (IL-8), Interleukin 12 (IL-12), tumour necrosis factor-alpha (TNF- α), and Interferon-gamma (IFN- γ). The group of anti-inflammatory cytokines contains transforming growth factor-beta (TGF- β), Interleukin 4 (IL-4), Interleukin 9 (IL-9), Interleukin 10 (IL-10), Interleukin 11 (IL-11), Interleukin 13 (IL-13). Soluble tumour necrosis factor inhibitors, soluble IL-1 receptors, IL-1 receptor antagonist and IL-18 binding protein are also thought to act as anti-inflammatory agents⁶⁴.

Pro-inflammatory mediators are released to engage more immune cells in the battle against infectious microbes, resulting in a profound inflammatory response. To prevent an inadequate hyper-inflammatory response with tissue injury, the immune system induces the production of anti-inflammatory mediators. A dysregulated balance of pro-inflammatory and inflammatory mediators can negatively affect the outcome of infection⁶³. The dominance of the release of pro-inflammatory cytokines after initiation of immune responses could lead to a hyper-inflammation, known as systemic inflammatory response syndrome (SIRS), which may lead to cardiovascular decompensation, shock, organ dysfunction and ultimately death. An overflow of anti-inflammatory agents results in the compensatory inflammatory response syndrome (CARS), which causes immune decompensation and failure to fight infection, leading to sepsis and death. An imbalanced production of mediators favouring either pro-inflammatory or anti-inflammatory cytokines

can often cause failure in fighting the infectious agent and increase the risks for morbidity and mortality⁶⁵.

Studies with sepsis mouse models and clinical data from septic patients document substantial increases of pro-inflammatory cytokines in blood and lavage fluids during the first hours of sepsis^{66–68}. An overload of pro-inflammatory mediators, mostly IL-6, TNF- α , IL-1, IFN- γ , was correlated with high sepsis severity and increased mortality. For this reason, many cytokines were proposed as prognostic factors for sepsis outcomes⁶⁶. For example, IL-6 is routinely used as a marker of neonatal infection and sepsis⁶⁹. Furthermore, the role of anti-inflammatory cytokines during CARS was investigated in mouse sepsis models. It was suggested that high levels of anti-inflammatory cytokines during ongoing bacterial sepsis increase the risk of progression to lethal septic shock with increased levels of bacterial CFUs due to immunosuppression^{70,71}.

2.1.5 Chemokines and inflammatory response

Chemokines are chemotactic cytokines. Chemokines are small proteins, that play an essential role in the development, homeostasis and regulation of the innate and adaptive immune system⁷². Chemokines are divided into four groups according to the position of their disulfide-bond forming cysteine residues: XC, CC, CXC, CX3C⁷³. The development of immune cells in the bone marrow is guided by CXCL12/CXCR4⁷⁴. During acute bacterial infection or stimulation with bacterial lipopolysaccharide of gram-negative bacteria, tissue resident cells of the innate immune system, e.g. macrophages, produce chemokines to recruit other immune cells. For example, in mast-cell deficient mice, CXCL1 (GRO- α , mouse KC), CXCL2 (Gro- β , mouse MIP-2), CXCL8 (IL-8), CCL2 (MCP-1), CCL3 (MIP-1 α), CCL4 (MIP-1 β), CCL5 (RANTES) was produced by tissue macrophages⁷⁵. In contrast, mast cells showed production of CCL2, CCL3, CCL4, CCL5, CCL20 (MIP-3 α), CXCL1, CXCL2, CXCL8, CXCL9 (Mig), CXCL10 (IP-10), CXCL11 (I-TAC) after stimulation with bacterial LPS⁷⁵. These chemokines attract neutrophils, macrophages, lymphocytes and facilitate their migration to the site of infection. In vivo experiments showed that CC chemokine receptors (CCR1, CCR2, and CCR5) are found on PMN, macrophages, T-cells, lymphocytes, and mast cells⁷⁶. In addition, chemokines

can augment the production of cytokines during sepsis. For example, CCL2 (MCP-1) and CCL3 (MIP-1 α) induced the production of pro-inflammatory IL-6 in PMN cells.⁷⁷

2.1.6 The role of nitric oxide (NO)

Nitric oxide (NO) is produced through the enzymatic catalysis of NO synthase (NOS). There are three isoforms of NO-Synthase: endothelial NOS (eNOS), inducible NOS (iNOS), and neuronal NOS (nNOS)⁷⁸. NO is a water-soluble gas that regulates blood pressure and blood flow distribution. It also plays a role in the inactivation of oxygen free radicals, prevention of microvascular thrombosis by inhibiting platelet aggregation and leucocyte adhesion⁷⁹. In endotoxemia and CLP-induced sepsis of mice, it was found that iNOS production was induced, resulting in higher levels of NO⁷⁹. NO production mediated subsequent sepsis-induced hypotension, cardiodepression, and vascular hyporeactivity. Furthermore, LPS released after gram-negative bacterial infection and sepsis induced iNOS through cytokines release. For example, TNF- α , IL-1, and IFN- γ induced iNOS in the endothelium, vascular smooth muscle cells, macrophages, and different parenchymal cells^{78,80,81}. On the one hand, the release of NO from macrophages during sepsis aims to achieve pathogen eradication. On the other hand, an overload of NO may contribute to tissue injury. A synergistic effect of eNOS and iNOS in neutrophil migration was observed in sepsis-associated acute lung injury^{82,83}. Inorganic polyphosphates of a chain length from 14-130 Pi suppressed the production of iNOS and thus NO after LPS-induced endotoxemia in peritoneal macrophages⁵.

2.2 Sepsis and septic shock

2.2.1 Definition of sepsis and septic shock

According to the sepsis guidelines of 2016, sepsis is defined as a “life-threatening organ dysfunction caused by the dysregulated host response to infection”⁸⁴. The clinical diagnosis of sepsis is based on the presence of an infection and the clinical assessment of Sequential (Sepsis-related) Organ Failure Assessment Score (SOFA-Score)⁸⁵. Septic shock is defined as a “subset of sepsis with particularly profound circulatory, cellular, and

metabolic abnormalities associated with a greater risk of mortality than sepsis alone”⁸⁴. Septic shock is described by “Vasopressor requirement, required to maintain a MAP of >65 mm Hg and a serum lactate level >2 mmol/L in the absence of hypovolaemia”^{86,87}. The new definition for septic shock identifies patients with in-hospital mortality of >40%^{87,88}.

The current definition of sepsis was published in 2016 based on the work of a sepsis task force. The main evaluation instrument is the SOFA Score assessment to describe the organ manifestation and characterise a critically ill patient. For example, a SOFA-Score ≥ 2 Points indicates that a patient has a 2-25-fold mortality risk. Additionally, the quick SOFA-Score (qSOFA) assessment was proposed for quick bedside-evaluation purposes of possibly septic patients⁸⁴.

2.2.2 Incidence and mortality of sepsis

Sepsis remains one of the most common causes of multi-organ failure and mortality. The treatment of sepsis causes a cost explosion because of the interventional intensity. Although sepsis is one of the most common reasons for patients' death, the incidence figures and clinical data in many countries were not well assessed and analysed. The annual incidence of sepsis in the USA rose from 221 per 100,000 persons in 2000 to 377 per 100,000 in 2008, causing the death of more than 200,000 people in 2007⁸⁹. The annual cost of sepsis patients' treatment was estimated at 22.2 billion dollars in 2011⁹⁰. A global, multinational study analysed data across 195 countries and territories from 1990 to 2017 to estimate the worldwide incidence and mortality of sepsis⁹¹. It showed a decrease in sepsis cases from 60.2 million patients in 1990 to 48.9 million in 2017. The corresponding age-standardised incidence numbers decreased from 1074,7 per 100,000 persons in 2000 to 677.5 per 100,000 persons in 2017. The mortality rate fell from 15.7 million in 1990 (29.1% of total cases) to 11 million deaths in 2017 (20.1% of total cases). Countries with a lower socio-demographic index (SDI) had higher age-standardised incidence and mortality rate of sepsis patients ⁹¹.

An analysis of patient data using DRG (diagnosis-related-groups) statistics from all hospitals participating in the DRG system showed an increase in sepsis cases from

200,535 to 279,530 from 2007 to 2013 in Germany⁹². The annual incidence rose from 256 to 335 cases per 100,000 persons. Among all septic cases, 27% of patients had severe sepsis in 2007 compared to 41% in 2013. Although the annual incidence numbers increased, the mortality rate fell from 27% of all cases in 2007 to 24.3% in 2013⁹².

E. coli infection is one of the most common causes of bacteremia and sepsis. In 2001 approximately 40 000 deaths in the USA were related to *E. coli* sepsis, corresponding to 17% of all sepsis deaths⁹³. Furthermore, *E. coli* is the most common Gram-negative bacterium associated with early-onset neonatal sepsis⁹⁴. Pathogenic *E. coli* cause intestinal and extraintestinal infections, which progress to sepsis^{95,96}. *E. coli* bacteria can be divided into four main groups (A, B1, B2, D). The most virulent extraintestinal pathogenic *E. coli* strains belong to groups B2 and D⁹⁷, but all strains possess virulence factors^{98,99}, that augment the inflammatory response and influence the outcome of *E. coli* sepsis¹⁰⁰. In the past decades, there was an increase in antibiotic resistance of *E. coli* isolates in both adult¹⁰⁰ and newborn¹⁰¹ patients, which is believed to be associated with phylogenetic group and virulence factors. A prospective clinical study showed that the presence of virulence factor papGIII and septic shock is associated with higher mortality rate¹⁰².

2.2.3 The pathomechanism of sepsis

In sepsis, the inflammatory response begins after the binding of PAMPs to cell-surface bound PRRs and intracellular PRRs, which initiates signal transduction pathways. Gene regulators such as NF- κ B, MAPKs, IRFs are activated and upregulate the transcription of genes, that are involved in inflammation, such as TNF- α , IL-1, IL-8, IL-12, and type I IFNs, which promote the activation of other cytokines, chemokines and other components of the innate and the adaptive immune system³³. For example, LPS-triggered activation of NF- κ B pathway promotes the transcription of genes responsible for the production of adhesion molecules¹⁰³, pro-inflammatory cytokines¹⁰⁴ and tissue-factor (TF)^{105,106}, the initiator of the extrinsic system of blood clotting pathway. As a result, cell adhesion and vascular permeability increase and endothelial cells change to a pro-coagulant state¹⁰⁷. Furthermore, complement system activation results in a generation of complement anaphylatoxins such as C3a, C5a¹⁰⁸. C5a acts as a chemoattractant for neutrophils and

macrophages, enhancing the oxidative burst and as a regulator for chemokine and cytokine release¹⁰⁹. These characteristics of C5a are believed to contribute to tissue injury, vasodilatation and amplification of the inflammatory response, which are often related to organ failure¹⁰⁹. Experimental studies showed that blockade of C5a has improved the outcome of sepsis^{110,111}. As sepsis progresses, the hyperinflammatory state is often followed by a state of immunosuppression, especially in the late phase of sepsis, which results in an increase of bacteremia in blood cultures and opportunistic infections¹¹². Moreover, sepsis negatively influences the adaptive immunity. The analysis of blood cells of patients, that underwent sepsis, showed an increase in the numbers of an immature neutrophil phenotype with impaired phagocytic capacity¹¹³, a downregulation of monocyte cytokine production¹¹⁴ and elevated numbers of neutrophil-like myeloid-derived suppressor cells (MDSCs)¹¹⁵. MDSCs release anti-inflammatory cytokines such as IL-10, TGF β , reducing further the inflammatory response, resulting in poor sepsis outcome¹¹⁵. Sepsis also causes a reduction of the expression of the activating MHC-II component human leukocyte antigen D-related (HLA-DR), and an increase in the expression of the T-cell protein programmed death ligands 1 and 2 (PD-L1, PD-L2) by APCs. PD-L1 and PD-L2 bind to the inhibitory programmed death proteins 1 and 2 (PD1, PD2) receptors respectively, causing a further suppression of T-cell function^{112,116}. Immunosuppression and reduced pro-inflammatory and TH1 cytokine production by lymphocytes during the sepsis was confirmed by comparing spleen cell samples of septic against control patients¹¹². Apoptosis of lymphocytes during sepsis was unfavourable for the sepsis outcome^{117,118}, as lymphocytopenia increases overall mortality and could be used as a negative predictive factor of survival rate¹¹⁹.

Sepsis is often associated with multiple organ dysfunctions. The myocardial failure after myocardial depression with consecutive reduced ejection fraction¹²⁰ and hypoxia-induced tissue injury¹²¹ result in hypoperfusion and cardiovascular shock. Hypoperfusion results in a reduced blood flow to the kidneys, resulting in kidney failure¹²². Disseminated intravascular coagulation (DIC) is one of the most critical complications of sepsis. DIC has two clinical manifestations: a severe bleeding disorder due to excessive fibrinolysis and excessive thrombosis/embolism in small and medium blood vessels, which may progress to gangrene of the extremities¹²³.

2.2.4 Sepsis interventional management

Because sepsis can progressively lead to multi-organ failure and death, a quick reaction standardised protocol was needed to reduce the mortality rate and improve overall outcome. Therefore, the European Society of Critical Care Medicine, the International Sepsis Forum, and the Society of Critical Care Medicine collaborated and published the Surviving Sepsis Campaign (SSC). The first recommendations in the form of guidelines for sepsis interventional management were released in 2004, revised in 2008, and in 2012¹²⁴. The latest publication for sepsis and septic shock treatment for adult patients was published in 2016¹²⁵ and for children in 2020¹²⁶.

2.2.5 Murine sepsis models and evaluation of septic infection

Animal sepsis models are indispensable to imitate and further investigate sepsis at an experimental level. The animals that are mainly studied are rodents. Various models of sepsis are based on different principles¹²⁷. Among them, the most frequent were the LPS-endotoxemia shock model, the sepsis model after intravascular injection of live bacteria, and the peritonitis sepsis model^{127,128}. The murine peritonitis model could be caused after cecal ligation and puncture or after intraperitoneal fecal slurry injection or after live bacterial challenge or after the implantation of a bacteria-containing fibrin clot in the peritoneal cavity¹²⁷. Cecal ligation and puncture was thought to be the gold standard of peritonitis models due to the simplicity and the resulting mortality rate¹²⁹. In addition to those models, there are models imitating meningitis, pneumonia, and lung injury. Each of the models mentioned above was well investigated and allowed assumptions regarding animal sepsis. Still, the conclusions about such a complicated procedure as human sepsis were limited and critically seen¹³⁰.

The evaluation and quantification of sepsis and inflammatory response resulted in the development of scoring systems. The clinical status of mice with sepsis is evaluated by various parameters such as mouse appearance, activity, response to stimulus and respiration rate^{131,132}. The quantification of the bacterial load is defined by estimating the bacterial colony-forming units in blood or tissue or by bacterial 16sRNA quantification. The

levels of pro-inflammatory (IL-1 β , IL-6, TNF- α) and anti-inflammatory (IL-10) cytokines or inflammatory chemokines (MCP-1, IL-8) could be a part of the multi-biomarker approach for the estimation of sepsis severity and outcome¹³³.

2.2.6 Human endotoxemia experiments

E. coli-derived LPS injection was also performed in randomised control studies in healthy patients to test the effect of LPS-endotoxemia on humans and possible treatment methods. LPS-endotoxemia caused activation of p38 and p42/44 MAPK, but not of c-Jun N-terminal Kinase ((JNK)¹³⁴. Pre-treatment of the patients with recombinant IL-10 reduced LPS-induced activation of coagulation and fibrinolysis¹³⁵, whereas pre-treatment with prednisolone after LPS-injection resulted in a decrease of biomarkers released during human endotoxemia¹³⁶.

2.3 Inorganic polyphosphates

2.3.1 Introduction – a polymer with many functions

Inorganic polyphosphates are a polymer built up from phosphate monomers bound together by high-energy phosphoanhydride bonds. Polyphosphates can be found in all organisms, prokaryotes and eukaryotes¹³⁷. Furthermore, inorganic polyphosphates exist as a free macromolecule in rock formations, areas of geothermic activity and wastewaters. The concentration and chain length of inorganic polyphosphates differs between various species and organisms. While mammalian cells have granules that contain polyphosphate polymers of up to 100 monomers, microbes accumulate polyphosphates with a length of hundreds to thousands of monomers^{138,139}. The molar quantities of inorganic polyphosphates are often expressed as phosphate monomer concentration (Pi) because of limitations in detection methods and chain-length variations. This normalization method was applied for this dissertation.

During the past decades, a growing body of research was conducted in the field of inorganic polyphosphates. A. Kornberg described this polymer as a "molecule for many reasons"¹³⁹. Figure 1 shows a schematic representation of inorganic polyphosphates and

the action of microbial PolyP metabolising enzymes, polyphosphate kinase (Ppk), and exopolyphosphatase (Ppx).

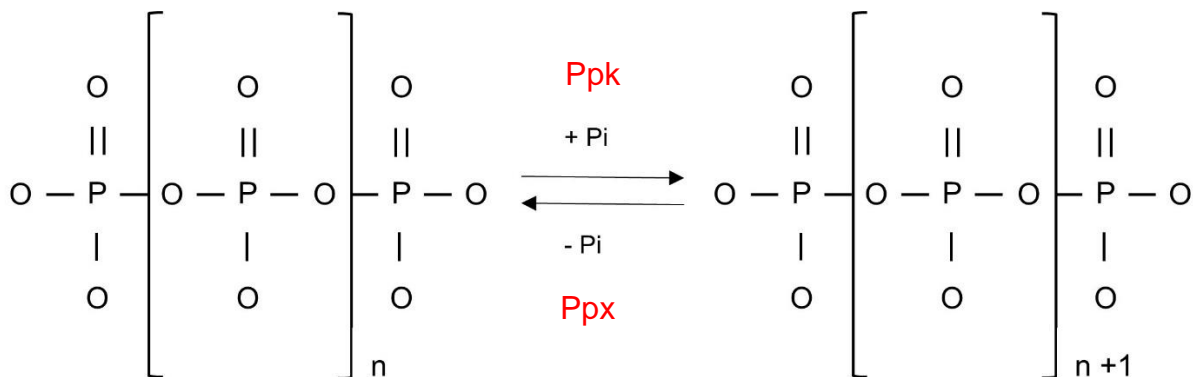


Figure 1: Schematic representation of inorganic polyphosphate polymer and its metabolism as regulated by Ppk and Ppx enzymes.

(modified from A. Kornberg, “Inorganic Polyphosphate: Toward Making a Forgotten Polymer Unforgettable”) ¹³⁹

2.3.2 PolyP in diverse organisms

Inorganic polyphosphates can be found in prokaryotes (bacteria), small eukaryotic cells (fungi), and mammalian cells such as platelets.

Bacterial polyphosphates consist of chains containing up to hundreds to thousands of monomers. Inorganic polyphosphates have an essential role in the survival and virulence of bacterial organisms. Studies on the biochemical activities, including inorganic polyphosphates, revealed that PolyP are a potential phosphate donor to AMP and ADP, resulting in ADP and ATP production, respectively, in bacteria and yeast^{140,141}. Inorganic polyphosphates were also found to act as a metal chelator in bacterial¹⁴² and yeast cells¹⁴³ and as a buffer during alkaline stress in algal cells¹⁴⁴.

Inorganic polyphosphate granules are a phosphate reservoir. PolyP metabolism is regulated by bacterial/yeast metabolising enzymes, based on the conditions that promoted either anabolism or catabolism. Polyphosphate kinases (Ppk) catalyse the addition of phosphate to the polyphosphate granules in a reversible reaction. The polyphosphatases catalyse the hydrolysis of phosphate groups or short-chain PolyP from PolyP. There are two well-studied types of bacterial polyphosphate kinases.

Polyphosphate kinase 1 (Ppk1), which is ATP dependent, and polyphosphate kinase 2 (Ppk2), which is ATP/GTP dependent¹⁴⁵. Polyphosphatases are found in prokaryotic and eukaryotic cells, where PolyP play an important metabolic role. There are two main groups of polyphosphatases: The exopolyphosphatases, which catalyse the breakdown of phosphate groups from terminal ends of PolyP, and the endopolyphosphatases, which catalyse the digestion of PolyP chains into smaller chains^{146,141,147}.

Inorganic polyphosphates and their metabolism play a vital role in many bacterial cells. The survival and virulence of bacteria seem to be directly dependent on PolyP metabolism, especially under stress conditions, including starvation and toxic reagents such as hypochlorite acid. Mutant bacterial cells of *Escherichia coli*, *Pseudomonas aeruginosa*, *Shigella flexneri*, *Salmonella enterica* serovar, and *Mycobacterium tuberculosis*, lacking Ppk, were described to display variable defects in growth rates, reduced heat/acid resistance, and reduced virulence, including mobility, biofilm formation, stringent response, and stress response^{148–155}. Moreover, inorganic polyphosphates have a chaperone-like function by stabilising unfolded bacterial proteins in wild-type and Ppx-deficient *E. coli* (thus longer PolyP chains), compared to Ppk-deficient (lacking PolyP) bacteria under stress conditions using hypochlorite acid and antibiotic treatment during in vitro experiments¹⁵⁶. Long starvation period as stress factor resulted in the accumulation of PolyP granules¹⁵⁷. Finally, it was shown that *Pseudomonas aeruginosa* mutant strains lacking Ppk1 and Ppk2 are more susceptible to antibiotic treatment, concluding that PolyP and their metabolism influences not only the virulence of bacteria but also the sensitivity of bacteria against antibiotic treatment¹⁵⁸. On the other side, investigations regarding the exopolyphosphatase activity indicated that loss of Ppx activity in *Neisseria meningitis* mutants provided resistance against complement attack and killing¹⁵⁹.

2.3.3 The effect of PolyP on blood coagulation in mammalian species

Inorganic polyphosphates with chain lengths of 70-75 Pi were biochemically identified in dense granules (also called δ -granules) of human platelets at a concentration of approximately 130 mM PolyP¹⁶⁰. Polyphosphate granules showed a similarity with acidocalcinosomes. Following thrombin exposure, PolyP were released, suggesting that platelet-derived polyphosphates could be involved in hemostasis¹⁶⁰. PolyP have a half-

life of approximately 90 minutes in blood plasma after release from granules due to degradation from plasma phosphatases. In further studies, it was found that PolyP can modulate and promote blood coagulation¹⁶¹.

Blood coagulation can be activated via two pathways, the intrinsic (also called contact pathway)¹⁶² and the extrinsic pathway (also called tissue factor pathway)¹⁶³, which merge into a common path of the conversion of prothrombin (Factor II, FII) into thrombin (FIIa). Thrombin cleaves fibrinogen into fibrin, resulting in the formation of a blood clot. The extrinsic pathway is initiated by the presence of tissue factor after injury and plays a crucial role, for example, after trauma. Infectious diseases can result in the activation of the contact pathway and progression into a coagulopathy¹⁶⁴.

The contact pathway is initiated when Factor XII (FXII) becomes activated to factor XIIa (FXIIa) in the presence of kininogen and kallikrein. FXIIa then activates Factor XI into Factor XIa, which activates Factor IX, resulting via contact pathway to the activation of Factor V (FV). Activation of the contact pathway also leads to the release of vasoactive and pro-inflammatory proteins of the kallikrein-kinin-system¹⁶². Inorganic polyphosphates bind to FXII activating proteins, thus promoting the initiation of the contact pathway¹⁶⁵. Simultaneously, S-PolyP, released from platelet granules, act as a cofactor for the inactivation of the tissue factor pathway inhibitor by activated factor XI¹⁶⁶. Inorganic polyphosphates accelerate the activation of factor V in the presence of activated factor X (FXa) and promote thrombin-mediated activation of factor XI and factor V¹⁶⁷. PolyP also increase the stabilisation of formed blood clots and protects them against fibrinolysis¹⁶⁸. FXII autoactivation amplifies the activation of the contact pathway and is triggered by inorganic polyphosphates. Long-chain polyphosphates were found to be a more potent amplifying procoagulant factor of FXII-autoactivation and FXIIa-mediated initiation of the contact pathway than S-PolyP. Nonetheless, S-PolyP resulted in an accelerated FXa activated coagulation in normal and FXII-deficient blood plasma and antagonised the action of tissue factor pathway inhibitor (TFPI)¹⁶¹.

In contrast, platelet-derived polyphosphates were found to have anticoagulative activities. The presence of short-chain PolyP led to delayed fibrin polymerisation times and alteration of the blood clot properties after evaluation using electron microscopy¹⁶⁹. Another study revealed that platelet-derived PolyP and FXII colocalize on the activated

platelet membrane and increase the affinity of tissue plasminogen activator (tPA), resulting in augmented fibrinolysis¹⁷⁰. Hence, while PolyP act predominantly pro-coagulatory, so anti-coagulatory effects seem to exist.

2.3.4 Interaction of PolyP with inflammatory mediators

The effects of inorganic polyphosphates in prokaryotes were described above. In this chapter, I will focus on the role of polyphosphates during inflammation in mammalian cells. PolyP activate the FXIIa/kallikrein-kinin axis, which is an intersection of coagulation and inflammation, supporting the idea that PolyP controls inflammatory processes^{171,172}. The activation of the kallikrein-kinin system causes the generation and release of bradykinin. Bradykinin acts as a vasodilator and increases vascular permeability, leading to septic shock. Furthermore, bradykinin induces the production and release of nitric oxide and prostacyclin, after binding to its receptor¹⁷³.

Short-chain polyphosphates, derived from platelets, were described to play a pro-inflammatory role by increasing endothelial leakage, promoting leukocyte migration in the peritoneal cavity after i.p polyphosphate injection, enhancing apoptosis, and increasing the production of the adhesion molecules vascular cell adhesion molecule-1 (VCAM-1), intercellular adhesion molecule-1 (ICAM-1) and E-selectin on endothelial cells. These effects of polyphosphates are mediated through the modulation of the NF- κ B pathway¹. Furthermore, it was proposed that these pro-inflammatory effects were related to the interaction of S-PolyP with histone H4, the high mobility box group 1 (HMGB1) and the receptors purinergic receptor Y1 (P2Y1) and receptor for advanced glycation end products (RAGE)³. Interestingly long-chain polyphosphates were found to have a higher binding affinity to these receptors than short-chain polyphosphates¹⁷⁴. In the same study, activated Protein C (APC) reduced the pro-inflammatory effects of inorganic polyphosphates¹⁷⁴. Inorganic polyphosphates, both S-PolyP and L-PolyP, activate the mammalian target of rapamycin complexes 1 and 2 (mTORC1, mTORC2) through interaction with RAGE and P2Y1 receptors³. Activation of mTORC1 led to phosphorylation of p70S6K and activation of the NF- κ B pathway, whereas activation of mTORC2 increased barrier leakage in vascular endothelial cells³.

Inorganic polyphosphates were detected in both mast cells and basophils. In both cell types, the length of detected polyphosphate was similar to the length of platelet-derived PolyP, approximately 60 Pi Units. Polyphosphate granules were co-localized with serotonin granules¹⁷⁵. IgE activation caused a simultaneous release of serotonin and polyphosphates. The role of polyphosphates derived from mast cells was not specified, but it was thought to support mast cells in their pro-inflammatory and procoagulant function¹⁷⁵. Based on the observation that *N. meningitidis* mutants, lacking Ppx and therefore having longer PolyP chains, were resistant to complement killing¹⁵⁹, the effect of inorganic polyphosphates on the complement system was investigated. Polyphosphates of medium and long size interacted with magnesium and calcium cations resulting in a destabilisation of the C5b/C6 complex and therefore in a downregulation of the complement system response through the terminal pathway⁴. The destabilisation of the C5b/6 complex results in a not-optimally formed membrane attack complex C5b-C9, which lacks lytic and phagocytotic potential, suggesting that platelet-derived polyphosphates could play a protective role for platelets against complement activation. Polyphosphates of approximately 120 Pi interacted as a cofactor with C1 Esterase inhibitor (C1INH) and its target C1s, resulting in the inhibition of complement activation via the classical pathway¹⁷⁶. Recent studies suggested that short-sized polyphosphates trigger neutrophil activation and induce the formation of neutrophil extracellular traps (NETs) and autophagy by cultured cells. NET formation and PolyP action were reduced in the presence of IL-29 (Interferon- λ) both in vitro and in vivo¹⁷⁷. The exact mechanism of PolyP-mediated NET formation is presumably mediated by activation and dephosphorylation of mTOR.

In addition, inorganic polyphosphates counteracted the gene expression of iNOS by peritoneal macrophages after LPS/TLR4-activation⁵. The exact mechanism was not yet described, but a correlation between PolyP and calcium-binding affinity was proposed. PolyP did not affect the TNF- α levels after LPS stimulation, arguing for the specificity of polyphosphate effects⁵. Bacterial-derived L-PolyP downregulated the LPS/TLR4-induced release of IFN β ¹⁷⁸. Short-chain polyphosphates have a binding affinity to the chemokine platelet factor 4 (PF4, CXCL4). After binding of inorganic polyphosphate to PF4, the structural and functional properties are altered, allowing binding of anti-PF4/heparin

antibodies¹⁷⁹. CXCL4 (PF4) is a member of the CXCL4 chemokine family and is released from α -granules during platelet activation. The binding to anti-PF4/heparin antibodies is a pathognomonic event in developing heparin-induced thrombocytopenia (HIT)¹⁸⁰. Moreover, PF4 binds to bacterial surfaces, and such opsonization facilitates pathogen phagocytosis¹⁸¹. The presence of S-PolyP increases the binding affinity of PF4 to bacteria (as demonstrated for *E. coli*) and upregulates phagocytosis, dependent on the soluble polyphosphates concentration¹⁷⁹.

Findings from our research group showed that L-PolyP are an immunoactive metabolite during *E. coli* infection, interfering and reducing the host defence response. L-PolyP affected the macrophage polarisation by decreasing iNOS expression and M1 polarisation, thus favouring M2 polarisation. Additionally, L-PolyP reduced the LPS-induced interferon release. Although the exact mechanism of polyphosphate release from bacterial cells is not known, long-chain polyphosphates were internalised by macrophages and likely to bind to a great number of macrophage proteins¹⁷⁸.

2.3.5 Working Hypothesis

The aim of this study was to investigate the effects of inorganic polyphosphates during sepsis.

The major working hypothesis is that bacteria-derived polyphosphates directly affect the host immune response and the protective immune cell functions during infection.

To test this hypothesis, *Escherichia coli* bacterial strains with different expressions of polyphosphate kinase, Ppk, and exopolyphosphatase, Ppx, resulting in varying levels of inorganic polyphosphates, were used. *Escherichia coli* MG1655, expressing both PolyP metabolising enzymes, was used as wild type, *E. coli* MJG 224 as Δ ppk strain, and *E. coli* MJG 315 as Δ ppx strain. I want to establish a sepsis model using intraperitoneal injection of live bacteria, whose suspension numbers would be calculated via flow-cytometry. The presence of long-chain inorganic polyphosphates, especially in the Δ ppx strain, will impair or improve the overall survival compared to the wild-type and Δ ppk strain. Furthermore, it was hypothesized that the presence of long-chain inorganic polyphosphates would increase pro-inflammatory cytokines and induce thrombosis in our murine models during sepsis.

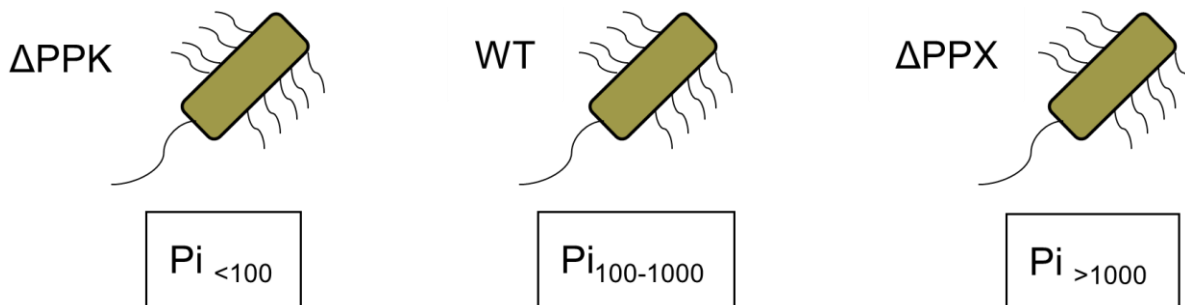


Figure 2: Schematic representation of *E. coli* strains.

E. coli MG1655 as wild-type bacteria with both metabolising enzymes Ppk and Ppx, *E. coli* MJG224 (Δ ppk), lacking Ppk1 thus expressing smaller or no polyphosphate chains, *E. coli* MJG315 (Δ ppx), lacking Ppx, thus expressing longer polyphosphate chains, as described by Gray, M. J. *et al.* Polyphosphate Is a Primordial Chaperone¹⁵⁶

3. Materials and methods

3.1 Material

3.1.1 *Consumable materials*

Table 1: Consumable material

Material	Manufacturer
Bottle top filter (0.22µm, 45mm, CA membrane)	Corning
Cannula (20G, 21G, 23G, 26G, and 30G)	Becton Dickinson
Cell culture flask 182.5 cm²	VWR
Cell culture flask 75 cm²	Greiner Bio-One
Cell lifter (18 cm)	Thermo Fisher Scientific
Cell strainer (100 µm)	Thermo Fisher Scientific
Cover slips	Menzel-Gläser
Cryo freezing container	Nalgene
Cryo tubes	Thermo Fisher Scientific
ELISA plates (96-well, Nunc - MaxiSorp)	Sigma-Aldrich
FACS tubes (5 ml)	Sarstedt
Filter tips (10 µl)	Molecular BioProducts
Filter tips (20, 200, and 1000 µl)	StarLab
Glassware	Schott
HisTrap FF 1ml Column	GE Healthcare
Inoculation loop	VWR
Microtest black (96-well)	Thermo Fisher Scientific
Microtest plate V-bottom (96-well)	Corning
Neubauer (improved) chamber	Brand
PCR-plate (96-well)	Bio-Rad
PCR-strips (0.2 µl with lid)	Thermo Fisher Scientific
PD-10 Desalting Columns	GE Healthcare
Petri dish (6 and 10 cm)	BD falcon
Pipette tips (200, 300, and 1000 µl)	Sarstedt

Pipettes (5, 10, 25, and 50 ml)	Greiner Bio-One
Pipetting basins (25 ml, RNase + DNase free)	VWR
Syringe (1, 10, and 20 ml)	Becton Dickinson
Syringe (2 ml)	Braun B. Melsungen
TC-treated plates (24-, 48-, and 96-well)	Corning
Tubes (1.5 ml, RNase + DNase free)	Sarstedt
Tubes (2 ml)	Sarstedt
Ultra-low attachment plated (24- and 96-well)	Corning
Whatman™ Syringe filter (0.2 µm)	GE Healthcare

3.1.2 Media and buffer

Table 2: Media and buffer

Buffer	Medium Composition / Manufacturer
Cryo-conservation medium	95% (v/v) Growth medium + 5% (v/v) DMSO
BD Cytofix	BD Bioscience
BD Cytofix/Cytoperm	BD Bioscience
BD Perm III	BD Bioscience
Bio-Plex sheath fluid	Bio-Rad
Blood agar plates	BD Bioscience
ELISA reagent diluent (1% BSA)	PBS + 1% (w/v) BSA
ELISA reagent diluent (0.1% BSA)	20 mM Tris base + 150 mM NaCl + 0.1% (w/v) BSA + 0.05% (v/v) Tween® 20
ELISA wash buffer	PBS + 0.05% (v/v) Tween® 20
FACS buffer	0.25% (w/v) BSA + 0.02% (w/v) sodium azide + 2mM EDTA in PBS
HBSS	Gibco
LB (Luria/Miller) medium	1% (w/v) tryptone, 0.5% (w/v) yeast extract, 1%(w/v) NaCl, pH 7.0 from Carl Roth
L929 cell medium	RPMI 1640 + 10% (v/v) FCS + 1% (v/v) P/S

L929 conditioned medium	49% (v/v) RPMI 1640 + 30% (v/v) L929 cell supernatant + 20% (v/v) FCS + 1% (v/v) P/S
Macrophage medium	RPMI 1640 + 0.1% (w/v) BSA + 1% (v/v) P/S
MH-S macrophages growth medium	RPMI 1640 + 10% (v/v) FCS + 1% (v/v) P/S
MLE-12 growth medium	RPMI 1640 + 2%(v/v) FBS + 1%(v/v) P/S + 1%(v/v) HEPES 1M + 1%(v/v) L-Glutamine 200mM + 0,5%(v/v) Insulin–Transferrin–Sodium selenite + 0,05%(v/v) α-Transferrin + 0,01%(v/v) Hydrocortisone 100µM + 0,01%(v/v) β- Estradiol
PBS (10x)	Thermo Fisher Scientific
PBS (1x)	Without Ca ²⁺ or Mg ²⁺ from Gibco
PBS + EDTA	PBS (1x) + 0.5 mM EDTA
Perm/Wash	BD Bioscience
RIPA lysis buffer	Merck Millipore
Rotiphorese® SDS-PAGE electrophoresis buffer	Carl Roth
RPMI 1640	With L-glutamine and 25 mM HEPES from Gibco
Resolving polyacrylamide gel (15%)	15% (v/v) Acrylamide Gel 30, 373 mM Tris (pH 8.8), 0.1% (w/v) SDS, 0.1% (w/v) APS, 0.04% (v/v) TEMED
Stacking polyacrylamide gel (5%)	5% (v/v) Acrylamide Gel 30, 125 mM Tris (pH 6.8), 0.1% (w/v) SDS, 0.1% (w/v) APS, 0.1% (v/v)
TAE buffer	AppliChem
TBE	89 mM Tris, 89 mM boric acid, 2 mM EDTA in ddH ₂ O, pH 8.3
TRIS buffer, pH 7.5	AppliChem

ScPPX purification – binding buffer	50mM Sodium phosphate buffer, 0,5M NaCl, 5mM imidazole (pH=8)
ScPPX purification – elution buffer	50mM sodium phosphate buffer, 0,5M NaCl, 0,5M imidazole (pH=8)
ScPPX dialysis buffer	20mM Tris HCl (pH=7,5), 50mM Kill, 10%(v/v) Glycerol (pH=7,5)
ScPPX activity reaction buffer	50nM HEPES, 175nM KCl, 1mM MgCl ₂ , (pH=8)

3.1.3 Reagents

Table 3: Reagents

Reagent	Manufacturer
123count eBeads™ Counting Beads	Thermo Fisher Scientific
3,3',5,5'-Tetramethylbenzidin (TMB)	eBioscience
4',6-diamidino-2-phenylindol (DAPI)	Sigma-Aldrich
Acrylamide Rotiphorese® Gel 30	Carl Roth
Agar-Agar	Carl Roth
Albumin fraction V (BSA)	Carl Roth
Ammonium persulfate (APS)	AppliChem
Benzonase® Nuclease, ≥250 units/μL S	Sigma-Aldrich
Bovine serum albumin (BSA) 35% (w/v) in DPBS (sterile)	Carl Roth
Bradford Ultra™	Expedeon
Bromphenol blue	Sigma-Aldrich
cOmplete protease inhibitor	Roche
Desderman®	Schülke & Mayr
Dimethyl sulphoxide (DMSO)	Sigma-Aldrich
Distilled water, RNase, and DNase free	Gibco
DL-Dithiothreitol (DTT)	Sigma-Aldrich
EDTA (0.5 M, sterile)	Promega

Ethanol (99.8%)	Carl Roth
Fetal calf serum (FCS)	Sigma-Aldrich
Filter paper	Bio-Rad
Fixable viability dye eFluor™ 780	Thermo Fisher Scientific
Formaldehyde 16% (w/v)	Thermo Fisher Scientific
Glycerol	Carl Roth
Glycine	AppliChem
HEPES	Gibco
Hydrocortisone	Sigma-Aldrich
Imidazole	Sigma-Aldrich
Insulin–Transferin– Sodium selenite	Sigma-Aldrich
Isoflurane	Abbott
Ketamine (50 mg/ml)	Hameln
L- Glutamine solution 200mM	Sigma-Aldrich
Lysozyme from chicken egg white (protein ≥90 %, ≥40,000 units/mg protein)	Sigma-Aldrich
Methanol (99.9%)	Carl Roth
Milk powder (nonfat, dried)	AppliChem
One comp eBeads	Thermo Fisher Scientific
Penicillin-Streptomycin (P/S) (10,000 U/ml penicillin, 10mg/ml streptomycin)	Thermo Fischer Scientific
Phenylmethylsulphonyl fluoride (PMSF)	AppliChem
pH-indicator strips (pH 0-14)	Merck Millipore
Phosphatase inhibitor cocktail 2	Sigma-Aldrich
Precision Plus Protein™ Kaleidoscope™	Bio-Rad
Propan-2-ol (99.8%)	Sigma-Aldrich
RNase AWAY™	Molecular Bioproducts
Rompun® (Xylazine)	Bayer
Roti-Stock SDS (20%, w/v)	Carl Roth

Sodium azide	Sigma-Aldrich
Sodium chloride	Carl Roth
Sodium hydroxide	Merck
Sodium nitrate	Sigma-Aldrich
Sulfuric acid (97%)	AppliChem
Terralin®	Schülke & Mayr
Tetramethylethylenediamine (TEMED)	Carl Roth
TRIS Base	AppliChem
Tris hydrochloride	AppliChem
Trypan Blue (0.4% w/v)	Sigma-Aldrich
Tween® 20	Sigma-Aldrich
Urea	Carl Roth
Xylene cyanol FF	Sigma-Aldrich
α-Transferrin	Sigma-Aldrich
β- Estradiol	Sigma-Aldrich

3.1.4 Assay kits

Table 4: Assay kits

Kit Manufacturer	Kit Manufacturer
BIOMOL® green	Enzo Life Sciences
BD Cell viability kit	BD Science
Bio-Plex Pro™ cell signaling reagent kit	Bio-Rad
Griess Reagent Kit	Thermo Fisher Scientific
iQ SYBR® Green Mastermix	Bio-Rad
Mouse CCL2/MCP1 ELISA	R&D Systems
Mouse CXCL1/KC ELISA	R&D Systems
Mouse CXCL10/IP-10 ELISA	R&D Systems
Mouse CXCL4/PF4 ELISA	R&D Systems
RNase-Free DNase Set Qiagen	Qiagen

RNeasy Mini Kit Qiagen	Qiagen
------------------------	--------

3.1.5 Biochemicals

Table 5: Biochemicals

Substance	Working concentrations	Source
L-PolyP (~200-1300mer)	50 μ M (Pi) <i>in vitro</i> 10 μ g (Pi)/g bodyweight <i>in vivo</i>	Prof. J. Morrissey, Champaign, IL, USA and Kerafast, Inc.
LPS (<i>E. coli</i> 0111:B4)	100 ng/ml	Sigma-Aldrich
S-PolyP (~25-125mer)	50 μ M (Pi) <i>in vitro</i> 10 μ g (Pi)/g bodyweight <i>in vivo</i>	Prof. J. Morrissey, Champaign, IL, USA and Kerafast, Inc.

3.1.6 Cells and *E. coli* strains

Table 6: Cell lines

Cell line	ATCC® identification
L929 fibroblasts	CRL-2648™
MH-S macrophages	CRL-2019™
MLE-12 epithelial cells	CRL-2110™

Table 7: *E. coli* strains

Strain	Genotype Source/Reference
MG1655	F- lambda- <i>ilvG</i> - <i>rfb</i> -50 <i>rph</i> -1 Prof. U. Jakob, Ann Arbor, MI, USA146
MJG224	Δ <i>ppk</i> (based on MG1655) Prof. U. Jakob, Ann Arbor, MI, USA146
MJG315	Δ <i>ppx</i> (based on MG1655)

	Prof. U. Jakob, Ann Arbor, MI, USA146
BL-21	New England Biolabs
MJG317	created after transfection of E. coli BL-21 competent bacteria with plasmid-vector, thus <i>overexpressing ScPPX</i> Prof. U. Jakob, Ann Arbor, MI, USA146

3.1.7 Antibodies

Table 8: Flow cytometry antibodies

Antigen/Isotype	Clone	Conjugate	Manufacturer
CD11b	M1/70	Pacific Blue™	BioLegend
CD206 (MRC1)	C068C2	Phycoerythrin- Cyanine7	BioLegend
CD80	16-10A1	Phycoerythrin	BioLegend
CD86	GL-1	Fluorescein -Isothiocyanate	BioLegend
F4/80	BM8	Allophycocyanin	BioLegend
Hamster IgG	eBio299Arm	Phycoerythrin	Thermo Fisher Scientific
IA/IE	M5/114.15.2	Phycoerythrin	BioLegend
iNOS (NOS2)	CXNFT	Alexa Fluor 488	Thermo Fisher Scientific
Ly6C	HK1.4	Phycoerythrin	BioLegend
Ly6G	1A8	Allophycocyanin	BioLegend
Rat IgG2a, κ	eBR2a	Alexa Fluor® 488	Thermo Fisher Scientific
Rat IgG2a, κ	RTK2758	Allophycocyanin	BioLegend
Rat IgG2a, κ	RTK2758	Fluorescein -Isothiocyanate	BioLegend
Rat IgG2a, κ	RTK2758	Phycoerythrin- Cyanine7	BioLegend
Rat IgG2b, κ	RTK4530	Pacific Blue™	BioLegend

3.1.8 Primers and vectors

Table 9: RT-PCR and qPCR primers and plasmid vectors

Target	(orientation) 5' – 3' Source/Reference
16S rDNA (forward)	GTGSTGCAYGGYYGTCGTCA
16S rDNA (reverse)	ACGTCRTCCMCNCCTTCCTC
GAPDH (forward)	TACCCCAATGTGTCCGTCGTG
GAPDH (reverse)	CCTTCAGTGGGCCCTCAGATGC
iNOS (forward)	TTCTGTGCTGTCCCAGTGAG
iNOS (reverse)	TGAAGAAAACCCCTTGTGCT
PPK forward	ACCGGTACCAAAACGGAGTAAAAGTGGTAATGGG
PPK reverse	CTTAAGCTTTTATTCAGGTTGTTCGAGTGATTTG
PPX forward	TGGCGATTTATGACTACATCAAATCACTCGAACAAC CTGAATAACCCTATGGTGTAGGCTGGAGCTGCTTC
PPX reverse	AAGTGCCTGAATAATGCGGGCCGACATTTCTCGTCG GCCCGCAAAGTATTACATATGAATATCCTCCTTAG
Vector:	pScPPX2

3.1.9 Instruments. Equipment and software analysis

Table 10: Instruments

Instrument	Manufacturer
Accurpette	VWR
ÄKTA Pure chromatography systems	GE Healthcare
Bacterial incubator HERATHERM	Thermo Fisher Scientific
Bio-Plex® 200 System	Bio-Rad
Bio-Plex® HTF	Bio-Rad
Bio-Plex® Pro II Wash Station	Bio-Rad
Cell culture incubator	Memmert
Centrifuge 5417 C/R	Eppendorf
Centrifuge Allegra X-15R	Beckman Coulter
Centrifuge Rotanta/RP	Hettich
FACSCanto II	BD Bioscience
FusionCapt Advance Solo 4	Vilber Lourmat

Gel Doc EZ Imager	Bio-Rad
Mastercycler ProS	Eppendorf
Microscope IX73	Olympus
Mini PROTEAN® Tetra Cell	Bio-Rad
Mixer MTS 2/4	IKA
Nano Drop 2000c	Thermo Fisher Scientific
Nutating Mixer	VWR
Opsys MR	Dynex Technologies
Orbital Shaker	VWR
pH-Meter HI2211 pH/ORP Meter	HANNA instruments
Pipettes	Gilson
Power Pac™ HC	Bio-Rad
Rotating Mixer Multi-1	StarLab
Rotating mixer RM Multi-1	StarLab
Scale AY612	Sartorius
Scale CPA1003P	Sartorius
SpectraMax i3	Molecular Devices
Thermal cycler C1000	Bio-Rad
Thermomixer comfort	Eppendorf
Vortex Genie 2	Scientific Industries
Waterbath	Julabo
Workbench Aura mini	Nunc
Workbench HERA safe	Thermo Fisher Scientific

Table 11: Software

Application (Software)	Version	Source/Reference
Bio-Plex® analyses (Bio-Plex® Manager)	6.1	Bio- Rad
Data depiction / Statistics (GraphPad Prism)	7-9	GraphPad Software Inc.

ELISA analyses (Revelation)	G3.2	Dynex® Technologies
Flow Cytometry Analyses(FlowJo®)	10.0.00003	FlowJo® LLC
qPCR analyses (CFX Manager)	3.1	Bio-Rad
Photometric measurements (NanoDrop)	2000	Thermo Fischer Scientific

3.2 Mouse strains

Table 12: Mouse strains

Strain	Age/Sex	Source
C57BL/6J	8-9 weeks old, males	Janvier

Methods

3.3 In vivo Experiments

3.3.1 *Establishment of live E. coli sepsis model*

For all sepsis experiments, sex- and age-matched, male mice of 8-9 weeks were used. An overnight bacterial culture (B-On) was inoculated in LB growth medium from an E. coli stock. The incubation conditions were set at 37 °C and 200rpm. The next day, a bacterial culture (B1) was inoculated from the overnight culture (B-On) in LB medium in a ratio of 1:100 and incubated under the same conditions. When the OD₆₀₀ of the bacterial suspension (B1) reached 1.2-1.5, it was transferred in a new tube and was centrifuged at 2500G and room temperature (RT). The supernatant was removed, and the bacterial pellet was resuspended in an equal volume of PBS (approximately 35-40ml). The bacterial numbers were counted using flow cytometry using the BD cell viability kit and following the manufacturer's instructions (BD Science). The bacterial cell numbers were estimated using FACS-Flow Cytometry. The bacterial suspension was centrifuged down, the supernatant was removed, and the pellet was resuspended in prewarmed PBS (37 °C) to achieve the CFU numbers per volume as needed. Before the injection, the weight and temperature of the mice were measured. 100µl of the bacteria suspension was carefully intraperitoneally (i.p) injected in each mouse with a 30G-subcutaneous needle, about 1 cm over the left limb. Any injury of the inner and outer body parts was avoided. The injection method is schematically presented in Figure 3.

In survival studies, the clinical status of the mice was observed and documented for seven days, including an evaluation of clinical severity scoring (adopted from Gonert et al.)¹³², weight, and temperature measurements. The clinical assessment of sepsis on different aspects of mouse behaviour was performed using the clinical severity scoring system shown in Table 13.

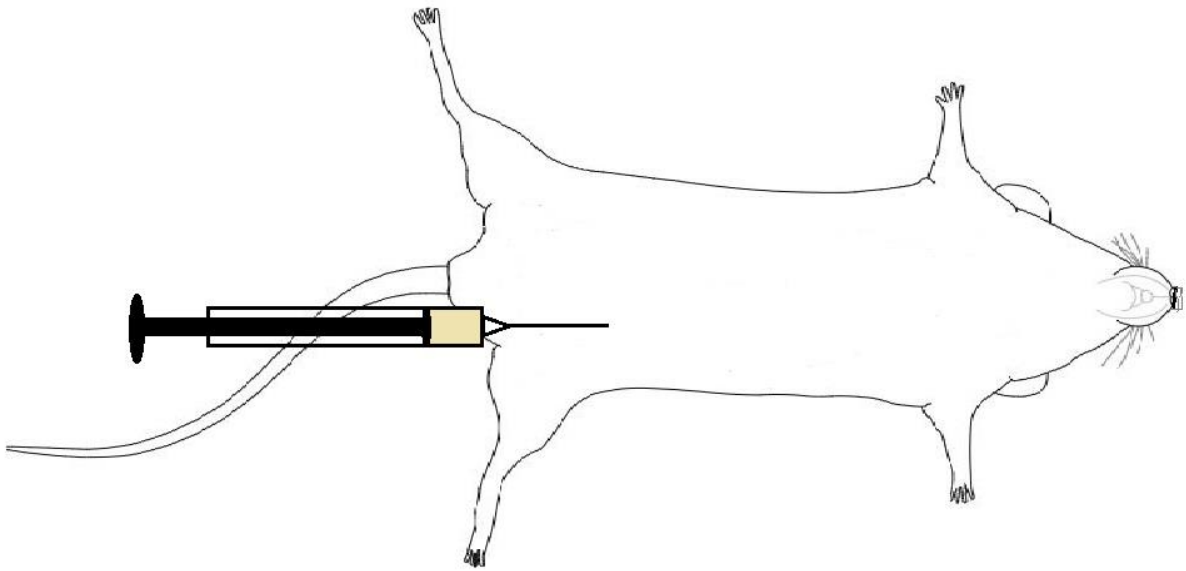


Figure 3: Schematic representation of the intraperitoneal injection of the bacterial suspension in sex- and age-matched C57BL/6 mice.

Table 13: Clinical severity scoring system

Grade	Criteria			
	Quality	Spontaneous activity	Reaction to exogenous stimuli	Posture
1	No signs of illness	Active, strong	curious	Quick movements
2	Low grade	Less active with occasional interruptions in activity	Reduced alertness, but adequate response	Slightly hunched
3	Mid-grade	Slow, sleepy, move with difficulty	Limited and delayed	Hunched
4	High-grade	Lethargic, motionless, no movement	None	Severely hunched
5	Dead	-		

The remaining mice were euthanized using CO₂ at the end of the experiment. In subsequent studies, as part of an investigation of the inflammatory response during live *E. coli* sepsis, the mice that survived 20-24h after sepsis induction were euthanized using CO₂. Their cells and body fluids were further investigated, as described below in Chapter 3.3.4.

All studies with mice were approved by the State Investigation Office of Rhineland-Palatinate and were in accordance with the guidelines of the German Animal Protection Act¹⁸², and the Federation of European Laboratory Animal Science Associations, directive 2010/63/EU of the European Parliament and the Council of the European Union. All experiments with mice were supervised by animal welfare officers. All mice were housed in a 45–60% humidity, 22 ± 2 °C ambient temperature, controlled light/dark (12 h/12 h) cycle, with free access to food and water, were used as sex–age-matched cohorts for experiments and maintained in a specific pathogen-free environment.¹⁷⁸

3.3.2 Live E. coli sepsis and administration of inorganic polyphosphates.

The experiments were performed as described above in section 3.3.1. In this series of experiments, long-chain polyphosphates P700 and short-chain polyphosphates P70 were studied during live *E. coli* sepsis. After dilution of the PolyP stock solution to 1mg/ml, inorganic polyphosphates of 10µg/ml per gram bodyweight of the mice were mixed with 100µl wild-type bacterial solution (*E. coli* MG1655) of the concentration needed at RT, until homogenisation. A mixture of bacteria and PBS of 10µg/ml per gram bodyweight of the mice was prepared for the control group. The mixture was then i.p injected in mice using a 30-G needle. For this experiment, a survival study for seven days and an analysis of body fluids after euthanasia of the mice using CO₂ were performed.

3.3.3 Live E. coli sepsis and treatment with recombinant exopolyphosphatase from Saccharomyces cerevisiae (ScPPX).

The bacterial cultures and infection to induce peritoneal sepsis were performed, as described in chapter 3.3.1. Recombinant ScPPX was diluted in normal saline (NaCl 0.9%) and prewarmed at 37 °C to activate the enzyme. ScPPX of 2µg/g bodyweight was

intraperitoneally injected in the mice, using a 30-G needle at 3-6 hours after infection, when CSS=3. The control group received normal saline of the same concentration as ScPPX. For this experiment, a survival study for seven days was performed.

3.3.4 Extraction of blood plasma and peritoneal lavage after sepsis

At the end of the experiments described above, the mice were euthanized using CO₂. Following blood collection, the abdominal skin was disinfected and carefully removed to reveal the outer peritoneal tissue layers. Using a 23G needle, 7-8ml ice-cold PBS was flushed in the peritoneal cavity and then transferred in a 15ml tube on ice. In a dilution series (1:10⁵-1:10⁶), 100µl of the diluted peritoneal lavage were evenly distributed on sheep blood agar plates. The plates were then incubated at 37 °C for 24-48 hours to determine the peritoneal CFU counts. Some lavage fluid was immediately centrifuged at 300G, 4 °C for 5 minutes and used for the flowcytometric cell analysis. Another portion of the suspension was centrifuged at 20,000G, 4 °C and for 10 minutes to allow cell precipitation. The supernatant was stored at -80C for further analysis.

3.4 In vitro experiments

3.4.1 Bacterial growth curve

An overnight bacterial culture was inoculated from the bacterial stock solution in LB-Medium (Luria Miller). The overnight culture was incubated at 37 °C under continuous shaking (200rpm). The next day, a new bacterial culture was started in LB-Medium after dilution (1:100) of the overnight culture and incubated at the same conditions. A sample from the bacterial culture was collected at different time points to measure the optical density (OD). The optical density was measured at 600nm on a Nanodrop 2000c Spectrophotometer.

This experiment was also performed to test the effect of exogenous L-PolyP addition to a final concentration of 0.2mM and ScPPX (diluted to 1:400 from a stock concentration of 1.27mg/ml) on bacterial growth.

3.4.2 Flow cytometric count of the bacterial inoculum for live *E. coli* sepsis

A bacterial solution was resuspended from an overnight bacterial culture and incubated at 37 °C and vigorous shaking. When the optical density reached 1.0-1.2, 2ml of the bacterial culture was centrifuged at 2,500G for 5 min at 4 °C. The pellet was resuspended in PBS. This step was repeated twice. 500µl of the solution was heated at 70 °C for 15min to kill the bacteria. The heat-killed bacteria were used as a control suspension for dead bacteria in the bacterial suspension. Each sample tube for flow cytometry contained 490µl staining buffer (PBS with 0.01% Tween 20, 1mmol/L EDTA, sterile filtered using 0.22µm Filter), 10µl bacterial suspension, 5µl thiazole orange, 5µl propidium iodide, and 50µl counting beads. The control tube did not contain any bacteria, and no counting beads were added in the tube containing the heated bacterial suspension. The bacterial count was performed using a FACS Canto II flow cytometer and FACS Diva software. The flow cytometry data were analysed using FlowJo.

3.4.3 Purification of *Saccharomyces cerevisiae* exopolyphosphatase (ScPPX)

The purification procedure of ScPPX was performed according to the protocol of Michael J. Gray, who provided us with the pScPPX2 plasmid.¹⁸³ Following the product transformation protocol of competent *E. coli* BL-21¹⁸⁴, a new bacterial strain, *E. coli* MJG 317, was created, which contained the pScPPX2 plasmid.¹⁸³ A colony of *E. coli* MJG317 was resuspended in 5ml LB medium and incubated overnight under continuous shaking (200rpm) at 37 °C. On the next day, 1L of LB medium containing 100mg Ampicillin was inoculated with the bacterial solution. Ampicillin was added, so that no bacteria other than the plasmid-containing *E. coli* could grow in the culture. The bacterial suspension was incubated for 3-4 hours at 37 °C under shaking (120rpm). After the addition of another 100µg/ml Ampicillin and Isopropyl β-D-1-thiogalactopyranoside (IPTG) to 1mM to the solution, the culture was incubated overnight at 37 °C and vigorous shaking (150rpm). IPTG was added to bind to the lac-repressor in the lac-operon of *E. coli* MJG317, thus inducing gene transcription and protein expression. The next day, the bacteria were harvested by centrifugation in 50ml Falcon tubes (20 minutes, 4,000G, RT). The pellet was stored at -80 °C or used directly for the purification, as described below. The pellet from the ScPPX overexpression culture was defrosted on ice and resuspended in binding

buffer (50mM Sodium phosphate buffer, 0,5M NaCl, 20mM imidazole, pH=8) for a total of 5ml. More binding buffer (10-15ml final volume) was added, if the suspension was of high viscosity. Lysozyme (1mg/ml), MgCl₂ (to a final concentration of 2mM), Benzonase (50U/ml) and complete proteinase inhibitor mix were added to the suspension (ScPPX can bind nucleotide polymers, so nuclease digestion is critical). After an incubation of 30-60 minutes on ice, the cells were lysed by sonification (on ice, two cycles of 3 min, 10s on + 10s off, with a break of 3min in between). The mixture was centrifuged to remove cell debris (20min, 20,000G, 4 °C), and bacterial lysate (supernatant) was collected. The lysate was loaded on a 1ml Histrap HP column. The purification was performed on an ÄKTA Pure chromatography instrument according to the manufacturer's protocol. The elution fractions were collected after rinsing the column with elution buffer (50mM sodium phosphate buffer, 0.5M NaCl, 0.5M imidazole, pH=8). The protein suspension was desalted using Dialysis buffer (20mM Tris HCl (pH=7.5), 50mM KCl, 10% per vol. Glycerol) on PD-10 desalting columns and sterile filtered with 0.22µm membrane filters. Protein electrophoresis on an SDS-Gel was performed in order to compare bacterial lysate, flow-through and elution fractions. The estimated size of ScPPX is around 45kDa. The protein concentration of purified ScPPX was estimated by Bradford protein assay, and the enzymatic activity was measured using a Biomol green assay. The protein was stored at 4 °C because ScPPX is reported to lose activity when frozen. The activity and the concentration of the protein were monitored in periodic intervals.

3.4.4 Bacterial killing assay by macrophages

The following method was based on the bacterial ingestion assay as published by Drevets et al. in 2015¹⁸⁵. 10ml LB (Luria Miller) growth medium was inoculated from an overnight bacterial culture and incubated (37 °C, 200rpm) until the OD_{600nm} was measured 0.3-0.5. Next, 1ml bacterial suspension was centrifuged (2,500G, 5 min, RT). The supernatant was discarded, and the bacterial pellet was washed with PBS by pipetting up and down. The washing procedure was repeated at least two times by discarding the supernatant each time. Finally, the bacterial pellet was resuspended in 1 ml assay buffer (RPMI 1640, FBS 10%) and incubated for 3 minutes at 37 °C. To perform the bacterial killing assay, MH-S macrophages and bone-marrow-derived macrophages were used. Macrophages

were resuspended in assay buffer to a final concentration of 5×10^5 cells/ml allowed to rest for 1 hour at 37 °C. Subsequently, the bacterial and the macrophage suspension were equally mixed in the presence or absence of L-PolyP (P700, to a final concentration of 1mM) and incubated at 37 °C under continuous rotation end-over-end. Before starting the experiment, a diluted bacterial suspension ($1:10^4$) was plated on sheep blood agar plates to determine CFU count at time point $t=0$ minutes. A control suspension of macrophages and bacteria were produced by dissolving the suspension in assay buffer. After 15 minutes, 45 minutes and 90 minutes, suspension samples were collected, a dilution series was prepared ($1:10^4$, $1:10^5$, $1:10^6$ in PBS), and plated on sheep blood agar plates. All plates were incubated at 37 °C for 24 hours before counting of CFUs, which corresponds to the extracellular bacteria after phagocytosis at each time point under different incubation conditions.

3.4.5 Preparation of bone marrow-derived macrophages

To generate bone marrow-derived macrophages (BMDM), healthy C57BL/6J mice were euthanized using CO₂. After skin disinfection and careful soft tissue preparation, both femurs and tibias were removed and washed with ice-cold PBS in a 10ml petri dish. The following steps were performed under sterile conditions. The bones were disinfected for 15 sec in a mixture of 1-propanol 35% (p.v) and ethanol 25% (p.v) and then washed with ice-cold PBS. Next, both ends of the bones were clipped and the marrow was removed by flushing with ice-cold PBS from a syringe with a 23G sterile needle. The collected cells were filtered through a 100- μ m mesh. The cell suspension was centrifuged at 300G for 5 min at 4°C. The supernatant was removed and the cells were suspended in 100 ml of cell-conditioned BMDM differentiation medium. 10 ml of cell suspension were transferred in 10 cm Petri dishes. On the third day of BMDM generation, a fresh aliquot of differentiation medium (10 ml) was added to the cultured cells. The cells were incubated for 7-10 days at 37°C, 5% CO₂, and >95% humidity.

To harvest BMDMs, the cell culture medium was removed, followed by a brief cell wash with 5 ml prewarmed PBS. After discarding the washing buffer, PBS containing 0.5 mM EDTA was added to detach the cells. Any still adherent cells were detached using a cell scraper. The cell suspension was centrifuged at 300G for 5 min. The supernatant was

removed, and the cell pellet was resuspended in 10 ml of macrophage medium, followed by a cell count using trypan blue staining in a Neubauer chamber. For most experiments, 5×10^5 cells/ml solution was used for further experiments. The cells were allowed to rest and incubated under the conditions stated above for ≥ 2 hours before the start of stimulation. The purity of BMDM preparation was determined by flow cytometry and was typically $\geq 98\%$ F4/80+CD11b+ macrophages.

3.4.6 MH-S macrophage culture

MH-S macrophages is an SV40 transformed, alveolar macrophage cell line obtained from a healthy mouse¹⁸⁶. To prepare an MH-S culture, a cryovial was defrosted on ice. The cryorecovered suspension (containing DMSO 5%) was carefully mixed with a 48.5 ml growth medium, followed by centrifugation at 1500rpm for 5 minutes. The supernatant was discarded, and the pellet was resuspended in a 10ml MH-S growth medium, which was transferred in a culture flask and incubated at 37°C, 5% CO₂, and >95% humidity. Every 2-3 days the cells were transferred/split to new flasks. The suspension containing non-adherent MH-S macrophages was transferred to a 15ml/50ml centrifuge tube. After a washing step using 10ml prewarmed PBS, the adherent cells were treated with 2ml Trypsin EDTA solution and allowed to incubate at 37 °C for 1-2 minutes until the cells detached. Thereafter, 8ml growth medium solution was added to stop the procedure. The suspension was either mixed with the non-adherent cells and centrifuged at 1,500rpm for 5 minutes or dispersed into new flasks containing fresh growth medium to a final subcultivation ratio of 1:5 to 1:10. After centrifugation, the medium was discarded and the pellet was resuspended in macrophage medium. The macrophage cells were counted using trypan blue staining in a Neubauer chamber. For most experiments, a cell amount of around 5×10^5 cells/ml (1ml/well of a 24-well plate) was used to perform in vitro experiments or the bacterial killing assay.

3.4.7 MLE-12 cell culture

MLE-12 cells are murine, lung epithelial cells obtained from a healthy mouse.¹⁸⁷ To prepare an MLE-12 cell culture, a cryovial was defrosted. The vial's cryopreserved content (containing DMSO 5%) was mixed with a 48.5ml growth medium, followed by

centrifugation at 1500rpm for 5 minutes. The supernatant was discarded, and the pellet was resuspended in a 10ml MLE-12 cell growth medium, which was transferred in a culture flask and incubated at 37°C, 5% CO₂, and >95% humidity. Every four days the cells should be split/transferred in a new flask. The solution containing non-adherent MLE-12 cells was transferred to a centrifugation tube. After a washing step with 10ml prewarmed PBS, the adherent cells were treated with 1.5ml Trypsin EDTA solution and allowed to incubate at 37 °C for 2 minutes until the cells detached. MLE-12 cells are sensitive to Trypsin EDTA solution; thus, the detaching procedure needed to be short. Furthermore, cell detachment using a cell scraper was avoided. Next, 8.5 ml growth medium (containing FCS with Antitrypsin) was used to stop the process. The suspension was centrifuged at 1500rpm for 5 minutes and dispersed into new flasks containing fresh growth medium to a final subcultivation ratio of 1:5. After centrifugation, the medium was discarded and the pellet was resuspended in a fresh growth medium. The epithelial cells were counted using trypan blue staining in a Neubauer chamber. For most experiments, a cell amount of around 5 x 10⁵ cells/ml (1ml/well of a 24-well plate) was used to perform in vitro experiments.

3.4.8 Determination of cell numbers for in vitro experiments

MH-S macrophages or bone marrow-derived macrophages were resuspended in 5 ml macrophage medium and MLE-12 cells in the same amount of MLE-12 growth medium. The cell suspensions were diluted 1:5 or 1:10 in trypan blue and loaded on an improved Neubauer chamber. Only the viable cells (without uptake of trypan blue) were counted. Cell numbers were calculated as follows:

$$\mathbf{N\ of\ cells} = \text{Cells counted} \times \frac{\text{Dil. factor}}{(5\ \text{or}\ 10)} \times \frac{10,000}{\text{ml}} \times \text{Vol. of cell solution}$$

3.4.9 In vitro stimulation and sample preparation

The cells were incubated at 37°C and 5% CO₂ for 2 hours to rest. Thereafter, the cells were stimulated, as described in the figure legend of each experiment. For most experiments, LPS of a final concentration of 100 ng/ml and L-PolyP of a final

concentration of 50 μ M (corresponding to monophosphate Pi) were used, unless indicated otherwise. The cells were usually stimulated for 24-48 hours. At the end of the incubation period, the supernatants were transferred to fresh reaction tubes and centrifuged at 650G, 4°C for 5 minutes, to remove any remaining cells. Finally, the supernatants were collected and stored at -80C for further investigation.

3.5 Biochemical methods

3.5.1 DNA extraction from bacteria using Trizol Reagent

Bacteria were harvested by centrifugation (2,500G, 5 min, RT). The nonparticulate supernatant, consisting of bacterial growth medium, was gently removed. The following procedure was performed under a ventilated hood. 0.25ml of the bacterial suspension was resuspended in 0.75 ml Trizol Reagent, followed by continuous up and down pipetting until the pellet was lysed entirely. After 5-minute incubation at room temperature, 0.2 ml chloroform/ml Trizol was added. The sample was vigorously mixed for 15 sec. and was incubated for 2-3 min. Next, the sample was centrifuged for 15 min at 12,000G and 4°C. The aqueous phase (RNA) was transferred into a new tube. 0.4ml EtOH (99.8% p.v) per 1ml Trizol was added to the organic phase and the interphase. The mixture was shaken by hand and incubated for 2-3 minutes at RT. After centrifugation (2,000G for 5 minutes at 4°C), the supernatant was removed and eventually used for protein purification. The pellet containing the bacterial DNA was washed with 1ml washing buffer (0.1M Sodium Citrate, 10% EtOH) per 1ml Trizol and was incubated in washing buffer for 30 minutes at RT. The DNA wash was repeated twice after spinning the mixture at 2,000G for 5 minutes at 4°C between the washing steps. Following centrifugation, the pellet was resuspended in 1.5-2.0ml 75% EtOH and incubated for 10-20 minutes at RT under periodical mixing. The homogenate was stored at 4°C for several hours or at -20C for several days. The suspension was centrifuged (2,000G for 5 minutes at 4 °), and the pellet was resuspended in 300-500 μ l NaOH (8mM)/ml Trizol. After spinning (12,000G for 10 minutes) to precipitate cell residuals, the supernatant containing the DNA was transferred to another tube and used for PCR-based DNA amplification and analysis.

3.5.2 Genotyping of *E. coli* by polymerase-chain-reaction (PCR)

The DNA sample extraction is described above (Paragraph 2.2.4). To create the PCR samples, 12.5µl HotStart Green PCR Mastermix, 5µl forward primer, 5 µl reverse primer, and 2.5µl bacterial DNA (Total volume: 25µl) were mixed. An annealing temperature gradient program for primer binding was used to find the optimal genotyping conditions. The temperature varied from 52.9-60.4 °C in 8 steps. The optimal temperature for primer binding was determined as 57.5 °C. Therefore, this annealing temperature was used for subsequent DNA amplification experiments involving the ppk and ppx primers. An agarose gel (10-12%) was prepared using 200 ml TAE-Puffer(1x). The DNA samples were carefully pipetted onto the gel. The gel electrophoresis was then performed under constant 100V-voltage. Finally, the gel was stained with GelRed under shaking for 30 minutes and digitally photographed in a gel documentation chamber.

3.5.3 Enzyme-linked immunosorbent (ELISA) assay

The quantification of secreted proteins in cell culture supernatants or cell-free body fluids was performed using CXCL4/PF4, MIP-1 α , CXCL1/KC, CXCL10, IL-6, TNF- α enzyme-linked immunosorbent assay (ELISA) kits from R&D systems. For accurate and reliable results, the assays were performed according to the protocol provided with each kit.

The principle of the sandwich ELISA assay is based on specific binding and detection of the targeted protein. A capture antibody, which is specific to binding sites of the protein, is at first adapted to the bottom of the testing well. After the addition of the sample, this antibody binds to the protein. A detection antibody, specific for other binding sites of the protein, which contains biotin, is then added and attaches to the protein. Then, a conjugate, containing avidin and peroxidase (Streptavidin-HRP), which has a high affinity for biotin, was added, followed by the addition of a peroxidase substrate. A brief washing step is necessary between the incubation steps. The exact procedure is described below. The colourimetric quantification of the metabolite, released during the enzymatic reaction of peroxidase with its substrate, enables the targeted protein quantification using a standard curve of samples with known concentration.

Description of the procedure: A capture antibody with specificity to the target protein was coated onto the ELISA plate and incubated at RT overnight. The next day, the plate was washed three times with 300 µl of PBS + 0.05% (v/v) Tween® 20. Then, the addition of

300 µl of PBS + 1% BSA, followed by incubation for 1 hour at RT, enabled the blocking of unspecific binding sites. After incubation of the plate, the washing procedure was repeated, as described above. 100 µl of diluted samples, standard series, and blank were added onto the coated wells and allowed to rest for 2 hours at RT. The sample dilution was performed to fit the sample values within the range of the standard curve. As reagent diluent, PBS + 1% BSA was used for all the ELISA-assays except for the CXCL4/PF4 ELISA, for which 0.1% BSA, 0.05% Tween® 20 in Tris-buffered saline was used. Afterwards, the washing was repeated, and 100 µl of detection antibody, dissolved in reagent diluent, was added. The plate was again incubated at RT for 2 hours, followed by a washing procedure, as described above. Then 100 µl of Streptavidin-HRP, resuspended in reagent diluent, was added for 20 min, followed by another brief washing step. 100 µl TMB substrate was added and incubated for 15-20 minutes until colour development. The enzymatic reaction of peroxidase was stopped after adding 50 µl 2N H₂SO₄. Optical densities were measured at the wavelength 450 nm with a correction at 550 nm (Opsys MR Microplate Reader, DYNEX). A four-parameter sigmoid curve was constructed, which allowed the targeted protein (antigen) quantification in relation to the standard dilution series.

3.5.4 Sample preparation for quantitative PCR analysis

In order to perform qPCR analysis, the first steps in the workflow are cell lysis followed by RNA isolation. At the end of the experiments, the cells were directly lysed in cell culture plates after careful removal of supernatant. The cells, which were obtained from in vivo experiments as described above, were centrifuged (300G, 5 min, 4°C) and lysed.

Cell lysis was performed using the Qiagen RNeasy mini kit according to the manufacturer's instructions. The samples were lysed for 5 min in 350 µl lysis buffer by pipetting carefully up and down. Next, ethanol 70% (v/v) was added to the sample and the solution was thoroughly mixed. The mixture was loaded on Qiagen columns and centrifuged for 15 s at 8,000G. The flow-through was discarded. Afterwards, the columns were washed with 700µl buffer RW1, followed by centrifugation for 15 s at 8,000G, discarding the flowthroughs. Then, a washing step using 500µl buffer RPE was performed twice. Centrifugation for 2 min at 8,000G removed any extra fluid so that the columns

could dry. The dried columns were placed in fresh PCR clean tubes, and 30µl of nuclease-free H₂O was added, followed by incubation for 1 min at RT. The RNA was collected after a centrifugation step for 1 min at 8,000G and was either directly used for analysis or stored at -20°C.

The “High-Capacity cDNA Reverse Transcription” kit from Applied Biosystems was used for reverse transcription and cDNA synthesis from the sample RNA. The RNA concentration of each sample was photometrically measured at 260 nm by Nanodrop 2000c (Thermo Fisher Scientific) before synthesising cDNA based on a reverse transcription procedure. RNA concentrations were adjusted to 0.2-2 µg of RNA per 20µl sample. cDNA synthesis was performed based on the manufacturer’s instructions in the thermal cycler Mastercycler pro S (Eppendorf). The following PCR protocol was used (Table 14):

Table 14: Preparation of cDNA

Step	Temperature (°C)	Time (min)
1	25	10
2	37	120
3	85	5
4	10	∞

To perform qPCR analysis, the synthesized cDNA was adjusted to a concentration of 2-20 ng/µl and was identical in each experiment. 2µl cDNA from these samples was used as a template for qPCR reaction. The total reaction volume was 20µl, including 2-fold iQ SYBR green mix and specific forward and reverse primers of the targeted genes to a final concentration of 0.5 µM. For the qPCR reaction, a C1000 with a CFX96 real-time PCR detection system (Bio-Rad) was used. All qPCR runs were followed by a melting point analysis, which can be shown in the following table (Table 15):

Table 15: qPCR program

Step	Temperature (°C)	Time (s)	Cycles
1	95	180	1x
2	95	15	40x
3	58	30	40x
4	60 to 95	4	70x

The Ct value represents the amplification cycle at which threshold and amplification lines interfere. All results were compared to the expression of the housekeeping gene mouse glyceraldehyde 3-phosphate dehydrogenase (GAPDH). Furthermore, the target gene expression was set to 1 for unstimulated conditions using the $2^{-\Delta\Delta Ct}$ method¹⁸⁸:

$$\Delta Ct = Ct_{\text{target gene}} - Ct_{\text{reference gene}}$$

$$\Delta\Delta Ct = Ct_{\text{condition}} - Ct_{\text{control}}$$

$$\text{Ratio} \left(\frac{\text{Expression in condition}}{\text{Expression in control}} \right) = 2^{-\Delta\Delta Ct}$$

3.5.5 Bioplex assay

Simultaneous detection and analysis of 23 mouse cytokines and chemokines, found in peritoneal lavage and blood plasma, was performed using the BioPlex Pro™ mouse cytokine assay, 96-well, 23-Plex Group I (BioRad, USA). The analytes were: IL-1 α , IL-1 β , IL-2, IL-3, IL-4, IL-5, IL-6, IL-9, IL-10, IL-12(p40), IL-12(p70), IL-17, Eotaxin (CCL11), G-CSF, GM-CSF, IFN- γ , KC (CXCL1), MCP-1 (CCL2), MIP-1 α (CCL3), MIP-1 β (CCL4), RANTES (CCL5) and TNF- α , as described in previous study from the working group of PD Dr. med. Bosmann¹⁸⁹. The samples were diluted 4-fold in sample diluent (BioRad) after centrifugation at 1,000G for 15 minutes at 4°C. A standard series was constructed using sample diluent. The run of the Bio-Plex Mouse assay was performed according to the manufacturer's instructions.¹⁹⁰ An Aurum™ vacuum manifold (BioRad) was used for the washing steps. The samples were analyzed on the Luminex xMAP™/Bioplex-200 System with BioPlex Manager™ Software 5.0. Statistical analysis was performed with the aid of GraphPad Prism Version 8/9.

3.5.6 Flow cytometry of mouse cells

The peritoneal lavage cells from in vivo experiments were isolated as described above in section 3.3.4. Aliquots of the samples were used for CFU counts, while the lavage cells were centrifuged at 300G for 5 min at 4°C. The supernatant was carefully transferred into a new tube and further processed for analysis. The following steps, including processing and staining live cells, were performed on ice to avoid antigen internalization or clustering. Furthermore, each washing step was followed by a centrifugation at 300G, 4 °C for 5 minutes. The cell pellet was suspended in 220 µl ice-cold PBS. Next, all the samples were transferred to a 96-well V-bottom plate, and the washing step with 220µl ice-cold PBS was repeated. After discarding the supernatant, the pellet was dissolved in a mixture, containing 100 µl FACS Stain buffer and 2µl TruStain® fcX block (anti-CD16/CD32) – for every 100 µl FACS Staining buffer 2 µl of TruStain® fcX were added, achieving a 1:50 dilution. The cell suspension was incubated for 15 minutes on ice. Afterwards, the surface staining antibodies were added to the cell suspensions, followed by incubation for 30 min. Then, the cell suspensions were washed twice with 220 µl of FACS buffer.

For the surface staining workflow, the cells were fixed in 2% (v/v) formaldehyde in FACS buffer for 20 min at RT, followed by a centrifugation. The supernatant was discarded, and the cells were suspended in 200µl FACS buffer.

If additional intracellular staining of antigens was needed in the workflow, the cell pellet was resuspended in 100 µl Cytofix/Cytoperm (BD Bioscience) and incubated for 20 min at RT. Next, a washing step with 220µl of Perm/Wash buffer (BD Bioscience) was performed. The cells were resuspended in 100 µl of Perm/Wash buffer, the intracellular antibodies were added, and the cell suspension was incubated for 30 min on ice. Thereafter, a washing step with 220µl Perm/Wash was performed twice. The cells were finally suspended in 200 µl FACS buffer, containing 2% PFA. An isotype antibody control was used to compare the fluorescent intensity of unspecific cell staining with specific antibodies. The isotype control antibodies were commercially purchased and corresponded to fluorochromes, species, and immunoglobulin subclass.

A volume of 20 µl of counting bead suspension was added to the samples before the flow cytometric measurement, which enabled the quantification of analysed cells. The flow

cytometry was performed on a BD FACSCanto II (BD Bioscience) for acquiring 50,000 events per sample. Cell numbers were calculated, as shown below:

$$N_{\text{absolute cells}} = \frac{N_{\text{cell count}} \times V_{\text{beads}}}{N_{\text{bead count}} \times V_{\text{sample}}} \times C_{\text{beads}} \times V_{\text{absolute cell lavage}}$$

3.5.7 Bradford assay

Diluted or undiluted samples of the isolated protein (mostly ScPPX samples, purification procedure described above) were tested using Bradford assay. 10 µl of sample or standard were mixed with 140 µl Bradford Ultra™ in a 96 well microplate. After colour development, the samples were photometrically measured at OD595nm using Opsys MR Microplate Reader (DYNEX). The protein concentration was calculated after estimating the linear regression of the standards. Standards were made by mixing BSA with PBS 1x as dilution buffer. For more accuracy, a high-protein-concentration standard dilution series (range: 1.5mg/ml to 100µg/ml and blank) and low-protein-concentration standard dilution series (range: 150µg/ml to 10µg/ml and blank) were made. Samples were tested against both dilution series.

3.5.8 Griess assay

To quantify the production of NO after cell stimulations or after in vivo sepsis experiments, a colorimetric Griess assay to estimate the concentration of released nitrite was performed. Nitrite is a metabolite of NO under oxidative conditions. Samples from body fluids or cell culture supernatants (75 µl per sample or diluted sample) were mixed with 10 µl of Griess reagent and 65 µl deionized water. A serial dilution of nitrite concentrations was used as control standards. Following a 30 min incubation at RT, the absorbance was measured at a wavelength of 550 nm (Opsys MR Microplate Reader, DYNEX223).

3.5.9 Enzymatic activity measurement of ScPPX using Biomol Green assay

A 96-Well plate with a dilution series of phosphate standards was prepared. H₂O was used as assay reagent and HCl 2N as stop solution to terminate the ScPPX reaction.

Each well, except the wells that contained the phosphate standard series, was prefilled with 35 μ l cold HCl 2N. 20 μ l ScPPX and 980 μ l H₂O were transferred in two 1.5 ml Eppendorf tubes and allowed to rest at 37 °C for 10 minutes. ScPPX was activated and equilibrated at its optimal working temperature. Thereafter, L-PolyP (P700) was added as final concentrations of 100 μ M to Tube 1 and 200 μ M to Tube 2 for starting the reaction. 15 μ l of each tube's solution was removed and pipetted in the corresponding wells every minute for about ten minutes after the initiation of the reaction. Next, 100 μ l Biomol green was added to each well. The plate was then incubated in the dark at RT for 20-30 minutes until a green colour developed. A photometric measurement of the released monophosphate was performed at 620nm using a Opsys MR Microplate Reader. A Michaelis-Menten Kinetic curve was prepared for the PPX activity, which was expressed in nmol Pi x mg⁻¹ScPPX x min⁻¹.

3.5.10 Statistical analysis

All experiments were performed three times as independent biological replicates. Unless otherwise indicated, the experiments were performed in technical replicates (e.g. two wells of the same condition). Furthermore, assays such as ELISA and qPCR were performed as technical replicates for all samples. Data are represented as mean with standard error of the mean (S.E.M.). Statistical analysis was performed with GraphPad Prism 8/9 and its statistical algorithms. The results of survival studies were evaluated by performing Log-rank Mantel-Cox tests. The statistical comparison between more than two groups was investigated using two-way ANOVA. The comparison between two groups was tested for significant differences using the two-sided Student's *t*-test. The result's statistical significance was indicated, when the *p*-value was less than 0.05. The statistical significance of data is noted in figures and figure legends using asterisks as follows: **p*≤0.05, ***p*≤0.01, ****p*≤0.001, and *****p*≤0.0001, n.s: not significant.

4. Results

4.1 Estimation of bacterial concentration needed for in vivo bacterial sepsis

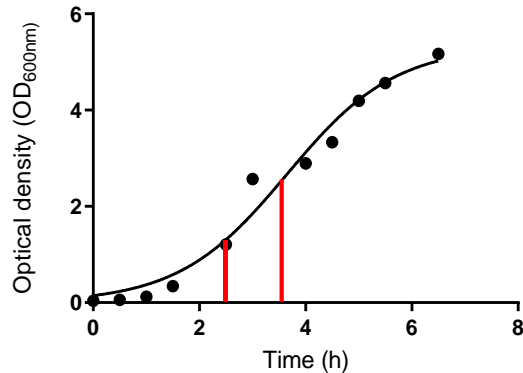


Figure 4: Growth curve of E. coli MG1665 based on optical density.

Bacteria of the E. coli MG1655 strain (wild-type bacteria) were inoculated from an overnight culture in LB-medium (Luria-Miller). The bacterial suspension was incubated at 37 °C at 200rpm. At different time points, the optical density was measured using a Nanodrop 2000c at 600nm (OD_{600nm}). Bacterial growth is expressed in terms of OD_{600nm}. Data are presented as mean \pm S.E.M as Gompertz growth curve.

To perform live E. coli sepsis experiments, it was required to study the bacterial strain characteristics, which would be used. Therefore, a growth curve of E. coli MG1655, the wild type bacterial strain containing both ppk and ppx, was estimated. Live E. coli challenge was performed with bacteria that underwent log-phase growth and more specifically, bacteria that underwent incubation for 2.5-3.5h, as indicated by the red lines in Figure 4.

E. coli bacteria were isolated by centrifugation, and their concentration was estimated by flow cytometry as described in chapter 3.4.2. Figure 5 shows the gating strategy for the quantification of bacterial numbers using FlowJo. To control the flow cytometric measurement efficiency by another method, bacterial samples were plated for CFU count on sheep blood agar plates.

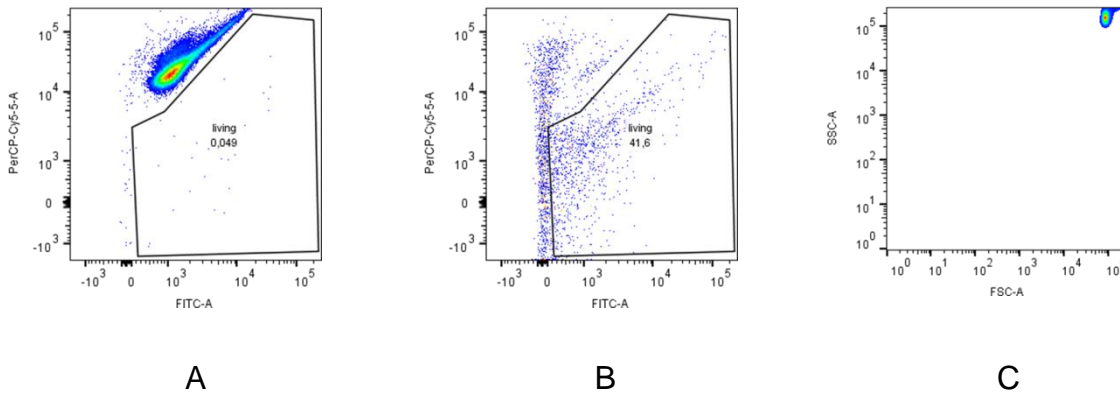


Figure 5: Gating strategy for quantification of injected *E. coli* bacteria.

Before injection into mice, aliquots of the bacterial suspension were stained and analyzed by flow cytometry. The gating of heat-killed dead bacteria (A) as positive control, live bacteria (B) and the counting beads (C) are shown on the diagrams.

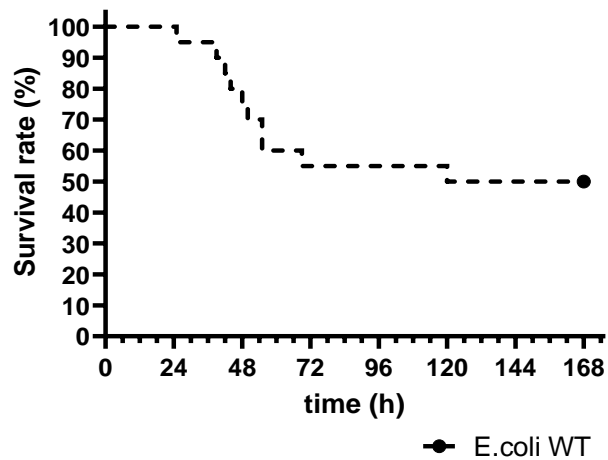


Figure 6: Survival rate after live *E. coli* sepsis induction with *E. coli* MG1655 (wt-bacteria).

C57BL/6J male mice (8 weeks old) were injected intraperitoneally with *E. coli* MG1665 bacteria. The clinical status and the survival of mice after peritonitis and sepsis induction were observed for one week. This curve represents the overall survival in percentage. At the end of the experiment, 50% of the animals died.

It was found that a bacterial concentration in a range of $8,5 \times 10^8$ – $1,7 \times 10^9$ CFUs/ml could cause a mortality rate of 50% after sepsis, as seen in Figure 6. Therefore, this bacterial concentration served as a control for subsequent in vivo experiments, testing survival rates compared to sepsis with wild-type E. coli.

4.2 Sepsis from bacterial strains deficient of polyphosphate metabolising enzymes resulted in an altered outcome

Although the mutant bacteria originated from the same strain (E. coli MG1655), the difference in growth characteristics of all three bacterial strains during the log-phase had to be estimated before performing comparative in vivo sepsis experiments. Figure 7 confirms that the growth of our bacterial strains is not influenced by the absence of PolyP-metabolising enzymes under optimal growth conditions.

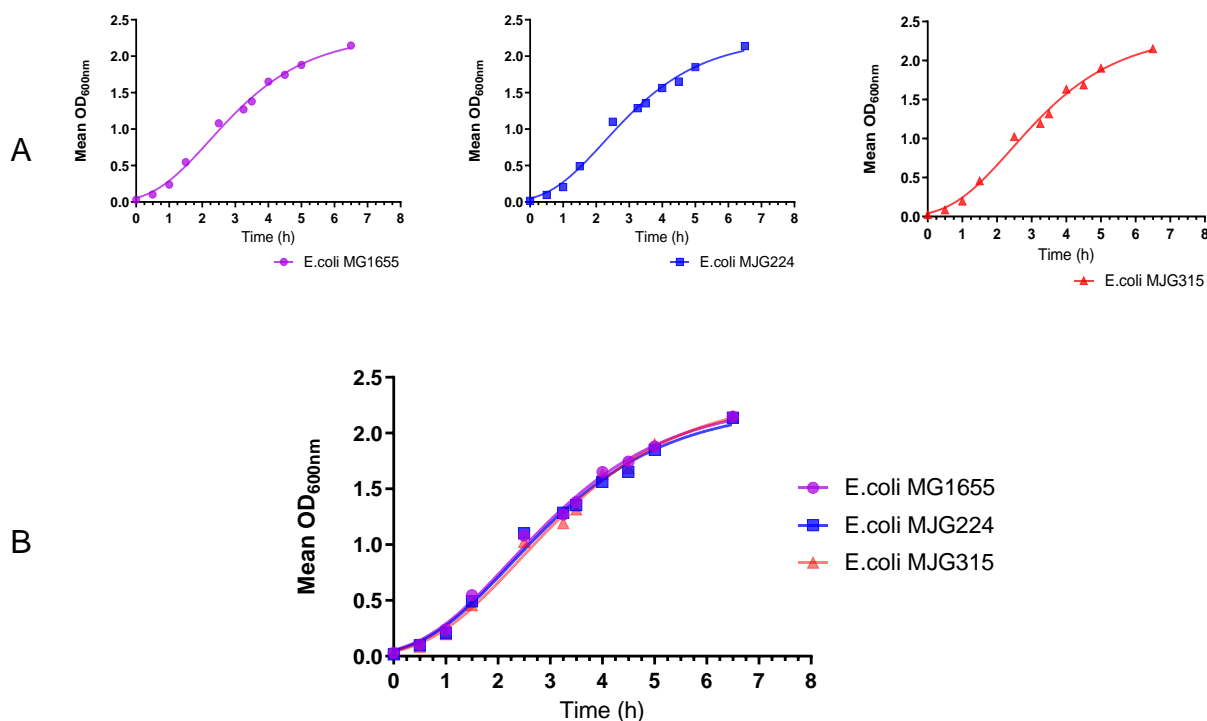


Figure 7: Growth curve of used bacterial stains in terms of optical density.

E. coli MG1655 (wild-type bacteria), E. coli MJG224 (Δ ppk) and E. coli MJG315 (Δ ppx) were incubated at 37 °C at 200rpm. At different time points,

the optical density of the suspension was measured using Nanodrop 2000c at 600nm (OD600nm). **A.** Bacterial growth of each strain individually is expressed in terms of OD600nm. **B.** Comparison of growth curves of every bacterial strain. Data are presented as mean \pm S.E.M as Gompertz growth curve.

After injection of the bacterial suspension in male mice (8-9 weeks old), survival rate and clinical severity scoring were studied for one week. The sepsis outcome after infection with mutant bacteria was compared to the outcome of infection with wild-type bacteria (Figure 8).

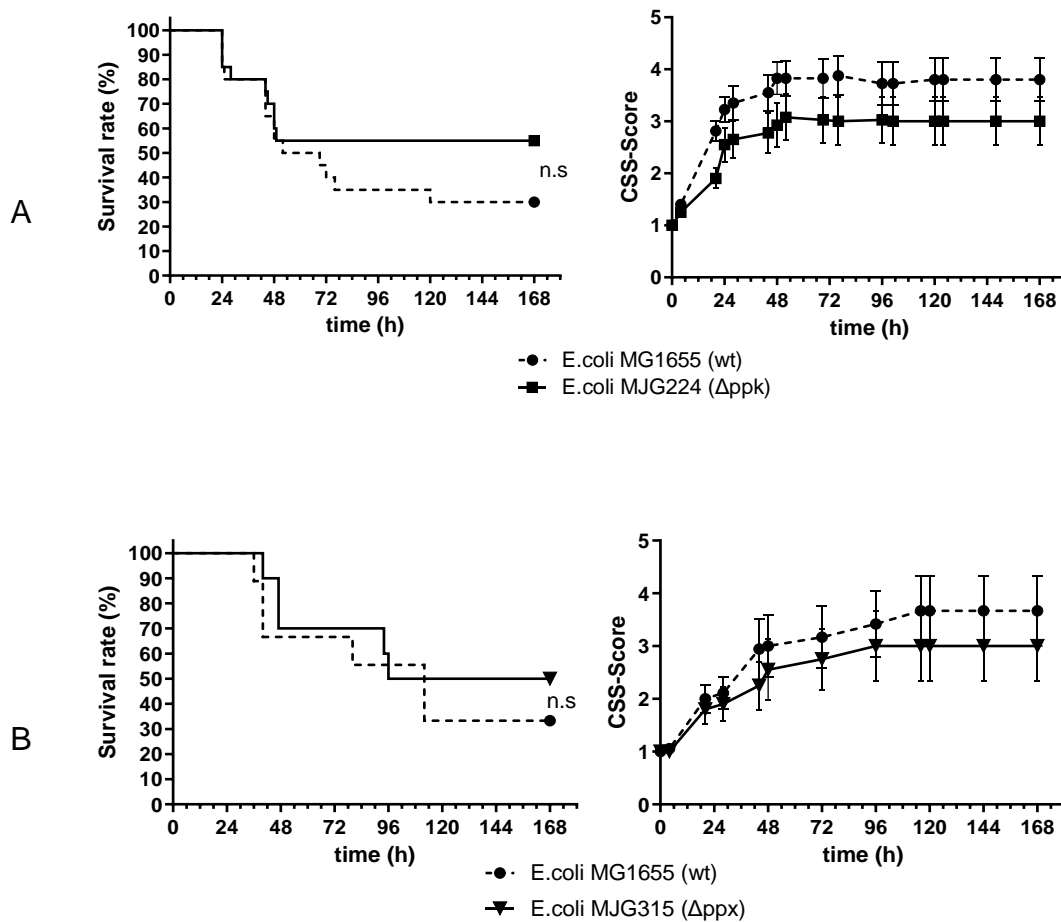


Figure 8: Sepsis experiments with E. coli strains deficient of polyphosphate metabolising enzymes.

E. coli bacterial solution (concentration range 9.31×10^8 - 1.58×10^9 CFUs/ml) was intraperitoneally injected in male mice to provoke peritonitis and sepsis. A: Induction of sepsis with Δ ppk E. coli trended to a non-significant increase in survival rate and a lower clinical severity (CSS) of the outcome. Pooled data from two independent experiments with n=20 mice/group. B: Induction of sepsis with Δ ppx E. coli trended to a non-significant increase in survival rate and a lower clinical severity (CSS) outcome. Pooled data from two independent experiments with n=10 mice/group. Survival curves were analyzed using the Log-Rank Mantel-Cox Test, CSS-Scoring was evaluated as mean \pm S.E.M by a 2-Way ANOVA Test. n.s: not significant

55% of mice that underwent sepsis with Δ ppk E. coli survived compared to 30% of the mice injected with wild-type bacteria. The difference in the overall survival and the difference in the mean clinical status, favouring Δ ppk E. coli, were statistically not significant. Surprisingly, the mortality rate during infection with E. coli Δ ppx (MJG315) was also 17% lower than for sepsis with wild type bacteria, resulting in the death of 50% of mice as compared to 33.3% of mice that were infected with wt-E. coli (Figure 9). These results were also not significant.

4.3 L-PolyP dysbalance the inflammatory response and impair the outcome of E. coli sepsis

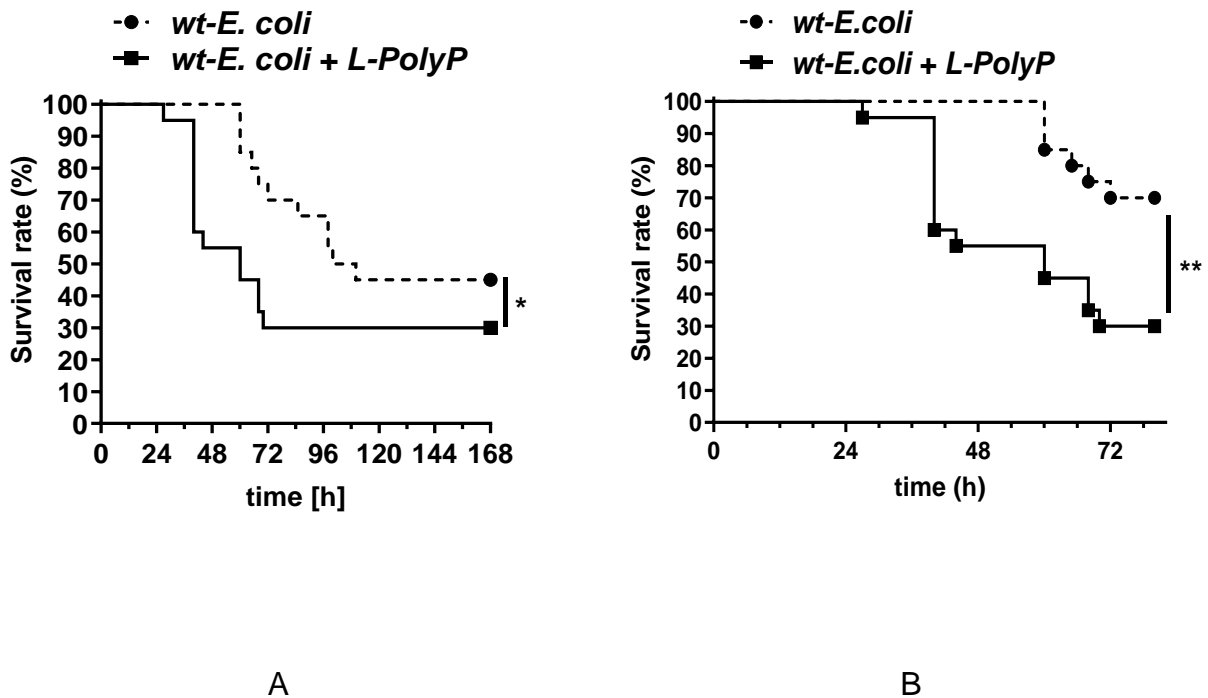


Figure 9: The administration of L-PolyP increases mortality rates during E. coli bacteremia.

Wild-type *E. coli* bacteria (*E. coli* MG1655) and L-PolyP (around 700 Pi-monomers) of a concentration 10 μ g/g bodyweight were intraperitoneally injected in mice to induce sepsis. A: The presence of L-PolyP aggravates the survival rate significantly. (Gehan-Breslow-Wilcoxon test). B: The most significant difference in mortality between the groups was observed 72h after sepsis induction. (Log-rank test). The raw data analysed for graph B are the same as the data of Graph A. The data are pooled from two individual experiments with n=20 mice pro group. *p \leq 0.05, **p \leq 0.01.

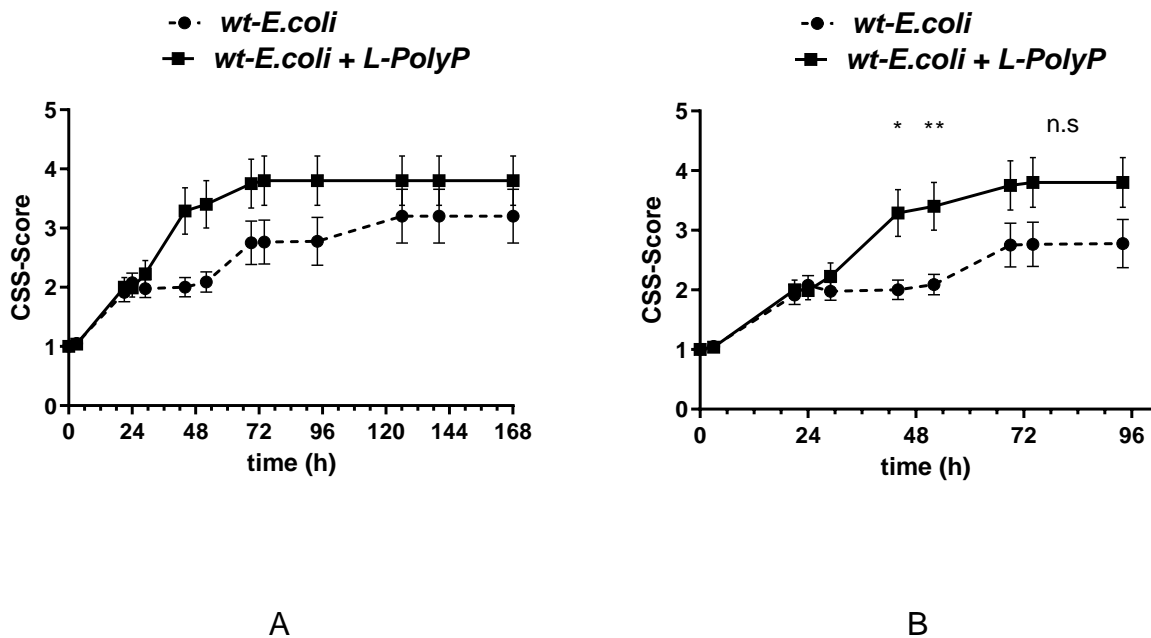


Figure 10: L-PolyP increased clinical severity score (CSS) in septic mice.

The presence of L-PolyP during *E. coli* sepsis increased the mortality rate and the CSS compared to the control group. The raw data were analysed with focus on different time points. A: Administration of L-PolyP shows an overall non-significant alteration of outcome with higher CSS-Score. B: Administration of L-PolyP significantly changes the outcome, resulting in higher clinical severity 44 and 56 hours after sepsis. The data are pooled from two individual experiments with $n=20$ mice per group. CSS-Scoring was evaluated as mean \pm S.E.M by a 2-Way ANOVA Test. * $p \leq 0.05$, ** $p \leq 0.01$, n.s: not significant.

The administration of exogenous L-PolyP during *E. coli* sepsis with wild-type bacteria resulted in a reduction of the survival rate. More specifically, 30% of the mice, which underwent sepsis with simultaneous treatment with L-PolyP, survived compared to 45% of the control group population. Furthermore, most of the deaths occurred within 72 hours after injection of the L-PolyP-bacteria suspension. The early increase in mortality rate led me to an investigation of body fluids of infected mice, in order to analyse the differences in the development of the inflammatory response in the presence or absence of L-PolyP in vivo.

Before euthanasia, 40% of the L-PolyP group mice were deceased, while only 13.3% of the control group mice died. The mean clinical severity sepsis score, indicating the expression of sepsis symptoms such as low activity, altered posture and low reaction to stimuli, was significantly higher for mice treated with L-PolyP. A peritoneal CFU count was performed to quantify the extent of bacterial burden.

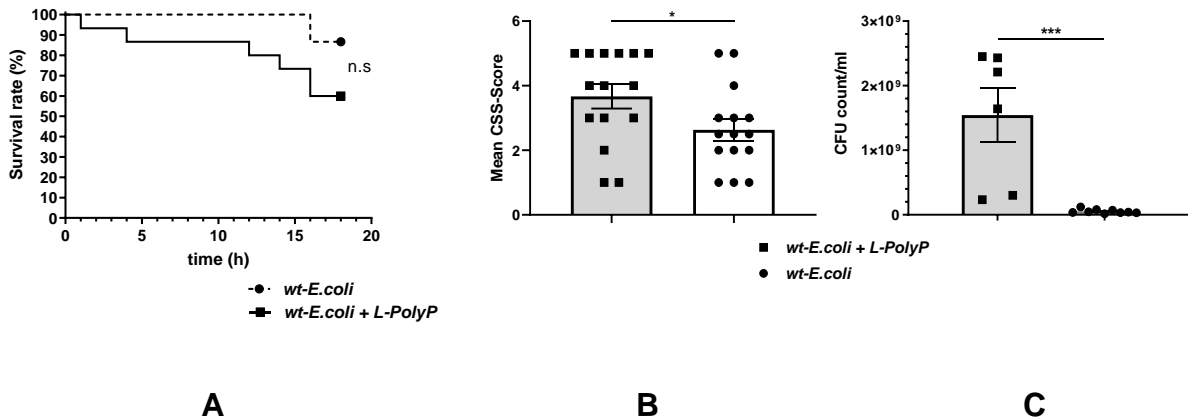


Figure 11: L-PolyP increase bacterial burden and aggravate symptoms of sepsis.

20h after sepsis induction with wt-E. coli plus L-PolyP (10µg/g body weight) injection or PBS (vehicle) injection, mice were euthanized. A: Overall survival of septic mice before euthanasia (Log-rank Mantel-Cox test), n=15 mice/group. B: Comparison of clinical severity scores of both groups before euthanasia (n=15 mice per group). C: Bacterial CFU count of live mice that presented clinical signs of sepsis. n=6 E. coli + L-PolyP group and n=10 E. coli+PBS group. Data of frames B, C were evaluated as mean ± S.E.M and analyzed by Student's t-test. *p≤0.05, ***p≤0.001, n.s: not significant.

The presence of L-PolyP during septic peritonitis resulted in a significant increase in the peritoneal lavage's bacterial burden. Two mice from the L-PolyP group and three mice from the control group were excluded from the analysis, due to undetectable CFUs in more than three lavage dilutions (1:10, 1:100, 1:1000000), suggesting an absence of sepsis. The mean CFU count of L-PolyP treated mice was more than 10-fold higher than the controls. (Mean CFU concentration ± S.E.M = $1.54 \times 10^9 \pm 3.95 \times 10^8$ CFUs/ml in L-PolyP-bacteria group vs. $5.26 \times 10^7 \pm 1.01 \times 10^7$ CFUs/ml in control group).

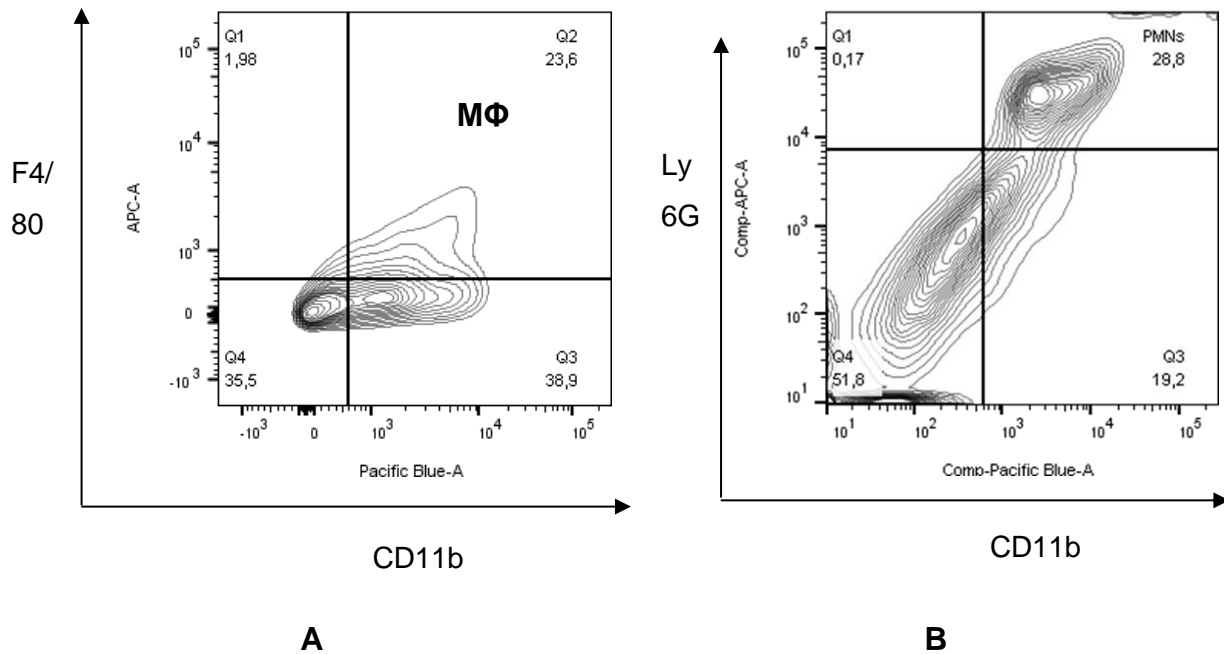


Figure 12: Gating strategy for quantification of peritoneal cells.

A: Gating of macrophages in peritoneal lavage. **B:** Gating of polymorphonuclear neutrophil in peritoneal lavage. The gating was done before flow cytometric count of peritoneal cells and analysis using FlowJo.

Since the development of peritonitis and sepsis is associated with the recruitment of immune cells, I further investigated the peritoneal lavage 20h after sepsis induction, focusing on innate immune cells in flow cytometry. The presence of L-PolyP was associated with a significant increase in the levels of polymorphonuclear neutrophils (PMNs) and macrophages

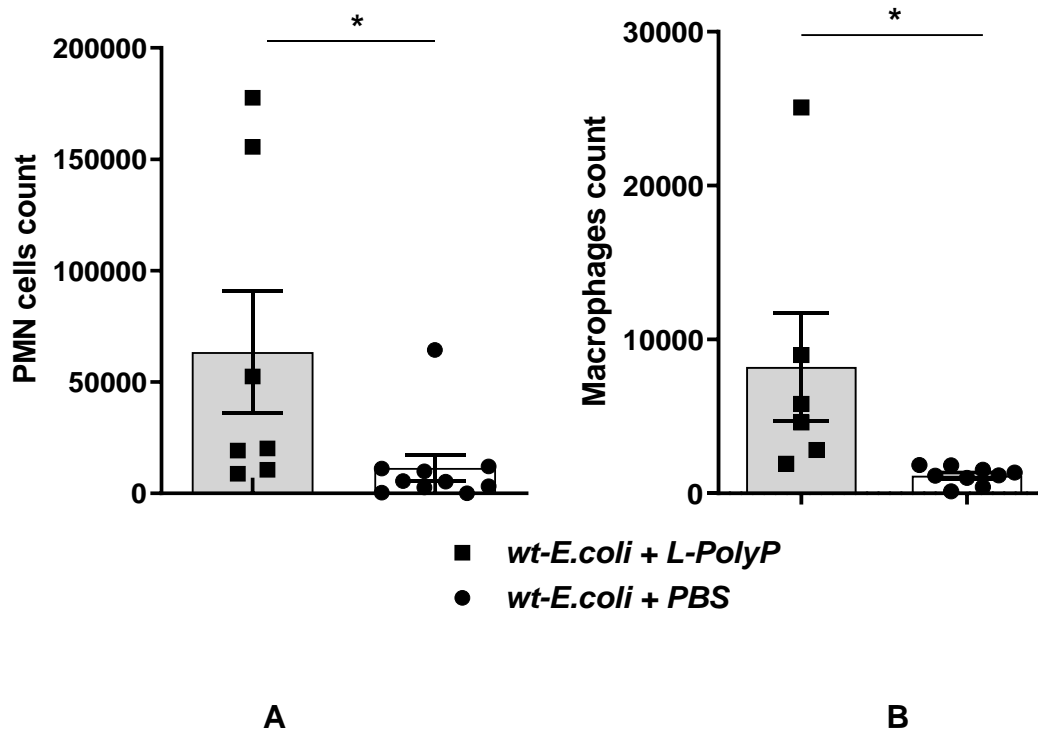


Figure 13: Quantification of peritoneal immune cells during E. coli sepsis.

Mice were sacrificed 20h after intraperitoneal E. coli injection. Cells were quantified by flow cytometry. **A:** Polymorphonuclear neutrophil count in peritoneal lavage. **B:** Macrophages count in peritoneal lavage. Data are presented as mean \pm S.E.M with n=7 for the L-PolyP Group, n=10 for the control group and were evaluated by t-test. * p \leq 0.05.

The bacterial infection in the peritoneal cavity activates the innate immune response, which aims for eliminating of the pathogen and preventing disease progression. The immune response is facilitated and orchestrated by the release of chemokines and cytokines. I quantified a series of different chemotactic factors, which can be secreted from the immune cells at the site of infection and are known to attract monocytes (CXCL10, MIP1 α) and neutrophils (KC – keratinocyte chemoattractant) by ELISA (Figure 14). The concentrations of the chemokines, MCP-1, Eotaxin-1 and RANTES were determined by BioPlex assay (Figure 16). Furthermore, the production of pro-inflammatory (IL-1 β , IL-6, TNF α) and anti-inflammatory cytokines (IL-10) was evaluated using ELISA- and BioPlex-Assays, to compare the innate immunity response in the

presence or absence of L-PolyP during *E. coli* sepsis (Figure 15). The presence of L-PolyP resulted in an increased immune response compared to the control group, because the examined chemotactic and inflammatory cytokines were significantly increased.

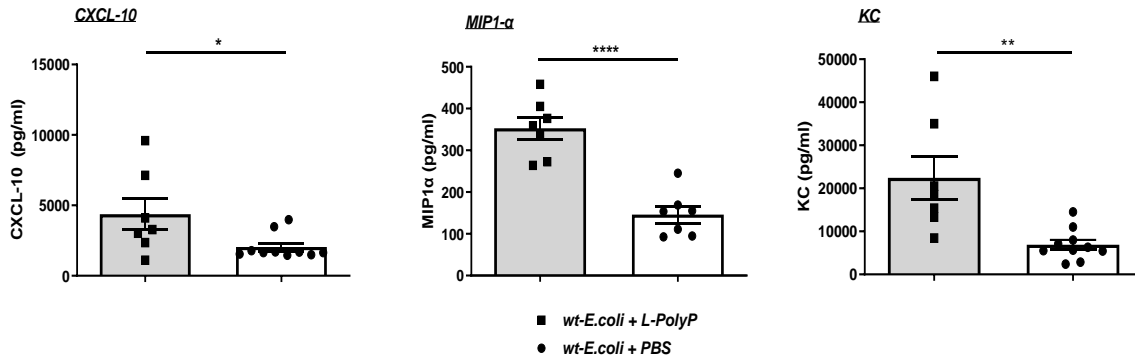


Figure 14: Quantification of chemokines in the peritoneal lavage in the presence or absence of exogenous L-PolyP during *E. coli* sepsis.

Mice were euthanised 20h after intraperitoneal *E. coli* injection. Chemokines of the peritoneal lavage were quantified using ELISA. Graphically shown are the concentrations of CXCL-10, MIP1- α and KC. Data are presented as mean \pm S.E.M with n=7 for the L-PolyP group, n=10 for the control group and were evaluated by t-test. * $p \leq 0.05$. ** $p \leq 0.01$, **** $p \leq 0.0001$.

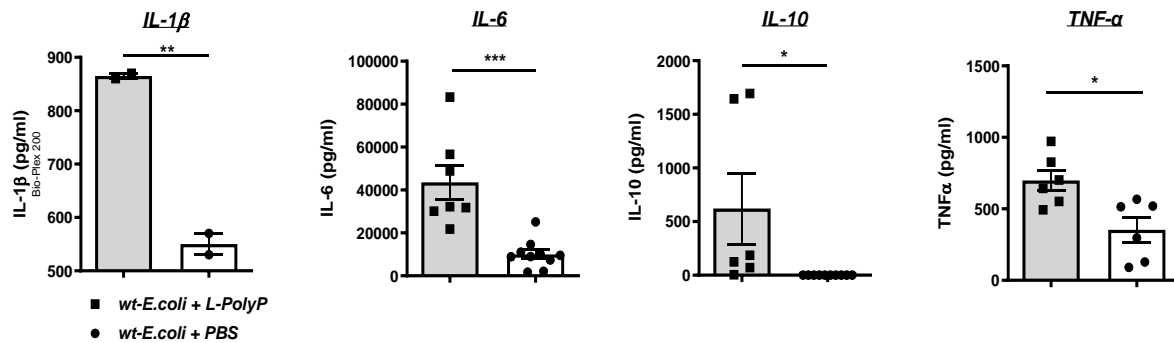


Figure 15: Quantification of pro- and anti-inflammatory cytokines in the peritoneal lavage in the presence or absence of L-PolyP during *E. coli* sepsis.

Mice were euthanised 20h after intraperitoneal *E. coli* injection. Cytokines of the peritoneal lavage were quantified using ELISA and BioPlex-200.

Graphically shown are the concentrations of IL-1 β , IL-6, IL-10, TNF- α . Data are presented as mean \pm S.E.M with n=7 for the L-PolyP group and n=10 for the control group (ELISA) and pooled samples from n=5 mice/group for BioPlex (IL-1 β). Data were evaluated by t-test. * p \leq 0.05. ** p \leq 0.01, *** p \leq 0.001.

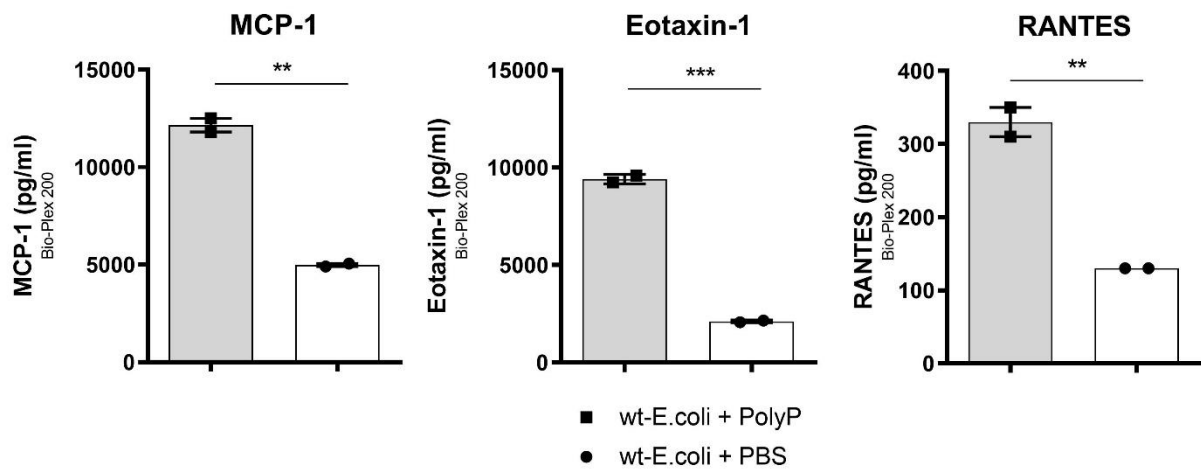


Figure 16: Quantification of chemokines in the peritoneal lavage in the presence or absence of L-PolyP during E. coli sepsis (Bioplex assay).

Mice were euthanised 20h after intraperitoneal E. coli injection. Cytokines and chemokines of the peritoneal lavage were quantified using BioPlex-200. Graphically shown are the concentrations of MCP-1, Eotaxin-1, RANTES. Data are presented as mean \pm S.E.M from pooled samples of n=5 mice/group for the L-PolyP group and control group. The experiment was done only in duplicates due to cost limitations. Data were evaluated by t-test. ** p \leq 0.01, *** p \leq 0.001.

4.4 Short-chain polyphosphates do not influence E. coli sepsis survival

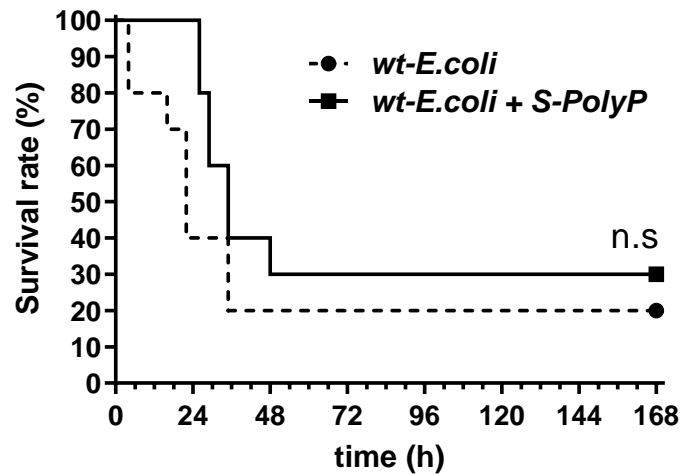


Figure 17: The presence of S-PolyP does not affect survival during E. coli sepsis.

Wild-type E. coli bacteria (E. coli MG1655) and S-PolyP (P70, around 70 Pi-monomers) of a concentration 10µg/g body weight were intraperitoneally injected in mice to induce sepsis. Number of mice per group was n=10. The data were analyzed by the Log-Rank (Mantel-Cox) test and the Gehan-Breslow-Wilcoxon test. n.s: not significant.

E. coli MG1655 bacteremia in the presence of short-chain polyphosphates (S-PolyP) resulted in a survival rate of 30%. The survival rate of the control group that received wt-bacteria and PBS was 20%. Although there is a 10% difference in mortality and survival between the two groups, the overall difference was not significant (Figure 17). For this reason, it was decided not to investigate further the sepsis effects in the presence of S-PolyP, although some previous studies described inflammatory effects for S-PolyP in other models of disease^{1,2,4,174}.

4.5 Recombinant exopolyphosphatase improved the outcome of E. coli sepsis

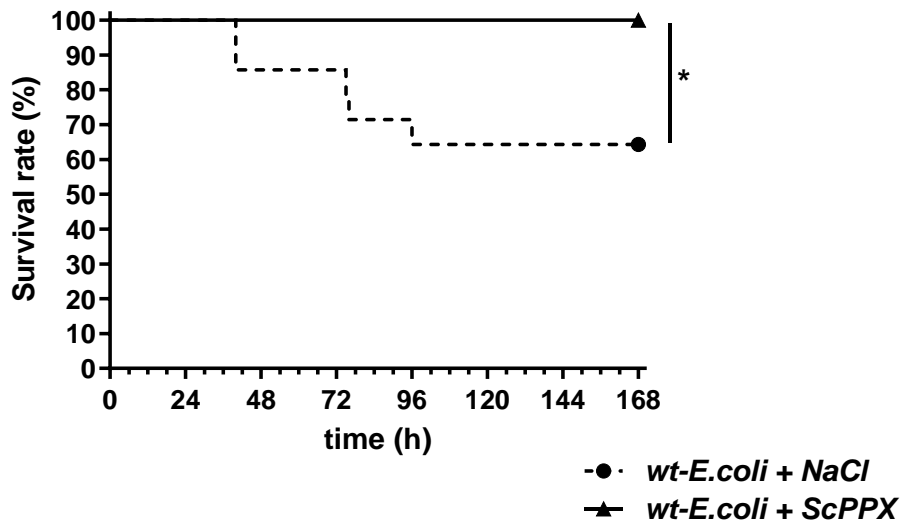


Figure 18: Treatment with recombinant exopolyphosphatase from *Saccharomyces cerevisiae* improves the survival rate during *E. coli* sepsis.

Wild-type *E. coli* bacteria (*E. coli* MG1655) were intraperitoneally injected into mice to induce peritonitis and sepsis. ScPPX (2 μ g/g body weight) was intraperitoneally injected at 3-6h after infection or when the average CSS-Score was greater than 3. The CSS-Scoring was recorded for 7 days. The stock concentration of ScPPX was 1.361mg/ml, estimated by Bradford assay. The enzyme activity was estimated by activity assay, as described above in chapter 3.5.9: 790.9 nmol Pi mg⁻¹PPX min⁻¹. The numbers were n=15 mice for the ScPPX group, n=14 for the control group that received sterile NaCl as empty vehicle. The data were originated from one experiment. The significance was tested by Log-rank (Mantel-Cox) Test. *p \leq 0.05.

The administration of recombinant ScPPX as a treatment for the septic infection caused a significant improvement of the survival rate compared to the control group (Figure 18). Although the 50% survival target in the control group was not achieved due to lower CFU count of the injected bacterial suspension as estimated, 25.8% of the control mice died,

while none of the ScPPX-mice passed away during the experiment. Furthermore, a significant improvement in the clinical symptoms of sepsis was observed in the ScPPX treatment group (Figure 19).

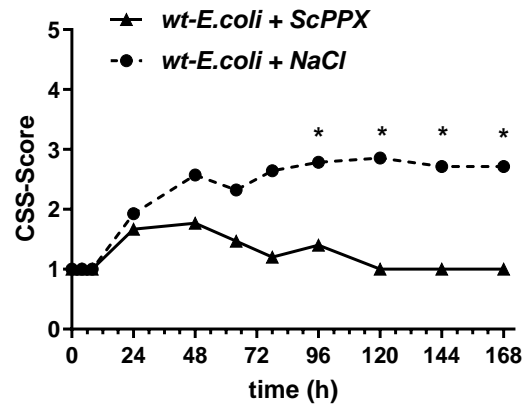


Figure 19: Treatment with recombinant exopolyphosphatase from *Saccharomyces cerevisiae* improves the clinical signs of sepsis.

Mean CSS-Score after intraperitoneal sepsis with wild-type *E. coli* bacteria (*E. coli* MG1655). ScPPX (2 μ g/g body weight) was intraperitoneally injected 4h after infection or when the average CSS-Score was greater than 3. The CSS-Scoring was recorded for 7 days. Stock concentration of ScPPX was 1.361mg/ml. The enzymatic activity was estimated by activity assay, as described above in section 3.5.9.: 790.9 nmol Pi mg⁻¹PPX min⁻¹. n=15 mice for the ScPPX group, n=14 mice for the control group that received sterile NaCl as empty vehicle. One mouse from the control group was euthanised and excluded from the analysis due to injury. Data were evaluated by two-way ANOVA test. *p \leq 0.05.

A further investigation of the effect of ScPPX during sepsis was obtained after euthanasing the septic mice and counting the CFUs in the peritoneal lavage. A higher concentration of CFUs was observed in the control group lavages than in the lavages of ScPPX treated C57BL/6J mice. (Mean CFU \pm S.E.M: in ScPPX group 7.33x10⁶ \pm 5.96x10⁵ CFUs/ml, in control group 12.77x10⁶ \pm 2.41x10⁶ CFUs/ml). The differences in CFU counts could explain the difference in mortality between the two groups.

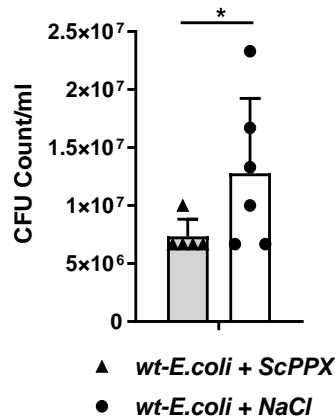


Figure 20: ScPPX treatment caused a decrease in bacterial burden during E. coli sepsis.

E. coli infection and mice treatment with ScPPX were followed by collecting peritoneal lavages after 24 h. Peritoneal lavage was diluted in sterile PBS and plated on sheep blood agar plates. The plates were incubated at 37 °C for 24h before the count. Mouse numbers: n=6 E. coli+ScPPX group and n=5 E. coli+NaCl group. Data were evaluated as mean ± S.E.M and tested by Student's t-test. * p≤0.05.

4.6 Administration of L-PolyP during endotoxemia in mice

Gram-negative bacteria such as E. coli contain lipopolysaccharides (LPS) in their outer bacterial membrane. We found that LPS injection (12.5µg/g body weight) caused a survival rate of ~50% in healthy C57BL/6J mice. To check if L-PolyP influences the mortality in this endotoxemia model, we intraperitoneally injected L-PolyP in a concentration of 10µg/g body weight. The overall survival of mice in the presence of L-PolyP was 70%, while 50% of the mice that underwent LPS-induced sepsis without L-PolyP treatment died. This difference in survival rate was not significant (Figure 21).

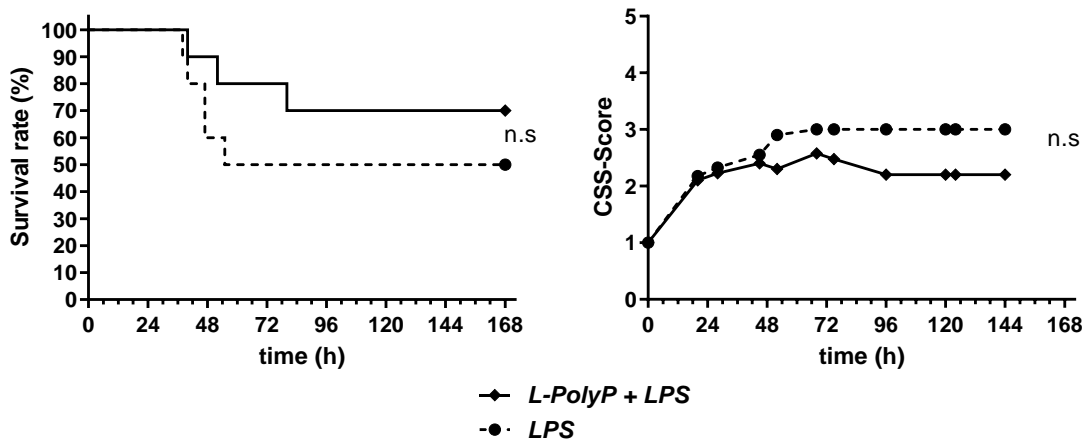


Figure 21: Studies on the administration of L-PolyP in LPS-induced endotoxemia.

To induce endotoxemia-associated shock, mice were i.p. injected with LPS (12.5µg/g body weight) in the presence or absence of L-PolyP (10µg/g body weight). Survival rate **(A)** and sepsis symptoms, evaluated by CSS-Score **(B)**, were documented for one week after injection. The data were obtained with N=10 mice per group. The significance was tested by Log-Rank test **(A)** and 2-Way ANOVA Test **(B)**. n.s. not significant.

In cell cultures, we also examined the effect of L-PolyP on NO production using LPS activated MH-S macrophages. The evaluation of NO release was performed using the Griess assay, taking advantage of a catalytic reaction releasing NO₂⁻. The presence of L-PolyP in cell culture media containing LPS reduced the LPS-induced NO-release (Figure 22).

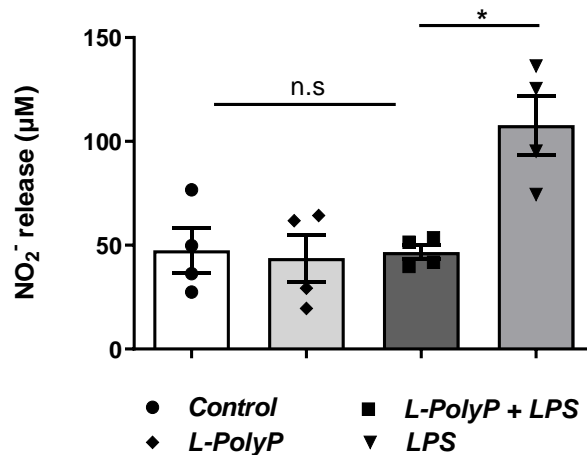


Figure 22: L-PolyP reduce iNOS activity in the context of LPS-induced TLR4 signalling.

MH-S macrophages were stimulated for 24h with *E. coli*-derived LPS (100ng/ml) in the presence or absence of L-PolyP (50µM), with L-PolyP alone or remained untreated (control group). NO release was assessed in the supernatant using Griess assay, by photometrically measuring NO₂⁻ as reaction product of NO. The data are pooled from two experiments and shown as mean ± S.E.M. Significance was tested by t-test. * p≤0.05, n.s not significant.

4.7 L-PolyP triggered CXCL4 release during *E. coli* sepsis

As stated before, S-PolyP, stored in granules of platelets, interacts with the blood coagulation pathways. In this study, we intended to examine the relationship between the inflammation response and blood clotting in dependency of L-PolyP. In *E. coli* sepsis using wt-*E. coli* with or without L-PolyP treatment, we quantified Platelet-factor 4 production in the collected peritoneal lavage and blood plasma, using a PF4/CXCL4 ELISA assay. The presence of L-PolyP during live *E. coli* sepsis led to a highly significant increase in PF4 release (Figure 23).

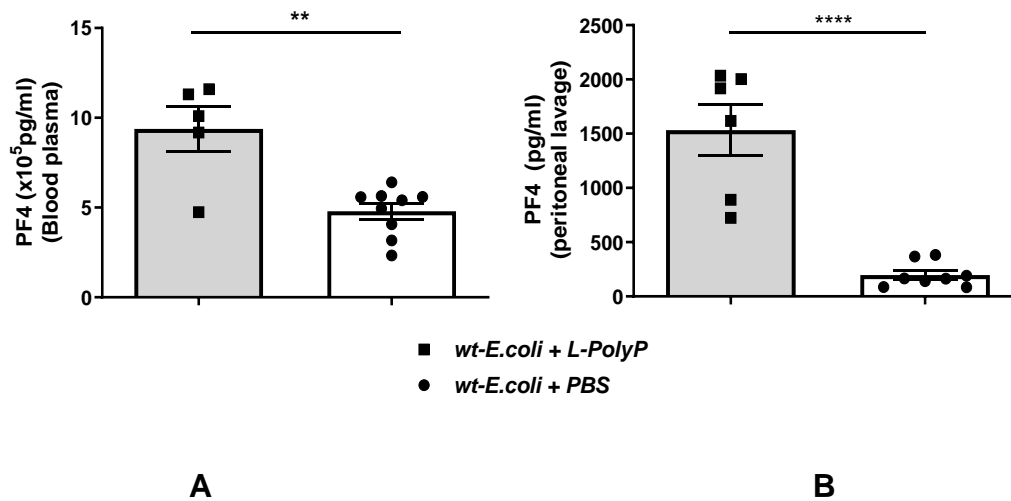


Figure 23: L-PolyP increase platelet-factor 4 release in blood plasma and peritoneal lavage during E. coli sepsis

Mice were sacrificed 20h after intraperitoneal E. coli sepsis. Blood plasma and peritoneal lavage were isolated from mice. PF4/CXCL4 production in blood plasma **(A)** and peritoneal lavage **(B)** was quantified using ELISA. Data are presented as mean \pm S.E.M with n=7 for the L-PolyP group and n=10 for control group and were evaluated by t-test. ** $p \leq 0.01$, **** $p \leq 0.0001$.

Additionally, we measured PF4 production in the collected, cell-free supernatant of MH-S murine, lung macrophages stimulated with L-PolyP (50 μ M) and bacterial lipopolysaccharide (LPS, 100 ng/ml) isolated from E. coli. L-PolyP increased the CXCL4/PF4 chemokine release similarly to bacterial LPS. The combination of both stimulating factors resulted in a massive augmentation of CXCL4/PF4 production from macrophages (Figure 24).

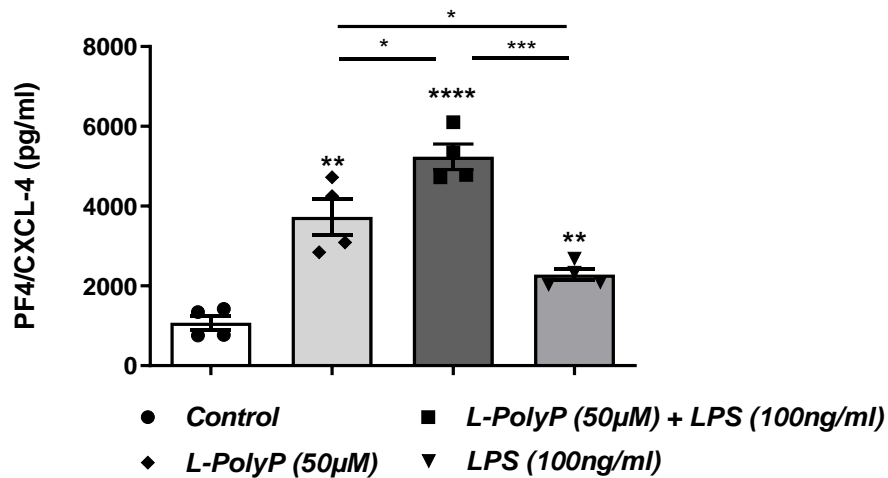


Figure 24: L-Polyp result in platelet-factor 4 release from MH-S macrophages.

MH-S macrophages were stimulated with L-PolyP (50µM) in the presence or absence of *E. coli* derived LPS (100ng/ml) or remained untreated (control group) for 24h. CXCL4/PF4 release was measured by ELISA. The data shown are derived from two pooled experiments. Data are presented as mean ± S.E.M and were evaluated by t-test. * p≤0.05. ** p≤0.01, *** p≤0.001, **** p≤0.0001.

4.8 The presence of L-PolyP decreased bacterial killing by macrophages

An essential aspect of the immune response is the ingestion of pathogens from macrophages, known as phagocytosis. To study the effect of L-PolyP on phagocytosis, we performed in vitro bacterial killing assays with the wild-type *E. coli* strain.

A bacterial suspension (10-fold higher concentration than macrophages) was mixed with either bone-marrow-derived macrophages or MH-S macrophages and incubated at 37 °C under continuous rotation in the presence of L-PolyP or remained untreated. Extracellular CFU count was measured to define the efficiency of bacterial killing during 90 minutes of incubation.

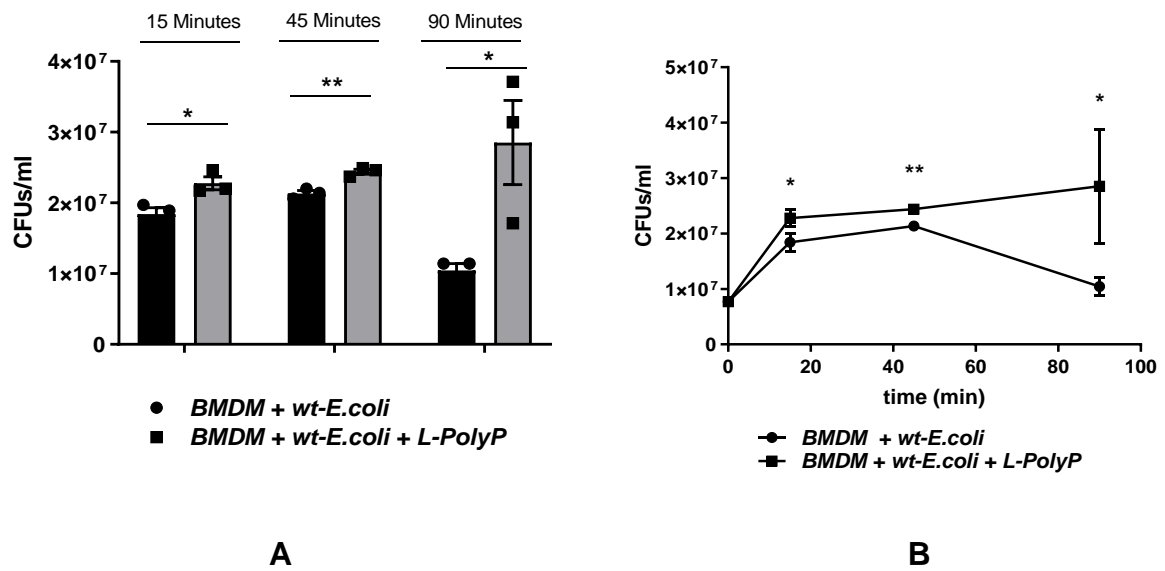


Figure 25: L-PolyP reduce the efficiency of phagocytosis in vitro.

Bacterial suspension of *E. coli* strains MG1655 (wt) was inoculated from overnight culture was mixed with BMDM and incubated at 37 °C under rotation in the presence of L-PolyP or remained untreated (control group).

A: Extracellular CFU count at different time points. **B:** Bacterial killing assay for wt *E. coli* based on extracellular CFU count. Graphs A and B represent the same data in different presentation form. Representative data of individual experiments. The experiment was performed twice with BMDMs and twice with MH-S with the same tendencies. Data are presented as mean ± S.E.M. The significance was tested by t-test. * p≤0.05, ** p≤0.001.

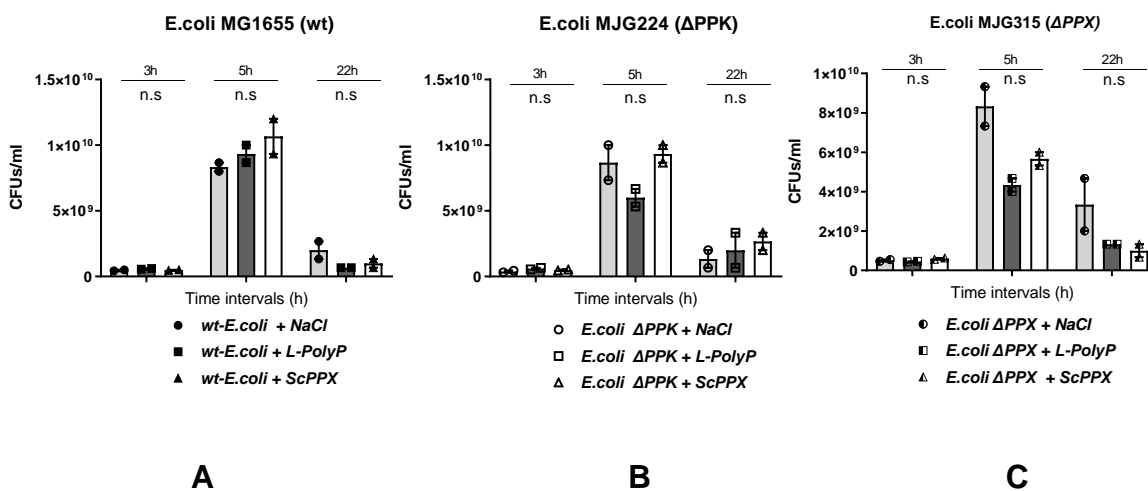
The presence of L-PolyP resulted in a significant increase of extracellular CFU count during bacterial killing assay. Specifically, during bacterial killing of wt-bacteria after 15 minutes of incubation the extracellular CFU count (mean ± S.E.M) for untreated bacterial-macrophage suspension was $1.84 \times 10^7 \pm 7.59 \times 10^5$ CFUs/ml, while for L-PolyP group it was $2.28 \times 10^7 \pm 7.52 \times 10^5$ CFUs/ml. After 45min the CFUs measured for the control group were $2.13 \times 10^7 \pm 3.31 \times 10^5$ CFUs/ml, whereas the L-PolyP group $2.44 \times 10^7 \pm 2.94 \times 10^5$ CFUs/ml. The extracellular CFUs count at t=90min was $1.84 \times 10^7 \pm 9.82 \times 10^5$ CFUs/ml for the control group and $2.28 \times 10^7 \pm 9.21 \times 10^5$ for the L-PolyP group (Figure 25).

4.9 The bacterial growth of E. coli is not affected by exogenous L-PolyP and ScPPX

As seen in previous experiments, the administration of L-PolyP or ScPPX influenced the bacterial growth, measured by CFU count, in murine sepsis models. Therefore, I wanted to examine if exogenous L-PolyP or ScPPX affects the bacterial growth in vitro.

The bacterial suspension was incubated in LB Medium at 37 °C and 200rpm. The bacterial growth was assessed in terms of OD_{600nm}. In addition, the aliquots of the bacterial samples were collected for CFU count at time points 3h, 5h, 22h after the start of incubation.

None of the reagents resulted in a significant change of the bacterial growth, as shown in Figure 27. In conclusion, the E. coli strains could grow physiologically because L-PolyP and ScPPX showed non-toxic characteristics in vitro (Figure 26).



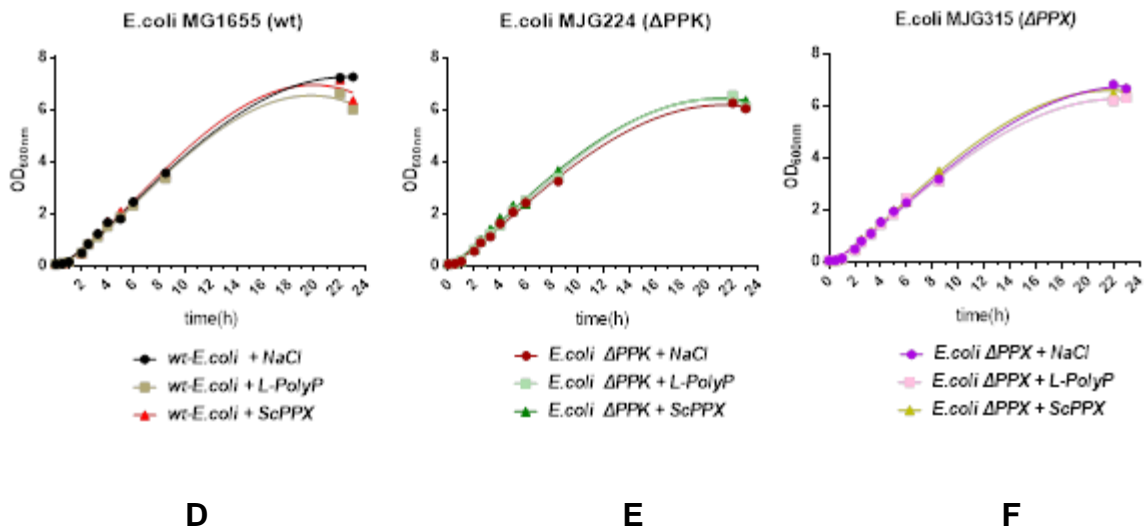


Figure 26: L-PolyP and ScPPX do not influence *E. coli* bacterial growth in vitro

Bacteria of *E. coli* strains MG1655 (wt), MJG224 (Δ PPK), MJG315 (Δ PPX) were inoculated from overnight culture. The bacterial suspension was incubated at 37 °C at 200rpm in LB-medium (Luria-Miller) in the presence of L-PolyP or ScPPX or NaCl 0.9% (untreated). **A-C**: CFU count at different time points. **D-E**: Bacterial growth is expressed in OD600nm at different time points. Data (A-C) are presented as mean \pm S.E.M. Growth curves (D-E) are presented as Beta growth and then decay. Representative data of individual experiments. Significance was tested by t-test (A-C). n.s not significant

5. Discussion

5.1 Establishment of live E. coli sepsis model

Sepsis is a worldwide challenge for public health. It is associated with high mortality rates and high hospitalisation costs^{91,93}. In Germany, the annual incidence was 335 cases per 100,000 persons and the mortality rate was 24.3% in 2013⁹². E. coli infection is one of the common sources of bacteremia and sepsis, resulting in approximately 40,000 deaths alone in the USA (17% of all sepsis deaths) in 2001⁹³. The increase in antibiotic resistance of E. coli isolates in both adult¹⁰⁰ and newborn¹⁰¹ patients is a major problem in the treatment of E. coli associated sepsis. In these experiments, one of my aims was to analyse the growth behaviour of the three E. coli strains, which differed in the expression of PolyP metabolising enzymes and were later used for sepsis studies in mice. I decided to study a sepsis model of intraperitoneal injection of live E. coli to compare these three strains. The infectious dose (CFUs) and application methods for sepsis induction varied between established methods of E. coli bacterial sepsis in rodents¹⁹¹, baboons^{192,193}, pigs¹⁹⁴ and sheep¹⁹⁵. For this reason, I wanted to establish a sepsis model using E. coli MG1655 as wild-type bacterium to achieve 50% mortality rate. After observing that there were no differences in growth or macroscopic appearance between the used E. coli strains, when the bacteria were grown in LB medium under a constant temperature of 37 °C and continuous shaking, I isolated bacteria in the log-phase, so that the number of vital bacteria would be higher. The greatest challenge of this method was the estimation of the lethal dose to achieve 50% survival (LD₅₀) of the mice. Measurement of OD_{600nm} to estimate the LD₅₀ was not accurate because it is based on light scattering, which can be influenced by solution contamination. The CFU count to estimate the infectious dose is a procedure that requires an incubation for at least 24 hours, so it was only used as a control after bacterial intraperitoneal injection. Using FACS flow cytometry and cell gating analysis, I have managed to make an accurate estimation of the bacterial cell counts that were i.p injected in our mouse strain.

I performed many experiments to titrate LD₅₀ in the control group (wt E. coli injection) using CFUs in the range of 8.5×10^8 – 1.7×10^9 CFUs/ml. Although the growth conditions, the preparation and the injection procedure were standardised, the bacterial numbers of the injected groups were not always the same, suggesting that there might be a possible

source of error. The flowcytometric estimation of LD₅₀ was used in all in vivo experiments of this study and provided a more accurate and standardised alternative for sepsis models, that are based on bacterial injection, compared to previous methods^{191,193-196}. Mouse sepsis models could mimic human sepsis due to the multiple correlations of gene expression patterns during the inflammatory response¹⁹⁷. However, animal sepsis models should be standardised and reproducible in order to ensure a better understanding of sepsis pathomechanisms and to enable the development of treatment strategies¹⁹⁸.

5.2 L-PolyP are a modulator of sepsis outcome

Inorganic polyphosphates play an important role during immune response, as described in chapter 2.3.4. In the in vivo experiments, I tested if overexpression of L-PolyP in bacterial cells influences the survival rate and disease severity in murine peritonitis and if the underlying mechanism was based on the effect of inorganic polyphosphate on the inflammatory host response. According to the literature, the absence of polyphosphates reduces virulence of *E. coli* and *Pseudomonas aeruginosa* under stress conditions, making the bacteria more susceptible to antibiotics¹⁵⁸. Other studies investigated the role of short-chain polyphosphates, rather than bacterial-derived long-chain polyphosphates. In my in vivo model, I observed a non-significant change of the survival rate after sepsis induction with Δ ppk bacteria, which was almost 25% higher than the survival rate after wt-*E. coli* sepsis. Although the mortality rate during the first 48 hours after infection was the same based on our Kaplan-Meier survival curve, the mortality and clinical severity score of the wt-group increased progressively. On the contrary, I observed that sepsis from live wild-type bacteria resulted in a slightly higher mortality rate than Ppx-deficient bacteria, but there was again a lack of statistical significance in the observations. Surprisingly, infection with Ppx-deficient *E. coli* (MJG315, Δ ppx) resulted in a higher survival rate and lower CSS than the control group with wt *E. coli*, although it was hypothesised that Δ ppx *E. coli* would increase the mortality rate after infection. A possible explanation is that bacterial strains grew in superfluous LB-medium and not under oxidative stress conditions, in order to overproduce L-PolyP, as shown by Gray et al.¹⁵⁶. However, these results were also statistically not significant. A larger number of mice could provide significant results based on the demonstrated tendency in my experiments

in future studies. Moreover, further experiments with bacteria, that underwent oxidative stress, could significantly alter the outcome of sepsis.

The next in vivo experiment involved i.p injection of wild-type bacteria and administration of body weight adapted L-PolyP (P700). A significant increase of the mortality rate and the clinical scoring compared to the control group mice (wild-type bacteria and bodyweight-adapted PBS solution) was observed. In vitro experiments showed that the presence of L-PolyP does not influence bacterial growth, suggesting that the presence of L-PolyP in our in vivo experiments had most probably an effect on the host immune system rather than on bacteria.

Although many studies described that, platelet-derived, short, inorganic polyphosphates regulate the inflammatory response^{1–4,159,172,175,176,199} and mediate the activation of blood coagulation^{160,161,166,167,199–201} during both in vitro and in vivo, sepsis from *E. coli* MG1655 as wild-type bacteria in the presence of bodyweight-adapted S-PolyP did not influence the survival rate of sepsis. This was a rather surprising result, but our murine models were based on intraperitoneal and not intravascular injection of inorganic polyphosphate or bacterial cells. The intravascular application route is likely to have more potent effects on coagulation and complement pathways. A previous study suggested that S-PolyP suppress the LPS-induced iNOS expression of peritoneal macrophages in vitro⁵, therefore it would be interesting to investigate these effects in vivo. My dissertation aimed primarily to investigate the effect of S-PolyP (10µg/g bodyweight) on the outcome of murine sepsis.

The effect of L-PolyP was also tested in LPS-induced endotoxemia. The presence of body-weight-adapted L-PolyP trended to improve the clinical severity and survival rate of septic mice, but the results were statistically not significant. The concentration of PolyP used was the same as in our peritonitis models (10µg/g bodyweight). It would also be meaningful to test, if S-PolyP would have shown the same effects on LPS-induced endotoxemia, as described in previous studies⁵. This study focussed on the effect of L-PolyP, which is ubiquitously present in bacterial cells.

Similar results were obtained from the work of Dr. rer. nat. Julian Röwe for his doctoral thesis. These data were recently published¹⁷⁸. He established a monomicrobial CLP-

sepsis model after monocolonisation of germ-free mice with wild-type (MG1655) and Ppk1 deficient (MJG224) E. coli bacteria. Monocolonisation with Δ ppk1 bacteria followed by CLP resulted in a higher survival rate. Interesting for further studies would be a monocolonisation with Δ ppx E. coli bacteria (MJG315) to investigate if the CLP sepsis outcome compared to a monocolonisation with wild-type bacteria would be similar to our live injection results.

The clinical scoring assessment in this study was based on an established sepsis severity scoring¹³² and correlated well with the survival data, suggesting that this scoring system could be used for further survival studies.

5.3 The presence of L-PolyP increases the systemic inflammatory response

To investigate the exact mechanism how L-PolyP affect severity and survival of bacterial sepsis, I performed further in vivo and in vitro experiments. The investigation of the effect of L-PolyP in sepsis relied on the administration of exogenous L-PolyP. Additionally, cell culture experiments using MH-S macrophages and BMDMs were performed to investigate the effect of chemically synthesized L-PolyP on macrophages.

The exogenous administration of L-PolyP during sepsis with wild-type bacteria increased mortality. After euthanasia and analysis of the peritoneal lavage, the bacterial CFU count was estimated. A significantly higher concentration of CFU was observed in mice that underwent sepsis with L-PolyP. L-PolyP causes a massive bacterial burden in sepsis. The difference in CFU numbers between both groups can be interpreted as a failure of the immune system to eradicate the bacteria, rather than an advantage in bacterial growth by L-PolyP.

To test if the immune system was compromised, the numbers of two essential cell types of the local immune response in the peritoneum were determined by flow-cytometry: macrophages and neutrophils. The numbers of macrophages and neutrophils were significantly higher in the peritoneal lavage of L-PolyP + E. coli mice. The administration of L-PolyP during wt E. coli sepsis appeared to modulate the host inflammatory response. The CFU count per organ at different infection sites was not determined in my

dissertation. It would be interesting though, to see how the bacterial burden influences extraperitoneal organ systems and how these systems react to bacterial presence.

The analysis of pro-inflammatory and anti-inflammatory cytokines showed that the presence of L-PolyP during sepsis increases the expression of sepsis-associated pro-inflammatory cytokines IL-1 β , IL-6, TNF α , and anti-inflammatory IL-10. L-PolyP also induced the expression of chemokines KC, CXCL10, and MIP-1 α , Eotaxin-1, MCP-1, RANTES, which act as chemoattractants and lead to chemotaxis to the site of infection, in this case, the peritoneal cavity. The effect of L-PolyP on the complement system during sepsis was not part of this study. Suppression of complement activation by PolyP could explain the higher bacterial burden, since polyphosphate of medium and long size after interaction with magnesium and calcium cations cause destabilisation of C5b/C6 complex and therefore of the membrane attack complex C5b-C9⁴. Additionally, S-PolyP inhibit the complement system activation via the classical pathway¹⁷⁶.

The presence of L-PolyP weakens the immune response and leads to an overstimulation of cell migration and activation. Overstimulation of the immune response with an overflow of cytokines and chemokines leads to systemic inflammatory response syndrome, which leads to a septic shock and increased mortality. L-PolyP, a polymer found in bacterial cells, are a modulator of the inflammatory response in bacterial sepsis.

In vitro phagocytosis assays using L-PolyP and live E. coli on bone-derived macrophages showed that the presence of L-PolyP resulted in a significant decrease of bactericidal ability of macrophages. Furthermore, L-PolyP impaired LPS-induced iNOS expression after stimulation of alveolar macrophages. In conclusion, these studies suggest that L-PolyP interfered with macrophage activity and phagocytotic capacity. LPS-induction of iNOS in macrophages leads to bacterial elimination in the beginning of infection⁸¹. iNOS deficiency also resulted in an increased mortality rate in iNOS knockout mice during sepsis after performing CLP²⁰². LPS-mediated NO release leads to bacterial lysis and contributes to hypotension and septic shock, thus increasing mortality. Different iNOS inhibitors can regulate the effects of NO overflow, improving survival and preventing hypotension⁷⁹. Furthermore, in findings from our working group, the presence of L-PolyP reduced iNOS expression and favoured M2 polarisation¹⁷⁸. In this dissertation, the

exogenous administration of L-PolyP increased mortality in bacterial sepsis, while an inhibitory effect of PolyP on iNOS expression was observed in cell cultures. The dose-dependent effect of released NO through iNOS expression in the presence of L-PolyP could be a possible explanation for the contradictory effect of L-PolyP on NO-release and sepsis outcome. The concentration-dependent effect of iNOS expression and thus NO release should be further investigated.

According to the results of this study, the increase in mortality rate occurred between 36-72h after bacterial infection. Further studies could focus on the analysis of cell migration and cytokine/chemokine expression in terms of mRNA induction of regulating genes and of concentration of released pro-inflammatory/anti-inflammatory agents at different time points (for example 48h, 72h). A histological or immunochemical tissue analysis could also provide information on the chemotactic cell migration and total cell population in every tissue. Since sepsis is related to multi-organ failure after the interplay between SIRS and CARS²⁰³, reactions of cell lines involved in defence of lung, heart, liver, spleen and kidney against pathogen could be tested against bacteremia in the presence of L-PolyP. Sepsis diagnosis and severity require the estimation of many different biomarkers (multi-marker approach)¹³³. It would also be interesting to estimate the polyphosphate concentration in blood plasma. Since it is not known if bacterial polyphosphate is released in the bloodstream or affects the immune system after bacterial phagocytosis, polyphosphate detection in blood of septic mice, undergoing sepsis with bacterial strains with modified expression of PolyP metabolising enzymes, e.g. *E. coli* MJG 224 (Δ ppk), *E. coli* MJG 315 (Δ ppx) compared to wild-type bacteria and sham mice (no sepsis), could be an interesting perspective of further studies. If the results are promising, future investigators could also test if inorganic polyphosphates expression in blood plasma of human sepsis patients could predict or could alter the clinical sepsis outcome.

The exact mechanism of immune regulation was analyzed by our group. We described that inorganic polyphosphates interfere with the immune system by influencing macrophage polarisation favouring anti-inflammatory M2 polarisation and altering iNOS expression, reducing type I interferon response, decreasing STAT1 activation and suppressing MCH-II antigen presentation¹⁷⁸. Live fluorescence microscopy revealed

phagocytosis of labelled PolyP by cultured macrophages. The exact mechanism is unknown, although the interaction of PolyP with mTOR pathway, P2Y1 and RAGE receptors was described in tumour proliferation and cell growth models^{204–206}. In vitro experiments with P2Y1 or RAGE knock-out macrophages showed that the L-PolyP-mediated inhibition of iNOS expression was not altered, indicating that P2Y1 and RAGE receptors do not have an essential role in the interference of L-PolyP with macrophages¹⁷⁸. It remains unclear how bacterial polyphosphates are released and interact on the molecular level with the immune system during bacterial sepsis.

The effect of inorganic polyphosphates in other immune cells has not been well studied so far. S-PolyP were identified in mast cell granules, colocalised with serotonin granules, and in basophils. The release of PolyP/serotonin followed IgE activation of the mast cells¹⁷⁵. The PolyP-mediated neutrophil activation and NET-formation through mTOR activation was recently described¹⁷⁷. In this dissertation, the exogenous administration of L-PolyP in sepsis upregulated the chemokine release and caused increased numbers of neutrophils, hinting towards that L-PolyP may also lead to neutrophil activation. Inorganic polyphosphates and especially bacterial-derived L-PolyP could influence the systemic inflammatory response by interfering with other pathways of the immune system, explaining the differences in survival rate in the presence of this multifunctional polymer.

5.4 L-PolyP induce PF4 (CXCL4) release during inflammatory response

Inorganic polyphosphates are detected in dense granules in human platelets and are released after platelet activation.¹⁶⁰ Platelets are also a major source for the release of PF4 (CXCL4)^{207,208}, although PF4 can also be produced at much lower levels by macrophages^{209–211}. In this dissertation, the presence of L-PolyP in alveolar macrophage cultures and in *E. coli* sepsis resulted in a greater release of PF4 compared to LPS and to control group, respectively. So far, it has been shown that S-PolyP have a high binding affinity to PF4¹⁷⁹. After binding of inorganic polyphosphates to PF4 the chemokine is structurally modified and allows binding of anti-PF4/heparin antibodies¹⁷⁹.

PF4 not only plays a modulatory role in coagulation (e.g. role in Heparin-induced-thrombocytopenia) but also regulates the immune response. PF4 binds to bacterial surfaces and facilitates pathogen phagocytosis^{179,180}. PF4 induces a macrophage subtype, M4 macrophage²¹², with ambivalent M1 and M2 macrophage characteristics, for example impaired bacterial phagocytosis (M2) and empowered cytokine secretion (M1)^{213,214}. PF4 interferes with the T-cell immune response by reducing IL-2 and IFN γ release and therefore the autoactivation and proliferation of T cells²¹⁵ and enhances the response of regulatory T-cells, indicating that PF4 could play a role in the development of inflammatory and autoimmune disorders associated with immune system interaction²¹⁶. L-PolyP induce a unique macrophage polarization type, differing in certain aspects from the M2a class¹⁷⁸. L-PolyP/PF4 interaction could be the trigger of macrophage polarization, opening therefore a new future research field. My dissertation focused primarily on the effects of inorganic polyphosphate on the inflammatory response. The only indirect association with the blood coagulation system was provided through the relationship between L-PolyP and PF4. Due to limitations, it was not possible to directly test if the blood coagulation system played a crucial role in the outcome of sepsis in the presence of L-PolyP.

5.5 ScPPX as a potential drug candidate for sepsis

ScPPX is an exopolyphosphatase that regulates PolyP in yeast cells. The purification of ScPPX was performed as described in the supplemental information of Gray et al. "Polyphosphate Is a Primordial Chaperone"²¹⁷, which was based on the initial purification of ScPPX by Andreeva et al.¹⁴¹. ScPPX has a molecular weight of approximately 40kDa and had a higher specific activity rate (220U/mg) than other microorganism-extracted exopolyphosphatases¹⁴¹. The enzymatic activity of exopolyphosphatase was estimated at around 790.9 nmol Pi mg⁻¹ min⁻¹ after hydrolysis of L-PolyP and as evaluated by Biomol assay to detect Pi released.

Purified bodyweight-adapted ScPPX was injected in septic mice after the mice developed a CSS = 3. The control group mice with severe sepsis symptoms (CSS=3) received saline solution.

The presence of ScPPX significantly improved the survival rate by 25.8% compared to the control group. Clinical sepsis severity was also improved when septic mice were treated with ScPPX. Wild-type bacteria have all metabolizing enzymes for inorganic polyphosphate. It is expected that they express PolyP of 100-1000 Pi monomers. Their virulence is not reduced and they can adapt their metabolising ability under stress conditions.

The improved outcome of sepsis in the presence of ScPPX demonstrated that i.p injected ScPPX acts as PolyP neutralization is beneficial. The exact mechanism is not known. There are three proposed mechanisms. The first and second proposed mechanism are based on the observations of Dr. rer. nat. Julian Röwe in his doctoral thesis. The first mechanism suggests that bacterial polyphosphates and bacterial cells are phagocytosed by macrophages and neutrophils; ScPPX is also endocytosed by phagocytosing cells and acts as neutralizing agent intracellularly after endocytosis. The second proposed mechanism suggests that inorganic PolyP are released in the peritoneal cavity after bacterial phagocytosis from migrated immune cells and interfere with the immune system resulting in a higher mortality rate and higher sepsis severity. At a critical time point, ScPPX is injected in murine models and degrades released PolyP intraperitoneally, minimizing the effect of PolyP on the immune response. The third mechanism suggests that ScPPX is absorbed by the bacterial cells and neutralizes PolyP intracellularly. Further analysis of the peritoneal lavage showed that ScPPX treatment decreased bacterial burden during wild-type *E. coli* sepsis.

We performed in vitro experiments to test if the presence of ScPPX influences bacterial growth or phagocytosis with BMDMs. In fact, the presence of ScPPX did not affect bacterial growth and phagocytosis in vitro. Therefore, an interaction of ScPPX and bacterial cells and PolyP neutralization from ScPPX in the bacteria, as suggested from the third interaction mechanism, does not seem to provide an explanation for the improved survival rate during sepsis. The effect of ScPPX on the immune cells and immune response was not examined in this study. Although ScPPX could be used as an alternative treatment against the polyphosphate metabolism of pathogens in septic patients, the effect of ScPPX against other polyphosphate-metabolizing pathogens was not examined. In septic patients, the antibacterial treatment is administered intravenously

and not intraperitoneally. Furthermore, the administration of fluids is part of the optimal treatment of sepsis²¹⁸. An i.v administration of ScPPX in septic mice could also be tested. Reactions of the host against yeast-extracted proteins like ScPPX were not studied in our murine sepsis model. The testing of ScPPX injection with other standardized murine models of bacterial infection can provide exciting avenues of research in future.

5.6 Conclusion

Inorganic polyphosphates are a modulator of the immune response in sepsis. Bacterial polyphosphates and specifically long-chain polyphosphates increase mortality, modulate the inflammatory response, interact with cells of the innate and adaptive immune system. The administration of L-PolyP results in a deterioration of the sepsis outcome and the clinical status of mice with sepsis. The treatment with ScPPX, which degrades PolyP to its monomers, improves survival rate, decreases clinical sepsis severity and bacterial burden. These observations provide rationale for a novel approach to developing sepsis therapies targeting inorganic polyphosphates.

6. Summary (Zusammenfassung)

Polyphosphate (PolyP) sind ein Polymer aus anorganischen Phosphatmonomeren (Pi), welche miteinander durch Phosphoanhydridverbindungen verbunden sind. Anorganische Polyphosphate sind in allen Zelltypen vorhanden. Die Kettenlänge variiert von kleinkettigen Polyphosphaten (short chain polymers, S-PolyP), bestehend aus einigen wenigen bis 100 Pi, bis hin zu langkettigen Polyphosphaten (long chain polymers, L-PolyP), bestehend aus 100-1000 Monomeren. S-PolyP wurden hauptsächlich in Säugetierzellen z.B. in Granula von Thrombozyten nachgewiesen. L-PolyP wurden in prokaryotischen Zellen (z.B. Bakterien) identifiziert.

Studien haben gezeigt, dass PolyP und PolyP-Metabolismus eine wichtige Rolle für die Homöostase von prokaryotischen Mikroorganismen spielen. Der PolyP Metabolismus basiert hauptsächlich auf zwei enzymatischen Reaktionen. Das Enzym Polyphosphatkinase (Ppk) katalysiert die Bindung von Pi Monomeren an die PolyP-Kette. Das Enzym Exopolyphosphatase (Ppx) katalysiert den Abbau von PolyP mit Freisetzung von Pi Monomeren. Polyphosphate dienen als Energiespeicher in Bakterien, weil sie als Pi-Quelle der Synthese von ATP dienen, und besitzen eine Protein-schützende Wirkung unter Stressbedingungen

Basiert auf den nachgewiesenen Effekten von Polyphosphaten in früheren in vitro und in vivo Studien, wurde der Effekt von anorganischen PolyP in der E. coli Sepsis untersucht. Die Hypothese dieser Studie ist, dass anorganische langkettige Polyphosphate von Bakterien eine entscheidende Rolle in der Pathogenese der bakteriellen Sepsis spielen. Die Anwesenheit von L-PolyP könnte das Überleben, den Schweregrad und die Immunantwort während der Sepsis beeinflussen. Es wurde ein Sepsismodell mit intraperitonealer bakterieller Injektion etabliert. Mäuse des Stamms C57BL/6J (männlich, 8-12 Wochen alt) wurden mit lebenden E. coli (wild-typ, Δ ppk, Δ ppx) intraperitoneal injiziert. Anschließend wurden der klinische Zustand und die Mortalitätsraten verfolgt. Des Weiteren wurde ein Sepsismodell mit intraperitonealer E. coli (wild-typ) und gewichtsadaptierter Injektion von L-PolyP (10mg/kg Körpergewicht) Injektion durchgeführt. Anschließend wurde eine Analyse der peritonealen Lavage zur Bestimmung von Immunzellen, Zytokinen und bakterieller Last erstellt. Im letzten Teil

wurde getestet, ob die Verabreichung von rekombinanter PPX aus *Saccharomyces cerevisiae* (ScPPX) einen Einfluss auf die Mortalitätsrate und den Schweregrad der Sepsis hatte.

Es wurden folgende Ergebnisse dokumentiert: Die Anwesenheit von L-PolyP führte zu einer signifikanten Steigerung der Mortalitätsrate und einer deutlichen Verschlechterung des klinischen Zustandes bei Sepsis. Die weitere Analyse von peritonealer Lavage und Blut der Mäuse zeigte, dass langkettige Polyphosphate eine Immunzellmigration und eine signifikante Freisetzung von Zytokinen/Chemokinen verursachten. Die bakterielle Last in Anwesenheit von L-PolyP während der Sepsis war ebenfalls signifikant höher. Die Behandlung mit ScPPX führte zu einer Besserung des septischen Verlaufs mit verminderter Mortalität und einem verbesserten klinischen Zustand im Vergleich zur Kontrollgruppe. Es konnte somit gezeigt werden, dass L-PolyP ein wichtiger Modulator des Immunsystems ist und einen Einfluss auf das Überleben während der Sepsis hat. Die Neutralisation von L-PolyP wäre ein potenzieller Angriffspunkt für neue Therapien der bakteriellen Sepsis oder anderer bakterieller Infektionen. Eine ScPPX-Behandlung könnte als Therapie erwogen werden, sobald der genaue Wirkmechanismus und die Verträglichkeit besser untersucht sind.

7. References

1. Bae, J. S., Lee, W. & Rezaie, A. R. Polyphosphate elicits pro-inflammatory responses that are counteracted by activated protein C in both cellular and animal models. *J. Thromb. Haemost.* **10**, 1145–1151 (2012).
2. Dinarvand, P. *et al.* Polyphosphate amplifies proinflammatory responses of nuclear proteins through interaction with receptor for advanced glycation end products and P2Y1 purinergic receptor. *Blood* **123**, 935–945 (2014).
3. Hassanian, S. M., Dinarvand, P., Smith, S. A. & Rezaie, A. R. Inorganic polyphosphate elicits pro-inflammatory responses through activation of the mammalian target of rapamycin complexes 1 and 2 in vascular endothelial cells. *J. Thromb. Haemost.* **13**, 860–871 (2015).
4. Wat, J. M. *et al.* Polyphosphate suppresses complement via the terminal pathway. *Blood* **123**, 768–776 (2014).
5. Harada, K. *et al.* Inorganic Polyphosphate Suppresses Lipopolysaccharide-Induced Inducible Nitric Oxide Synthase (iNOS) Expression in Macrophages. *PLoS One* **8**, 1–7 (2013).
6. Mao, L. & Franke, J. Symbiosis, dysbiosis, and rebiosis-The value of metaproteomics in human microbiome monitoring. *Proteomics* **15**, 1142–1151 (2015).
7. Rosenberg, E., Sharon, G., Atad, I. & Zilber-Rosenberg, I. The evolution of animals and plants via symbiosis with microorganisms. *Environ. Microbiol. Rep.* **2**, 500–506 (2010).
8. Redinbo, M. R. The microbiota, chemical symbiosis, and human disease. *Journal of Molecular Biology* vol. 426 3877–3891 (2014).
9. Milner, E. C. B., Anolik, J., Cappione, A. & Sanz, I. Human innate B cells: A link between host defense and autoimmunity? *Springer Semin. Immunopathol.* **26**, 433–452 (2005).

10. Festi, D. *et al.* Gut microbiota and metabolic syndrome. *World J. Gastroenterol.* **20**, 16079–16094 (2014).
11. Gagnière, J. *et al.* Gut microbiota imbalance and colorectal cancer. *World J. Gastroenterol.* **22**, 501–518 (2016).
12. Smyth, E. T. M. & Emmerson, A. M. Surgical site infection surveillance. *Journal of Hospital Infection* vol. 45 173–184 (2000).
13. Wiegel, J. Distinction between the gram reaction and the gram type of bacteria. *Int. J. Syst. Bacteriol.* **31**, 88 (1981).
14. Chan, J., Fan, X., Hunter, S. W., Brennan, P. J. & Bloom, B. R. Lipoarabinomannan, a possible virulence factor involved in persistence of *Mycobacterium tuberculosis* within macrophages. *Infect. Immun.* **59**, 1755–1761 (1991).
15. Medzhitov, R. Recognition of microorganisms and activation of the immune response. *Nature* **449**, 819–826 (2007).
16. Landgraeber, S., Jäger, M., Jacobs, J. J. & Hallab, N. J. The pathology of orthopedic implant failure is mediated by innate immune system cytokines. *Mediators Inflamm.* **2014**, (2014).
17. Janeway, C. A. Approaching the asymptote? Evolution and revolution in immunology. *Cold Spring Harb. Symp. Quant. Biol.* **54**, 1–13 (1989).
18. Mogensen, T. H. Pathogen recognition and inflammatory signaling in innate immune defenses. *Clin. Microbiol. Rev.* **22**, 240–273 (2009).
19. Wu, J. & Chen, Z. J. Innate immune sensing and signaling of cytosolic nucleic acids. *Annu. Rev. Immunol.* **32**, 461–488 (2014).
20. Kawai, T. & Akira, S. The role of pattern-recognition receptors in innate immunity: Update on toll-like receptors. *Nat. Immunol.* **11**, 373–384 (2010).
21. Takeda, K., Kaisho, T. & Akira, S. Toll-like receptors. *Annu. Rev. Immunol.* **21**, 335–376 (2003).

22. Kawai, T. & Akira, S. Toll-like Receptors and Their Crosstalk with Other Innate Receptors in Infection and Immunity. *Immunity* **34**, 637–650 (2011).
23. Inohara, N., Chamaillard, M., McDonald, C. & Nuñez, G. NOD-LRR proteins: Role in host-microbial interactions and inflammatory disease. *Annu. Rev. Biochem.* **74**, 355–383 (2005).
24. Kanneganti, T. D., Lamkanfi, M. & Núñez, G. Intracellular NOD-like Receptors in Host Defense and Disease. *Immunity* **27**, 549–559 (2007).
25. Gürtler, C. & Bowie, A. G. Innate immune detection of microbial nucleic acids. *Trends Microbiol.* **21**, 413–420 (2013).
26. Hoving, J. C., Wilson, G. J. & Brown, G. D. Signalling C-type lectin receptors, microbial recognition and immunity. *Cell. Microbiol.* **16**, 185–194 (2014).
27. Borriello, F., Zanoni, I. & Granucci, F. Cellular and molecular mechanisms of antifungal innate immunity at epithelial barriers: The role of C-type lectin receptors. *Eur. J. Immunol.* **50**, 317–325 (2020).
28. Martinon, F., Mayor, A. & Tschopp, J. The inflammasomes: Guardians of the body. *Annu. Rev. Immunol.* **27**, 229–265 (2009).
29. Martinon, F., Burns, K. & Tschopp, J. The Inflammasome: A molecular platform triggering activation of inflammatory caspases and processing of proIL- β . *Mol. Cell* **10**, 417–426 (2002).
30. Lamkanfi, M. & Dixit, V. M. Inflammasomes and their roles in health and disease. *Annu. Rev. Cell Dev. Biol.* **28**, 137–161 (2012).
31. Schroder, K. & Tschopp, J. The Inflammasomes. *Cell* **140**, 821–832 (2010).
32. Kumar, H., Kawai, T. & Akira, S. Pathogen recognition in the innate immune response. *Biochem. J.* **420**, 1–16 (2009).
33. Takeuchi, O. & Akira, S. Pattern Recognition Receptors and Inflammation. *Cell* **140**, 805–820 (2010).
34. Kawai, T. & Akira, S. Signaling to NF- κ B by Toll-like receptors. *Trends Mol. Med.*

- 13**, 460–469 (2007).
35. Akira, S., Uematsu, S. & Takeuchi, O. Pathogen recognition and innate immunity. *Cell* **124**, 783–801 (2006).
 36. Iwasaki, A. & Medzhitov, R. Control of adaptive immunity by the innate immune system. *Nat. Immunol.* **16**, 343–353 (2015).
 37. Chinen, J., Fleisher, T. A. & Shearer, W. T. Adaptive Immunity. *Middleton's Allergy Princ. Pract. Eighth Ed.* **1–2**, 20–29 (2013).
 38. Takahama, Y. Journey through the thymus: Stromal guides for T-cell development and selection. *Nat. Rev. Immunol.* **6**, 127–135 (2006).
 39. Smith-Garvin, J. E., Koretzky, G. A. & Jordan, M. S. T cell activation. *Annu. Rev. Immunol.* **27**, 591–619 (2009).
 40. Fabbri, M., Smart, C. & Pardi, R. T lymphocytes. *Int. J. Biochem. Cell Biol.* **35**, 1004–1008 (2003).
 41. Abbas, A. K., Murphy, K. M. & Sher, A. Functional diversity of helper T lymphocytes. *Nature* vol. 383 787–793 (1996).
 42. Vivier, E. *et al.* Innate or adaptive immunity? The example of natural killer cells. *Science (80-.)*. **331**, 44–49 (2011).
 43. LeBien, T. W. & Tedder, T. F. B lymphocytes: How they develop and function. *Blood* **112**, 1570–1580 (2008).
 44. Hodgkin, P. D., Lee, J. H. & Lyons, A. B. B cell differentiation and isotype switching is related to division cycle number. *J. Exp. Med.* **184**, 277–281 (1996).
 45. Schmidlin, H., Diehl, S. A. & Blom, B. New insights into the regulation of human B-cell differentiation. *Trends Immunol.* **30**, 277–285 (2009).
 46. Höfer, T. *et al.* Adaptation of humoral memory. *Immunol. Rev.* **211**, 295–302 (2006).
 47. Kaminski, D. A. & Stavnezer, J. Antibody class switching differs among SJL,

- C57BL/6 and 129 mice. *Int. Immunol.* **19**, 545–556 (2007).
48. Stavnezer, J. Immunoglobulin class switching Cytokines direct switching by regulating germline transcription. *Curr. Opin. Immunol.* **8**, 199–205 (1996).
 49. Manuscript, A. NIH Public Access. **13**, 555–564 (2014).
 50. Forman, H. J. & Torres, M. Reactive oxygen species and cell signaling: Respiratory burst in macrophage signaling. *Am. J. Respir. Crit. Care Med.* **166**, (2002).
 51. Macrophage, O. F. T. H. E. ANTIGEN-PRESENTING FUNCTION. **1**, (1984).
 52. Amoroso, M. *et al.* LPS-induced cytokine production in human monocytes and macrophages. *Crit. Rev. Immunol.* **31**, 379–446 (2012).
 53. Varol, C., Mildner, A. & Jung, S. *Macrophages: Development and tissue specialization. Annual Review of Immunology* vol. 33 (2015).
 54. Mills, C. D. *et al.* M-1/M-2 Macrophages and the Th1/Th2 Paradigm. (2019) doi:10.4049/jimmunol.164.12.6166.
 55. Underhill, D. M. & Ozinsky, A. PHAGOCYTOSIS OF MICROBES : Complexity in Action . *Annu. Rev. Immunol.* **20**, 825–852 (2002).
 56. Mowat, A. M., Scott, C. L. & Bain, C. C. Barrier-tissue macrophages : functional adaptation to environmental challenges. 1258–1270 (2017) doi:10.1038/nm.4430.
 57. Opal, S. M. The innate immune response to. *Parasite Immunol.* **28**, 127–137 (2000).
 58. Rosadini, C. V. & Kagan, J. C. Early innate immune responses to bacterial LPS. *Curr. Opin. Immunol.* **44**, 14–19 (2017).
 59. Ryu, J. K. *et al.* Reconstruction of LPS Transfer Cascade Reveals Structural Determinants within LBP, CD14, and TLR4-MD2 for Efficient LPS Recognition and Transfer. *Immunity* **46**, 38–50 (2017).
 60. van Lieshout, M. H. P., van der Poll, T. & van't Veer, C. TLR4 inhibition impairs

- bacterial clearance in a therapeutic setting in murine abdominal sepsis. *Inflamm. Res.* **63**, 927–933 (2014).
61. Sheikh, F., Dickensheets, H., Gamero, A. M., Vogel, S. N. & Donnelly, R. P. An essential role for IFN- β in the induction of IFN-stimulated gene expression by LPS in macrophages. *J. Leukoc. Biol.* **96**, 591–600 (2014).
 62. Thomas, K. E., Galligan, C. L., Newman, R. D., Fish, E. N. & Vogel, S. N. Contribution of Interferon- β to the Murine Macrophage Response to the Toll-like Receptor 4 Agonist, Lipopolysaccharide. *J. Biol. Chem.* **281**, 31119–31130 (2006).
 63. Zanotti, S., Kumar, A. & Kumar, A. Cytokine modulation in sepsis and septic shock. *Expert Opin. Investig. Drugs* **11**, 1061–1075 (2005).
 64. Dinarello, C. A. Overview of the IL-1 family in innate inflammation and acquired immunity. *Immunol. Rev.* **281**, 8–27 (2018).
 65. Osuchowski, M. F., Welch, K., Siddiqui, J. & Remick, D. G. Circulating Cytokine/Inhibitor Profiles Reshape the Understanding of the SIRS/CARS Continuum in Sepsis and Predict Mortality. *J. Immunol.* **177**, 1967–1974 (2014).
 66. Oberholzer, A. *et al.* Plasma cytokine measurements augment prognostic scores as indicators of outcome in patients with severe sepsis. *Shock* **23**, 488–493 (2005).
 67. Pallua, N., Low, J. F. A. & Von Heimburg, D. Pathogenic role of interleukin-6 in the development of sepsis. Part II: Significance of anti-interleukin-6 and anti-soluble interleukin-6 receptor- α antibodies in a standardized murine contact burn model. *Crit. Care Med.* **31**, 1495–1501 (2003).
 68. Hildebrand, F., Pape, H. C., Hoevel, P., Krettek, C. & van Griensven, M. The importance of systemic cytokines in the pathogenesis of polymicrobial sepsis and dehydroepiandrosterone treatment in a rodent model. *Shock* **20**, 338–346 (2003).
 69. Ganesan, P., Shanmugam, P., Sattar, S. B. A. & Shankar, S. L. Evaluation of IL-6, CRP and hs-CRP as early markers of neonatal sepsis. *J. Clin. Diagnostic Res.*

- 10**, 13–17 (2016).
70. Zisman, A. D. ANTI_INTERLEUKIN_12_THERAPY_PROTECTS_MICE_IN.6.pdf. (1997).
 71. Ashare, A. *et al.* Anti-inflammatory response is associated with mortality and severity of infection in sepsis. *Am. J. Physiol. - Lung Cell. Mol. Physiol.* **288**, 633–640 (2005).
 72. Esche, C., Stellato, C. & Beck, L. A. Chemokines: Key players in innate and adaptive immunity. *J. Invest. Dermatol.* **125**, 615–628 (2005).
 73. Tosi, M. F. Innate immune responses to infection. *J. Allergy Clin. Immunol.* **116**, 241–249 (2005).
 74. Sokol, C. L. & Luster, A. D. The Chemokine System in Innate Immunity. 1–20 (2016) doi:10.1101/cshperspect.a016303.
 75. De Filippo, K. *et al.* Mast cell and macrophage chemokines CXCL1/CXCL2 control the early stage of neutrophil recruitment during tissue inflammation. *Blood* **121**, 4930–4937 (2013).
 76. Engl, T. N. Luster 1998. (1998).
 77. Speyer, C. L. *et al.* Novel chemokine responsiveness and mobilization of neutrophils during sepsis. *Am. J. Pathol.* **165**, 2187–2196 (2004).
 78. Bogdan, C. Nitric oxide synthase in innate and adaptive immunity: An update. *Trends Immunol.* **36**, 161–178 (2015).
 79. Parratt, J. R. Nitric oxide in sepsis and endotoxaemia. *J. Antimicrob. Chemother.* **41**, 31–39 (1998).
 80. Nathan, C. & Xie, Q. W. Regulation of biosynthesis of nitric oxide. *J. Biol. Chem.* **269**, 13725–13728 (1994).
 81. Chan, E. D. & Riches, D. W. H. IFN- γ + LPS induction of iNOS is modulated by ERK, JNK/SAPK, and p38mapk in a mouse macrophage cell line. *Am. J. Physiol. - Cell Physiol.* **280**, (2001).

82. Razavi, H. M. *et al.* Pulmonary neutrophil infiltration in murine sepsis: Role of inducible nitric oxide synthase. *Am. J. Respir. Crit. Care Med.* **170**, 227–233 (2004).
83. Wang, L. *et al.* Specific role of neutrophil inducible nitric oxide synthase in murine sepsis-induced lung injury in vivo. *Shock* **37**, 539–547 (2012).
84. Singer, M. *et al.* The third international consensus definitions for sepsis and septic shock (sepsis-3). *JAMA - J. Am. Med. Assoc.* **315**, 801–810 (2016).
85. Vincent JL, de Mendonça A, Cantraine F, Moreno R, Takala J, Suter PM, Sprung CL, Colardyn F, B. S. Use of the SOFA score to assess the incidence of organ dysfunction/failure in intensive care units: results of a multicenter, prospective study. Working group on ‘sepsis-related problems’ of the European Society of Intensive Care Medicine. *Crit Care Med.* (**11**), 1793–800.
86. Seymour, C. W. *et al.* Assessment of clinical criteria for sepsis for the third international consensus definitions for sepsis and septic shock (sepsis-3). *JAMA - J. Am. Med. Assoc.* **315**, 762–774 (2016).
87. Shankar-Hari, M. *et al.* Developing a New Definition and Assessing New Clinical Criteria for Septic Shock. *Jama* **315**, 775 (2016).
88. Keeley, A., Hine, P. & Nsutebu, E. The recognition and management of sepsis and septic shock: A guide for non-intensivists. *Postgrad. Med. J.* **93**, 626–634 (2017).
89. Lagu, T. *et al.* Hospitalizations, costs, and outcomes of severe sepsis in the United States 2003 to 2007. *Crit. Care Med.* **40**, 754–761 (2012).
90. Torio, Celeste M., Andrews, R. M. National Inpatient Hospital Costs: The Most Expensive Conditions by Payer, 2011. *HCUP statistical Brief #160* (2013).
91. Rudd, K. E. *et al.* Global, regional, and national sepsis incidence and mortality, 1990–2017: analysis for the Global Burden of Disease Study. *Lancet* **395**, 200–211 (2020).

92. Fleischmann, C. *et al.* Hospital Incidence and Mortality Rates of Sepsis: An Analysis of Hospital Episode (DRG) Statistics in Germany From 2007 to 2013. *Dtsch. Aerzteblatt Online* (2018) doi:10.3238/arztebl.2016.0159.
93. Russo, T. A. & Johnson, J. R. Medical and economic impact of extraintestinal infections due to *Escherichia coli*: Focus on an increasingly important endemic problem. *Microbes Infect.* **5**, 449–456 (2003).
94. Schrag, S. J. *et al.* Epidemiology of invasive early-onset neonatal sepsis, 2005 to 2014. *Pediatrics* **138**, (2016).
95. Russo, T. A. & Johnson, J. R. Proposal for a new inclusive designation for extraintestinal pathogenic isolates of *Escherichia coli*: ExPEC. *J. Infect. Dis.* **181**, 1753–1754 (2000).
96. Micol, R. *et al.* *Escherichia coli* native valve endocarditis. *Clin. Microbiol. Infect.* **12**, 401–403 (2006).
97. Clermont, O., Bonacorsi, S. & Bingen, E. Rapid and simple determination of the *Escherichia coli* phylogenetic group. *Appl. Environ. Microbiol.* **66**, 4555–4558 (2000).
98. Johnson, J. R. & Russo, T. A. Extraintestinal pathogenic *Escherichia coli*: ‘The other bad *E coli*’. *J. Lab. Clin. Med.* **139**, 155–162 (2002).
99. Johnson, J. R. & Stell, A. L. Extended virulence genotypes of *Escherichia coli* strains from patients with urosepsis in relation to phylogeny and host compromise. *J. Infect. Dis.* **181**, 261–272 (2000).
100. Wang, M. C., Tseng, C. C., Chen, C. Y., Wu, J. J. & Huang, J. J. The role of bacterial virulence and host factors in patients with *Escherichia coli* bacteremia who have acute cholangitis or upper urinary tract infection. *Clin. Infect. Dis.* **35**, 1161–1166 (2002).
101. Cole, B. K., Ilikj, M., McCloskey, C. B. & Chavez-Bueno, S. Antibiotic resistance and molecular characterization of bacteremia *Escherichia coli* isolates from newborns in the United States. *PLoS One* **14**, 1–17 (2019).

102. Jauréguy, F. *et al.* Host and bacterial determinants of initial severity and outcome of Escherichia coli sepsis. *Clin. Microbiol. Infect.* **13**, 854–862 (2007).
103. May, A. E., Neumann, F. J. & Preissner, K. T. The relevance of blood cell-vessel wall adhesive interactions for vascular thrombotic disease. *Thromb. Haemost.* **82**, 962–970 (1999).
104. Bierhaus, A., Ph, D., Chen, J. & Nawroth, P. P. LPS and Cytokine-Activated Endothelium INFLAMMATORY CHANGES IN. **26**, (2000).
105. Mackman, N. Regulation of the tissue factor gene. *FASEB J.* **9**, 883–889 (1995).
106. Bierhaus, A. *et al.* Mechanism of the tumor necrosis factor α -mediated induction of endothelial tissue factor. *J. Biol. Chem.* **270**, 26419–26432 (1995).
107. Bierhaus, A. & Nawroth, P. P. Modulation of the vascular endothelium during infection--the role of NF-kappa B activation. *Contrib. Microbiol.* **10**, 86–105 (2003).
108. van der Poll, T. & Opal, S. M. Host-pathogen interactions in sepsis. *Lancet Infect. Dis.* **8**, 32–43 (2008).
109. Ward, P. A. The harmful Role of C5a on innate immunity in sepsis. *J. Innate Immun.* **2**, 439–445 (2010).
110. Rittirsch, D. *et al.* Functional roles for C5a receptors in sepsis. *Nat. Med.* **14**, 551–557 (2008).
111. Czermak, B. J. *et al.* Protective effects of C5a blockade in sepsis. *Nat. Med.* **5**, 788–792 (1999).
112. Boomer, J. S. *et al.* Immunosuppression in patients who die of sepsis and multiple organ failure. *JAMA - J. Am. Med. Assoc.* **306**, 2594–2605 (2011).
113. Taneja, R., Sharma, A. P., Hallett, M. B., Findlay, G. P. & Morris, M. R. Immature circulating neutrophils in sepsis have impaired phagocytosis and calcium signaling. *Shock* **30**, 618–622 (2008).
114. Munoz, C. *et al.* Dysregulation of in vitro cytokine production by monocytes during sepsis. *J. Clin. Invest.* **88**, 1747–1754 (1991).

115. Delano, M. J. *et al.* MyD88-dependent expansion of an immature GR-1 +CD11b+ population induces T cell suppression and Th2 polarization in sepsis. *J. Exp. Med.* **204**, 1463–1474 (2007).
116. Hynninen, M. *et al.* Predictive value of monocyte histocompatibility leukocyte antigen-DR expression and plasma interleukin-4 and -10 levels in critically ill patients with sepsis. *Shock* **20**, 1–4 (2003).
117. Hotchkiss RS, Swanson PE, Freeman BD, Tinsley KW, Cobb JP, Matuschak GM, Buchman TG, K. I. Apoptotic cell death in patients with sepsis, shock, and multiple organ dysfunction. *Crit Care Med.* (**7**), 1230–51 (1999).
118. Hotchkiss, R. S. *et al.* Prevention of lymphocyte cell death in sepsis improves survival in mice. *Proc. Natl. Acad. Sci. U. S. A.* **96**, 14541–14546 (1999).
119. Drewry, A. *et al.* Persistent lymphopenia after diagnosis of sepsis predicts mortality. *Shock* **42**, 383–391 (2014).
120. Sato, R. & Nasu, M. A review of sepsis-induced cardiomyopathy. *J. Intensive Care* **3**, 1–7 (2015).
121. Galley, H. F. Oxidative stress and mitochondrial dysfunction in sepsis. *Br. J. Anaesth.* **107**, 57–64 (2011).
122. Takasu, O. *et al.* Mechanisms of cardiac and renal dysfunction in patients dying of sepsis. *Am. J. Respir. Crit. Care Med.* **187**, 509–517 (2013).
123. Levi, M. & Sivapalaratnam, S. Disseminated intravascular coagulation: an update on pathogenesis and diagnosis. *Expert Rev. Hematol.* **11**, 663–672 (2018).
124. Dellinger, R. P. *et al.* Surviving sepsis campaign: International guidelines for management of severe sepsis and septic shock, 2012. *Intensive Care Med.* **39**, 165–228 (2013).
125. Rhodes, A. *et al.* *Surviving Sepsis Campaign: International Guidelines for Management of Sepsis and Septic Shock: 2016.* *Intensive Care Medicine* vol. 43 (Springer Berlin Heidelberg, 2017).

126. Weiss, S. L. *et al.* Surviving sepsis campaign international guidelines for the management of septic shock and sepsis-associated organ dysfunction in children. *Intensive Care Med.* **46**, 10–67 (2020).
127. Poli-de-Figueiredo, L. F., Garrido, A. G., Nakagawa, N. & Sannomiya, P. Experimental models of sepsis and their clinical relevance. *Shock* **30**, 53–59 (2008).
128. Rittirsch, D., Hoesel, L. M. & Ward, P. A. The disconnect between animal models of sepsis and human sepsis. *J. Leukoc. Biol.* **81**, 137–143 (2007).
129. Dejager, L., Pinheiro, I., Dejonckheere, E. & Libert, C. Cecal ligation and puncture: The gold standard model for polymicrobial sepsis? *Trends in Microbiology* vol. 19 198–208 (2011).
130. Esmon, C. T. P. Why do animal models (sometimes) fail to mimic human sepsis? *Crit. Care Med.* **32**, S219–S222.
131. Shrum, B. *et al.* A robust scoring system to evaluate sepsis severity in an animal model. *BMC Res. Notes* **7**, 1–11 (2014).
132. Gonnert, F. A. *et al.* Characteristics of clinical sepsis reflected in a reliable and reproducible rodent sepsis model. *J. Surg. Res.* **170**, e123–e134 (2011).
133. Cho, S. Y. & Choi, J. H. Biomarkers of Sepsis. *Infect. Chemother.* **46**, 1–12 (2014).
134. Van den Blink, B. *et al.* Human endotoxemia activates p38 MAP kinase and p42/44 MAP kinase, but not c-Jun N-terminal kinase. *Mol. Med.* **7**, 755–760 (2001).
135. Pajkrt, D. *et al.* Interleukin-10 inhibits activation of coagulation and fibrinolysis during human endotoxemia. *Blood* **89**, 2701–2705 (1997).
136. De Kruif, M. D. *et al.* The influence of corticosteroids on the release of novel biomarkers in human endotoxemia. *Intensive Care Med.* **34**, 518–522 (2008).
137. Harold, F. M. Inorganic polyphosphates in biology: structure, metabolism, and

- function. *Bacteriol. Rev.* **30**, 772–94 (1966).
138. J. Biol. Chem.-1995-Kumble-5818-22.pdf.
 139. Kornberg, A. Inorganic polyphosphate: Toward making a forgotten polymer unforgettable. *J. Bacteriol.* **177**, 491–496 (1995).
 140. Kornberg, S. R. Adenosine triphosphate synthesis from polyphosphate by an enzyme from *Escherichia coli*. *BBA - Biochim. Biophys. Acta* **26**, 294–300 (1957).
 141. Andreeva, N. A. & Okorokov, L. A. Purification and characterization of highly active and stable polyphosphatase from *Saccharomyces cerevisiae* cell envelope. *Yeast* **9**, 127–139 (1993).
 142. Archibald, F. S. & Fridovich, I. Investigations of the state of the manganese in *Lactobacillus plantarum*. *Arch. Biochem. Biophys.* **215**, 589–596 (1982).
 143. Dunn, T., Gable, K. & Beeler, T. Regulation of cellular Ca²⁺ by yeast vacuoles. *J. Biol. Chem.* **269**, 7273–7278 (1994).
 144. Pick, U. & Weiss, M. Polyphosphate hydrolysis within acidic vacuoles in response to amine-induced alkaline stress in the halotolerant alga *Dunaliella salina*. *Plant Physiol.* **97**, 1234–1240 (1991).
 145. Zhang, H., Ishige, K. & Kornberg, A. A polyphosphate kinase (PPK2) widely conserved in bacteria. *Proc. Natl. Acad. Sci. U. S. A.* **99**, 16678–16683 (2002).
 146. Akiyama, M., Crooke, E. & Kornberg, A. An exopolyphosphatase of *Escherichia coli*: The enzyme and its ppx gene in a polyphosphate operon. *J. Biol. Chem.* **268**, 633–639 (1993).
 147. Wurst, H., Shiba, T. & Kornberg, A. The gene for a major exopolyphosphatase of *Saccharomyces cerevisiae*. *J. Bacteriol.* **177**, 898–906 (1995).
 148. Rashid, M. H. *et al.* Polyphosphate kinase is essential for biofilm development, quorum sensing, and virulence of *Pseudomonas aeruginosa*. *Proc. Natl. Acad. Sci. U. S. A.* **97**, 9636–9641 (2000).
 149. Sanyal, S., Banerjee, S. K., Banerjee, R., Mukhopadhyay, J. & Kundu, M.

- Polyphosphate kinase 1, a central node in the stress response network of *Mycobacterium tuberculosis*, connects the two-component systems MprAB and SenX3-RegX3 and the extracytoplasmic function sigma factor, sigma E. *Microbiol. (United Kingdom)* **159**, 2074–2086 (2013).
150. Rao, N. N., Gómez-García, M. R. & Kornberg, A. Inorganic Polyphosphate: Essential for Growth and Survival. *Annu. Rev. Biochem.* **78**, 605–647 (2009).
 151. Rashid, M. H., Rao, N. N. & Kornberg, A. Inorganic polyphosphate is required for motility of bacterial pathogens. *J. Bacteriol.* **182**, 225–227 (2000).
 152. Rashid, M. H. & Kornberg, A. Inorganic polyphosphate is needed for swimming, swarming, and twitching motilities of *Pseudomonas aeruginosa*. *Proc. Natl. Acad. Sci. U. S. A.* **97**, 4885–4890 (2000).
 153. Rao, N. N., Liu, S. & Kornberg, A. Inorganic polyphosphate in *Escherichia coli*: The phosphate regulon and the stringent response. *J. Bacteriol.* **180**, 2186–2193 (1998).
 154. Rao, N. N. & Kornberg, A. Inorganic polyphosphate supports resistance and survival of stationary-phase *Escherichia coli*. *J. Bacteriol.* **178**, 1394–1400 (1996).
 155. Kim, K.-S., Rao, N. N., Fraley, C. D. & Kornberg, A. Inorganic polyphosphate is essential for long-term survival and virulence factors in *Shigella* and *Salmonella* spp. *Proc. Natl. Acad. Sci.* **99**, 7675–7680 (2002).
 156. Gray, M. J. *et al.* Polyphosphate Is a Primordial Chaperone. *Mol. Cell* **53**, 689–699 (2014).
 157. Rudat, A. K., Pokhrel, A., Green, T. J. & Gray, M. J. Mutations in *Escherichia coli* Polyphosphate Kinase That Lead to Dramatically Increased In Vivo Polyphosphate Levels. *J. Bacteriol.* **200**, 1–20 (2018).
 158. Ortiz-Severín, J., Varas, M., Bravo-Toncio, C., Guiliani, N. & Chávez, F. P. Multiple antibiotic susceptibility of polyphosphate kinase mutants (ppk1 and ppk2) from *Pseudomonas aeruginosa* PAO1 as revealed by global phenotypic analysis. *Biol. Res.* **48**, 1–6 (2015).

159. Zhang, Q., Li, Y. & Tang, C. M. The role of the exopolyphosphatase PPX in avoidance by *Neisseria meningitidis* of complement-mediated killing. *J. Biol. Chem.* **285**, 34259–34268 (2010).
160. Ruiz, F. A., Lea, C. R., Oldfield, E. & Docampo, R. Human platelet dense granules contain polyphosphate and are similar to acidocalcisomes of bacteria and unicellular eukaryotes. *J. Biol. Chem.* **279**, 44250–44257 (2004).
161. Smith, S. A. *et al.* Polyphosphate exerts differential effects on blood clotting, depending on polymer size. *Blood* **116**, 4353–4359 (2010).
162. Wu, Y. Contact pathway of coagulation and inflammation. *Thromb. J.* **13**, (2015).
163. Broze, G. J. Tissue factor pathway inhibitor and the revised theory of coagulation. *Annu. Rev. Med.* **46**, 103–112 (1995).
164. Dahlbäck, B. Blood coagulation. *Lancet* **355**, 1627–1632 (2000).
165. Morrissey, J. H. inflammation. **95**, 11–18 (2013).
166. Puy, C. *et al.* Platelet-derived short-chain polyphosphates enhance the inactivation of tissue factor pathway inhibitor by activated coagulation factor XI. *PLoS One* **11**, 1–17 (2016).
167. Choi, S. H., Smith, S. A. & Morrissey, J. H. Polyphosphate accelerates factor V activation by factor XIa. *Thromb. Haemost.* **113**, 599–604 (2015).
168. Smith, S. A. & Morrissey, J. H. Polyphosphate enhances fibrin clot structure. *Blood* **112**, 2810–2816 (2008).
169. Whyte, C. S. *et al.* Polyphosphate delays fibrin polymerisation and alters the mechanical properties of the fibrin network. *Thromb. Haemost.* **116**, 897–903 (2016).
170. Mitchell, J. L. *et al.* Polyphosphate colocalizes with factor XII on platelet-bound fibrin and augments its plasminogen activator activity. *Blood* **128**, 2834–2845 (2016).
171. Renné, T. & Stavrou, E. X. Roles of factor XII in innate immunity. *Front. Immunol.*

- 10**, 1–9 (2019).
172. Müller, F. *et al.* Platelet Polyphosphates Are Proinflammatory and Procoagulant Mediators In Vivo. *Cell* **139**, 1143–1156 (2009).
 173. Araújo, R. C. *et al.* Altered neutrophil homeostasis in kinin B1 receptor-deficient mice. *Biol. Chem.* **382**, 91–96 (2001).
 174. Hassanian, S. M., Avan, A. & Ardeshirylajimi, A. Inorganic polyphosphate: a key modulator of inflammation. *J. Thromb. Haemost.* **15**, 213–218 (2017).
 175. Moreno-Sanchez, D., Hernandez-Ruiz, L., Ruiz, F. A. & Docampo, R. Polyphosphate is a novel pro-inflammatory regulator of mast cells and is located in acidocalcisomes. *J. Biol. Chem.* **287**, 28435–28444 (2012).
 176. Wijeyewickrema, L. C. *et al.* Polyphosphate is a novel cofactor for regulation of complement by a serpin, C1 inhibitor. *Blood* **128**, 1766–1776 (2016).
 177. Chrysanthopoulou, A. *et al.* Interferon lambda1/IL-29 and inorganic polyphosphate are novel regulators of neutrophil-driven thromboinflammation. *J. Pathol.* **243**, 111–122 (2017).
 178. Roewe, J. *et al.* Bacterial polyphosphates interfere with the innate host defense to infection. *Nat. Commun.* **11**, (2020).
 179. Brandt, S. *et al.* Polyphosphates form antigenic complexes with platelet factor 4 (PF4) and enhance PF4-binding to bacteria. *Thromb. Haemost.* **114**, 1189–1198 (2015).
 180. Thachil, J. The prothrombotic potential of platelet factor 4. *Eur. J. Intern. Med.* **21**, 79–83 (2010).
 181. Krauel, K. *et al.* Platelet factor 4 binds to bacteria-inducing antibodies cross-reacting with the major antigen in heparin-induced thrombocytopenia. *Blood* **117**, 1370–1378 (2011).
 182. Tierschutzgesetz. <http://www.gesetze-im-internet.de/tierschg/index.html>.
 183. Li, B. *et al.* Supplemental information. *Biotechnol. Bioeng.* **53**, 1–9 (2010).

184. Biolabs, N. E. Transformation Protocol for BL21(DE3) Competent Cells (C2527). <https://international.neb.com/protocols/0001/01/01/transformation-protocol-for-bl21-de3-competent-cells-c2527>.
185. Drevets, D. A., Canono, B. P. & Campbell, P. A. Measurement of Bacterial Ingestion and killing by macrophages. *Curr. Protoc. Immunol.* **2015**, 14.6.1-14.6.17 (2015).
186. Mbawuike, I. N. & Herscowitz, H. B. MH-S, a murine alveolar macrophage cell line: Morphological, cytochemical, and functional characteristics. *J. Leukoc. Biol.* **46**, 119–127 (1989).
187. Wikenheiser, K. A. *et al.* Production of immortalized distal respiratory epithelial cell lines from surfactant protein C/simian virus 40 large tumor antigen transgenic mice. *Proc. Natl. Acad. Sci. U. S. A.* **90**, 11029–11033 (1993).
188. Livak, K. J. & Schmittgen, T. D. Analysis of Relative Gene Expression Data Using Real-Time Quantitative PCR and the $2^{-\Delta\Delta CT}$ Method. *Methods* **25**, 402–408 (2001).
189. Bosmann, M. *et al.* The outcome of polymicrobial sepsis is independent of T and B cells. *Shock* **36**, 396–401 (2011).
190. Measurements, C. M., Definitions, A. P. & Validation, A. Bio-Plex Pro Mouse Th17 Assays.
191. Pass, L. J., Schloerb, P. R., Pearce, F. J. & Drucker, W. R. Cardiopulmonary response of the rat to gram-negative bacteremia. *Am. J. Physiol. - Hear. Circ. Physiol.* **15**, (1984).
192. Pegbp30 Baboon Shock Jsr 1995.Pdf.
193. Taylor, J., Reinhart, K. & Vallet, B. Staging of the pathophysiologic responses of the primate microvasculature to *Escherichia coli* and endotoxin: Examination of the elements of the compensated response and their links to the corresponding uncompensated lethal variants. *Crit. Care Med.* **29**, (2001).

194. Dehring, D. J. *et al.* Comparison of live bacteria infusions in a porcine model of acute respiratory failure. *J. Surg. Res.* **34**, 151–158 (1983).
195. Di Giantomasso, D., May, C. N. & Bellomo, R. Vital organ blood flow during hyperdynamic sepsis. *Chest* **124**, 1053–1059 (2003).
196. Experimental Escherichia coli peritonitis in immunosuppressed mice : the role of specific and non- specific immunity. **24**, 33–39 (2019).
197. Fay, D. L. 濟無No Title No Title No Title. *Angew. Chemie Int. Ed.* **6**(11), 951–952. **112**, (1967).
198. Remick, D. G. *et al.* Premise for Standardized Sepsis Models. *Shock* **51**, 4–9 (2019).
199. Morrissey, J. H., Choi, S. H. & Smith, S. A. Polyphosphate: An ancient molecule that links platelets, coagulation, and inflammation. *Blood* **119**, 5972–5979 (2012).
200. Smith, S. A. & Morrissey, J. H. Polyphosphate: A new player in the field of hemostasis. *Curr. Opin. Hematol.* **21**, 388–394 (2014).
201. Faxälv, L. *et al.* Putting polyphosphates to the test: evidence against platelet-induced activation of factor XII. *Blood* **122**, 3818–3824 (2013).
202. Cobb, J. P. *et al.* Inducible nitric oxide synthase (iNOS) gene deficiency increases the mortality of sepsis in mice. *Surgery* **126**, 438–442 (1999).
203. Gyawali, B., Ramakrishna, K. & Dhamoon, A. S. Sepsis: The evolution in definition, pathophysiology, and management. *SAGE Open Med.* **7**, 205031211983504 (2019).
204. Wan, H. X., Hu, J. H., Xie, R., Yang, S. M. & Dong, H. Important roles of P2Y receptors in the inflammation and cancer of digestive system. *Oncotarget* **7**, 28736–28747 (2016).
205. Wang, L., Fraley, C. D., Faridi, J., Kornberg, A. & Roth, R. A. Inorganic polyphosphate stimulates mammalian TOR, a kinase involved in the proliferation of mammary cancer cells. *Proc. Natl. Acad. Sci. U. S. A.* **100**, 11249–11254

- (2003).
206. Riehl, A., Németh, J., Angel, P. & Hess, J. The receptor RAGE: Bridging inflammation and cancer. *Cell Commun. Signal.* **7**, 1–7 (2009).
 207. Huang, S. S., Huang, J. S. & Deuel, T. F. Proteoglycan carrier of human platelet factor 4. Isolation and characterization. *J. Biol. Chem.* **257**, 11546–11550 (1982).
 208. Rucinski, B., Niewiarowski, S., James, P., Walz, D. & Budzynski, A. Antiheparin proteins secreted by human platelets. purification, characterization, and radioimmunoassay. *Blood* **53**, 47–62 (1979).
 209. Gawaz, M. Platelets in the onset of atherosclerosis. *Blood Cells, Mol. Dis.* **36**, 206–210 (2006).
 210. Scheuerer, B. *et al.* The CXC-chemokine platelet factor 4 promotes monocyte survival and induces monocyte differentiation into macrophages. *Blood* **95**, 1158–1166 (2000).
 211. Weber, C. Platelets and chemokines in atherosclerosis: Partners in crime. *Circ. Res.* **96**, 612–616 (2005).
 212. Gleissner, C. A. Macrophage phenotype modulation by CXCL4 in atherosclerosis. *Front. Physiol.* **3 JAN**, 1–7 (2012).
 213. Gleissner, C. A. *et al.* CXCL4 downregulates the atheroprotective hemoglobin receptor CD163 in human macrophages. *Circ. Res.* **106**, 203–211 (2010).
 214. Varin, A., Mukhopadhyay, S., Herbein, G. & Gordon, S. Alternative activation of macrophages by IL-4 impairs phagocytosis of pathogens but potentiates microbial-induced signalling and cytokine secretion. *Blood* **115**, 353–362 (2010).
 215. Fleischer, J. *et al.* Platelet Factor 4 Inhibits Proliferation and Cytokine Release of Activated Human T Cells. *J. Immunol.* **169**, 770–777 (2002).
 216. Liu, C. Y. *et al.* Platelet Factor 4 Differentially Modulates CD4 + CD25 + (Regulatory) versus CD4 + CD25 – (Nonregulatory) T Cells . *J. Immunol.* **174**, 2680–2686 (2005).

217. Herndon, S. C. *et al.* Supplemental Information Section. **53**, 1–4.
218. Brunkhorst, F. M. *et al.* S3 Guideline Sepsis—prevention, diagnosis, therapy, and aftercare: Long version. *Medizinische Klin. - Intensivmed. und Notfallmedizin* **115**, 37–109 (2020).

V. Curriculum vitae

Personal information

Name: Stavrides, Georgios
Date of birth: 8th October 1990
Nationality: Cypriot
Place of birth: Lefkosia, Republic of Cyprus



Academic career

05.2019 until present **Varisano Klinikum Frankfurt Höchst**
Resident in General Surgery
Approbation 23.01.2019

07.2011– 11. 2018 **Universitätsmedizin Mainz (Johannes von Gutenberg University)**
Studies of Human Medicine
Grade (Staatsexamen): 2,83

09.2005-06.2008 **Pancyprian Gymnasium, Secondary school**
Grade: 1,1

Practical expertise

20.11.2017-21.10.2018 **Practical year**
Universitätsmedizin Mainz, Universitätsspital Basel,
General Hospital Nicosia, Rep. Cyprus

01.5.2016-31.05.2017 **Centre of Thrombosis and Hemostasis (CTH)**
Working Group PD Dr. Markus Bosmann

01.09.2014-01.09.2015
Research assistant/ doctoral candidate (Virchow fellowship)
Doctoral thesis: The role of inorganic polyphosphates in
Escherichia coli sepsis

Publications

Roewe, J., **Stavrides, G.**, Strueve, M. *et al.* Bacterial polyphosphates interfere with the innate host defense to infection. *Nat Commun* 11, 4035 (2020).